Nanomaterial-based Electrochemical Sensors for the Detection of Glucose and Cholesterol

By

Asieh Ahmadalinezhad

A thesis submitted in conformity with the requirements for the Degree of Doctor of Philosophy in Biotechnology
Faculty of Science and Environmental Studies
Department of Chemistry
Lakehead University

Abstract

Electrochemical detection methods are highly attractive for the monitoring of glucose, cholesterol, cancer, infectious diseases, and biological warfare agents due to their low cost, high sensitivity, functionality despite sample turbidity, easy miniaturization via microfabrication, low power requirements, and a relatively simple control infrastructure. The development of implantable biosensors is laden with great challenges, which include longevity and inherent biocompatibility, coupled with the continuous monitoring of analytes. Deficiencies in any of these areas will necessitate their surgical replacement. In addition, random signals arising from non-specific adsorption events can cause problems in diagnostic assays. Hence, a great deal of effort has been devoted to the specific control of surface structures. Nanotechnology involves the creation and design of structures with at least one dimension that is below 100 nm. The optical, magnetic, and electrical properties of nanostructures may be manipulated by altering their size, shape, and composition. These attributes may facilitate improvements in biocompatibility, sensitivity and the specific attachment of biomaterials. Thus, the central theme of this dissertation pertains to highlighting the critical roles that are played by the morphology and intrinsic properties of nanomaterials when they are applied in the development of electrochemical biosensors.

For this PhD project, we initially designed and fabricated a novel amperometric glucose biosensor based on the immobilization of glucose oxidase (GO_x) on a Prussian blue modified nanoporous gold surface, which exhibited a rapid response and a low detection limit of 2.5 μM glucose. The sensitivity of the biosensor was found to be very high (177 μA/mM) and the apparent Michaelis–Menten constant was calculated to be 2.1 mM. Our study has demonstrated that nanoporous gold provides an excellent matrix for enzyme immobilization. To adopt these advanced properties, we fabricated a highly sensitive and mediator-free electrochemical biosensor for the determination of total cholesterol. The developed biosensor possessed high selectivity and sensitivity (29.33 μA mM^{-1} cm^{-2}). The apparent Michaelis–Menten constant, K_M^{app} of this biosensor was very low (0.64 mM), which originated from both the effective immobilization process and the nanoporous structure of the substrate. The biosensor exhibited a wide linear range, up to 300 mg dL^{-1}, in a physiological environment (pH 7.4); making it a promising candidate for the clinical determination of cholesterol. The fabricated biosensor was tested further by utilizing actual food samples (e.g., margarine, butter and fish oil). The results

indicated that it has the potential capacity to be employed as a facile cholesterol detection tool in the food industry and for supplement quality control. To enhance the stability of the biosensors in the continuous monitoring of glucose, we designed a novel platform that was based on buckypaper. The fabricated biosensor responded to glucose with a considerable functional lifetime of over 80 days and detected glucose with a dynamic linear range of over 9 mM with a detection limit of 0.01 mM.

To investigate the effects of the physical dimensions of nanomaterials on electrochemical biosensing, we synthesized TiO_2 nanowires with controllable dimensions via a facile thermal oxidation treatment of a Ti substrate. To improve the conductivity of the TiO_2 nanowires and to facilitate the immobilization of enzymes, a thin layer of carbon was deposited onto the TiO_2 nanowires via a chemical vapour deposition method. Upon the immobilization of glucose oxidase as a model protein, direct electron transfer was observed in a mediator-free biosensing environment. Our electrochemical studies have revealed that the electron transfer rate of the immobilized glucose oxidase is strongly dependent on the dimensions of the carbonized TiO_2 nanowires, and that the designed glucose biosensor exhibits a wide linear range, up to 18 mM glucose, as well as high sensitivity and selectivity. Glucose measurements of human serum using the developed biosensor showed excellent agreement with the data recorded by a commercial blood glucose monitoring assay.

Finally, we fabricated an enzyme-free glucose sensor based on nanoporous palladium-cadmium (PdCd) networks. A hydrothermal method was applied in the synthesis of PdCd nanomaterials. The effect of the composition of the PdCd nanomaterials on the performance of the electrode was investigated by cyclic voltammetry (CV). Amperometric studies showed that the nanoporous PdCd electrode was responsive to the direct oxidation of glucose with high electrocatalytic activity. The sensitivity of the sensor for continuous glucose monitoring was 146.21 $\mu AmM^{-1}cm^{-2}$, with linearity up to 10 mM and a detection limit of 0.05 mM.

In summary, the electrochemical biosensors proposed in my PhD study exhibited high sensitivity and selectivity for the continuous monitoring of analytes in the presence of common interference species. Our results have shown that the performance of the biosensors is significantly dependent on the dimensions and morphologies of nanostructured materials. The unique nanomaterials-based platforms proposed in this dissertation open the door to the design and fabrication of high-performance electrochemical biosensors for medical diagnostics.

Acknowledgments

First, I want to thank my supervisor Prof. Aicheng Chen for all the hope he has put on me. He has enlightened me through his wide knowledge of electrochemistry and his deep intuitions about where it should go and what is necessary to get there. I also thank the committee members of my thesis research proposal and the internal examiners of my dissertation, Dr. Wensheng Qin and Dr. Kam Leung and the external examiner, Dr. Kagan Kerman. Thanks also to Dr. Heidi Schraft, the coordinator of Biotechnology PhD program for her great help.

Thanks to Dr. Aicheng Chen's research group, Dr. Guosheng Wu, Dr. Min Tian, Dr. Rasha Tolba, Monika Malig, Jiali Wen, Sapanbir Thind, Xiao Qu, Sharon Chen, Brian Adams, Matthew Asmussen, Ke Pan, Cassendra Ostrom, Paul Benvenuto, Nelson Matyasovsky, Samantha Nigro, Ke Pan, and Todd Lafleur for the wonderful chat, friendship and collaborations. I thank the rest of Chemistry Department including both the faculty and the students. During my Ph.D., I received support of my supervisor's grant from NSERC and by the graduate assistant position at Lakehead Univrsity.

I also thank friends I met in Thunder Bay for the wonderful friendship they offered me, like Richard Martin, Mehdi Dashtban, Saedeh Dadgar, Tylor Martin, Trish Fretwell, Dave Wilson, Jenifer Elm, Nolan Dobroski, Naeem Nematollahi, Namira Mohammadi, Leyla Vakili, Hassan Nasser, Zohreh and Bahram Dadgostar, Amirhossein Karami, Jamshid Khastoo, Fereshteh Ghashghaee, Karim and Rima Khatami, and all my friends.

Last but not least, a great thank to my family, specially my parents for their endless love. Still today, learning to love them and to receive their love makes me a better person.

List of Figures

List of Tables

List of Abbreviations and Symbols

A	Geometric area of the working electrode
BP	Buckypaper
C	Concentration
ChE	Cholesterol estrease
ChO_x	Cholesterol oxidase
CV	Cyclic Voltammetry
D	Diffusion coefficient of the probe molecule
E^0	Formal potential
EDS	Energy-dispersive X-ray spectroscopy
E_{pa}	Anodic peak potential
E_{pc}	Cathodic peak potential
F	Faraday constant
GO_x	Glucose oxidase
HRP	Horseradish peroxidase
I	Current
I_{max}	Maximum current
I_p	Peak current
I_{ss}	Steady state current
K_m, K_M^{app}	Michaelis–Menten constant
k_s	Interfacial electron transfer rate constants
n	Number of transferred electrons

PB	Prussian blue
Q	Charge
R	Gas rate constant
R.S.D.	Relative standard deviation
SEM	Scanning electron microscopy
T	Temperature
TEM	Trasmission electron microscopy
XRD	X-ray diffraction spectroscopy
α	Experimental electron transfer coefficient
Γ	Amount of the electroactive enzyme
ΔE_p	Peak-to-peak separation potential
υ	Scan rate

Table of Contents

Chapter 1

Introduction

Over the past few decades, a number of reports have highlighted the growing importance of electrochemical biosensing devices in both clinical and environmental analysis. This may not seem as surprising when one considers that electrochemical transduction processes have inherent advantages such as low cost; high sensitivity; independence from solution turbidity; simple miniaturization that is well-suited to microfabrication; low power requirements; and relatively straightforward associated instrumentation. These characteristics make electrochemical sensing methods highly attractive in myriad applications, including the detection of cancer, infectious diseases, glucose and cholesterol, and biological warfare agents, to name but a few.

1.1. Nanoscience development

Nanoscale molecular electrochemistry has followed a line of evolution that had its beginnings in the late 1970s via a new intimate interaction between electrochemistry on one side and both solid state physics and physical surface science on the other.[1] In the midst of this evolution, which was almost likened to a renaissance in electrochemical science, single-crystal electrodes with well-defined surface structures were, for example, introduced as a major breakthrough.[1-2] This laid the foundation for subsequent novel electrochemical technologies, not the least of which was scanning probe microscopy. At the same time a range of surface science techniques and theories were introduced and developed. These included spectroscopy (UV/vis, IR, Raman, and X-ray photoelectron spectroscopy (XPS); the development of the quartz crystal microbalance and other physical techniques; as well as both statistical mechanical and electronic structural theories and computations, all of which were warranted via the new electrochemistry.

Shortly afterward, with the onset of scanning probe techniques, STM, and atomic force microscopy (AFM), a dramatic enhancement of both the fields of surface science and interfacial electrochemistry enabled the capacity for unprecedented levels of elucidation. The atomic resolution of pure metals and semiconductor electrode surfaces, and at least the sub-molecular resolution of electrochemical adsorbates could now be achieved; opening new worlds through the visualization of micro/nanoscopic structures and processes, and novel approaches in electrochemical nanotechnologies.[3]

As nanotechnology research involves the design and creation of structures with at least one dimension that is below 100 nm, researchers may now routinely manipulate the optical, magnetic, and electrical properties of materials by altering nanostructured attributes such as size, morphology, and atomic composition. The capacity for the synthesis of nanomaterials has undoubtedly been a core enabler, since they exhibit unique properties, which have widespread applications encompassing electrochemistry, electrocatalysis, optics, electronics, analytical devices, energy devices, and so forth. For instance, quantum dots can exhibit green to red emission upon dimensional tuning, which is in turn related to changes in quantum confinement.[4] Regarding shape effects, gold nanorods and gold nanocages have strong near-infrared surface plasmon resonance (SPR) absorption, whereas Au nanoparticles exhibit only size-dependent visible SPR absorption.[5] Altering the composition of nanomaterials through the alloying of two types of semiconductors may produce new materials that display properties that are distinct not only from the properties of their bulk counterparts, but also from those of their parent semiconductors.[6] For the sensing of small molecules, carbon nanotubes/Au nanoparticle hybrids possess a higher electrochemical performance than that of the individual nanomaterials.[7] The aforementioned adjustments and characterizations may further affect the biocompatibility,

sensitivity and specific attachment of biomaterials in the construction of nanometric biosensing devices.

1.2. Electrochemical biosensors

A typical catalytic biosensor consists of an enzyme layer that is interfaced with a signal transducing device. There have been substantial research efforts devoted to the development of strategies for incorporating whole cells, components of cells, or subcellular elements from living microorganisms, animal and plant tissues into biosensors.

Insofar as the development of electrochemical biosensors, the facilitation of electron transfer between enzymes and electrodes constitutes a tremendous challenge due to the deeply embedded redox-active centers of metalloenzymes.[8-10] On one hand, great progress has been made toward the enhancement of electron transfer in the construction of enzyme-based biosensors, by utilizing mediators, promoters or other special materials such as peroxidases.[8-10] On the other hand, higher sensitivity is achievable via the integration of nanomaterials, due to their capacity for the intimate attachment of enzymes, which is enabled by their higher surface area, roughness, and extensive number of available binding sites, as well as their unique physical, electronic and chemical properties.

1.2.1. Enzyme-based biosensors

Because enzyme-based sensors tend to either produce or consume protons and/or electroactive species, the vast majority of enzyme sensors employ an electrode as the transducer, which will be the primary emphasis of this dissertation. To date, from a practical and commercial point of view, biosensors for the detection of only four compounds have been widely used: glucose (diagnosis and treatment of diabetes, food science, biotechnology), lactate (sports medicine, critical care, food science, biotechnology), urea (clinical applications), and glutamate/glutamine

(food science, biotechnology). However, glucose biosensors are by far, the most widely employed. Hence, there are ongoing research efforts being applied toward their improvement. Devices that are capable of monitoring blood glucose in vivo, as part of an "artificial pancreas", have been the subject of extensive research by many groups over the last few decades.[11-13] Most enzyme-based biosensors employ a class of enzymes known as oxidoreductases, and the two most frequently encountered subclasses are the oxidases and dehydrogenases. Their reaction sequences may be described by the following reactions:

$$S_{red} + E_{ox} \rightarrow S_{ox} + E_{red} \qquad (1)$$

$$S'_{ox} + E_{red} \rightarrow S'_{red} + E_{ox} \qquad (2)$$

If, for example, glucose oxidase (GO_x) is the enzyme employed, then S_{red}, S_{ox}, S'_{ox}, and S'_{red} correspond to glucose, gluconic acid, oxygen, and hydrogen peroxide, respectively. To make reaction eq 1 rate limiting, a large excess of S'_{ox} (typically oxygen) is required. This is accomplished by increasing the flux ratio of S_{red} to S'_{ox} into the enzyme reaction layer such that S'_{ox} is in large excess. When properly implemented, the sensor output is largely independent of oxygen partial pressure over a wide range down to 8 Torr. (Levels of oxygen in subcutaneous tissue are estimated at 20−30 Torr). [14]

The rate of the overall reaction sequence can be measured by monitoring the consumption of S'_{ox} or the formation of S'_{red}. In practical GO_x systems this relates to either the consumption of oxygen or the production of peroxide. The advantage of the former approach is the relative ease of separation of oxygen from other electroactive species through the use of a gas-permeable membrane. The disadvantage of this approach is that it is more complicated, requiring two measurements (concentration of oxygen in the presence and absence of the enzymatic reaction). However, it is capable of compensating for a significant fluctuation in

oxygen levels.[15] The measurement of peroxide has the advantage of being simpler, especially for small sensors. The drawback, however, is that a number of in vivo endogenous species (ascorbate and urate) are electroactive at the applied potential required for peroxide oxidation. It has been proven possible to use permselective membranes that may successfully exclude interfering species.[16] Monitoring of peroxide reduction is not possible because of the inability to find a potential at which peroxide, but not oxygen, is reduced. A porous Teflon membrane has been used to electrochemically detect hydrogen peroxide because of its "gaslike" properties,[17] thus enabling selectivity.

It is clear then, that two redox couples are necessary to carry out the enzyme-catalyzed redox reaction, one of which is the analyte. Thus, the other (S'_{ox}) must be introduced in some fashion. It is often desirable for the biosensor to be "reagentless". This means that a clever method for delivering the second substrate (cofactor) must be devised, or S'_{ox} must initially be present at sufficiently elevated levels that it does not affect sensor response. This is the reason for the overwhelming preference for oxidases, as oxygen is often naturally already present at the required levels. If the enzyme belongs to the dehydrogenase class, it will typically use NAD as a cofactor. Either NAD or NADH will have to be monitored electrochemically or by some other means. There are a large number of enzymes in this class, but the need to add reagent (NAD) and the relative complexity of NADH electrochemistry have precluded their use in in vivo applications.

Alternatively, S'_{ox} might be eliminated if the redox center of the enzyme was coupled *directly* to the electrode, thus making the electrode the "sink" for the electrons required to complete eq 2. With few exceptions, this has not proven to be feasible because enzyme redox centers are frequently well buried within the protein and thus, heterogeneous electron transfer is

prohibitively slow. Horseradish peroxidase, which is a very small enzyme, is able to communicate directly with the electrode in the case of carefully prepared carbon electrodes[18] or through the use of 30 nm gold particles deposited on a gold electrode.[19-20]

1.2.2 Nanomaterials as substrates for enzymes

Compelling combinations of the dimensional, compositional, and geometric properties of nanomaterials are required to impart unique functionality and applications. With this aim, the synthesis of certain functional nanomaterials with well-defined morphologies that are capable of interacting with specific organic compounds and polymers are a significant and ongoing challenge. The spontaneous adsorption of organic molecules on a variety of nanomaterials can generate films that are only a single molecule in thickness. These nanoscale, self-assembled monolayer (SAM) films have been extensively used to engineer surfaces with well-defined properties. Their utility has been demonstrated over a wide range of applications, including wetting, adhesion, lubrication, patterning, and molecular recognition. Although many SAM systems have been investigated, alkanethiols adsorbed on gold have been shown to be the most successful combination. This pairing offers a variety of advantages, including the ability to precisely tune the interfacial properties of a surface through well-established organic synthetic methodologies, which have been developed in the preparation of custom ω-terminated alkanethiols. Alkanethiolate monolayers are moderately stable at room temperature; however, these films degrade over time and readily desorb upon moderate heating. This shortcoming limits the use of SAMs in applications involving elevated temperatures or harsh environments. Accordingly, the necessity of utilizing other adsorbates with multiple bonding moieties has been important toward the enhancement of the stability and versatility of nanostructure-based biosensors. Chitosan has been used in the fabrication of biosensing devices because of its

biocompatibility, biodegradability, multiple functional groups, as well as its solubility in acidic aqueous media [21-23]. This naturally occurring polymer contains primary amines, hydroxyl and acetyl groups, which under weakly acidic conditions are protonated and have a tendency for inducing electrostatic interactions with metallic nanostructures.

Molecular electronic properties (molecular "electronics") and interfacial molecular electron transfer have evolved over the past few decades as a result of investigations into the intimate interactions between nanometric substrates and biomolecules. Here, we have aimed at working on particular facets of this exciting and broad interdisciplinary area; namely experimental and theoretical aspects associated with biomolecular electrochemistry.

1.3. Dissertation rationale and scope

The central theme of this dissertation pertains to highlighting the critical roles that are played by the morphology and intrinsic properties of nanomaterials when they are applied in the development of biosensors. Therefore, the objectives of my research are:

(1) Synthesis and characterization of novel, biocompatible, metal-based engineered nanomaterials

(2) Study of the interactions between nanomaterials and bio-recognition elements toward the evolution of an efficient immobilization procedure

(3) Development of electrochemical biosensors based on nanostructured materials for the detection of specific target biomolecules

(4) Adjustment of nanomaterial dimensions in order to achieve optimum sensitivity, stability and response time

I anticipate that the above objectives and methods will culminate in the establishment of strategies for enabling biocompatibility, high sensitivity, selectivity, rapid response, miniaturization, and low cost for biosensing.

In the following chapters, recent achievements in the development of various simple approaches for the synthesis of diverse nanomaterials with a variety of geometries are reported, along with their potential applications in electrochemical biosensors.

Chapter 2 will present a survey of existing biosensors along with a number of current issues that are thought to impede their performance. Finally, future perspectives for this field will be examined. In chapter 3, a general procedure for the fabrication of reported biosensors will be discussed. In chapter 4, we report on a novel glucose biosensor that is based on the immobilization of glucose oxidase (GO_x) on a Prussian blue modified nanoporous gold surface. The morphology and composition of the gold nanostructures were characterized by scanning electron microscopy (SEM), energy-dispersive X-ray spectroscopy (EDS). We describe a highly sensitive electrochemical biosensor for the determination of total cholesterol in chapter 5. The cholesterol biosensor was fabricated by the co-immobilization of three enzymes, including cholesterol oxidase (ChO_x), cholesterol esterase (ChE) and horseradish peroxidase (HRP), on nanoporous gold networks, which were grown directly on a titanium substrate. The morphology and composition of the fabricated nanoporous gold were characterized by scanning electron microscopy (SEM), energy-dispersive X-ray spectroscopy (EDS) and X-ray diffraction spectroscopy (XRD). The electrochemical behaviour of the cholesterol biosensor was studied using cyclic voltammetry. In chapter 6, we report on a novel platform based on buckypaper for the design of high-performance electrochemical biosensors. Using glucose oxidase as a model enzyme, we constructed a biocompatible mediator-free biosensor and studied the potential effect

of the buckypaper on the stability of the biosensor with both amperometry and FTIR spectroscopy. In chapter 7, we present a new methodology for the synthesis of carbon-modified titanium oxide (TiO_2) nanowires with controllable size. The surface morphology of a carbonized nanosensor network was further characterized for different sizes of nanowires. Upon enzyme immobilization, an electrochemical biosensor was developed for the detection of glucose in a human serum sample. To test the efficacy of nanomaterials in the direct oxidation of glucose, we report on a non-enzymatic palladium-cadmium (Pd-Cd) electrode in chapter 8. A hydrothermal method was applied in the synthesis of Pd-Cd nanoparticles. The non-enzymatic electrode was fabricated via the deposition of a Pd-Cd nanoparticle array on a glassy carbon electrode using Nafion. Direct glucose oxidation on the electrode was investigated in detail and we discuss the effect of electrode adhered nanomaterials on the electrocatalytic oxidation of glucose. Finally, in chapter 9, we conclude with a look at future challenges and prospects as relates to various aspects involved with the synthesis and application of nanomaterials-based biosensors.

References

1. Hubbard, A. T., Electrochemistry of Well-defined Surfaces. *Acc.Chem. Res.* **1980,** *13*, 177-184.

2. Clavilier, J.; Faure, R.; Guinet, G.; Durand, R., Preparation of Monocrystalline Pt Microelectrodes and Electrochemical Study of the Plane Surfaces Cut in the Direction of the {111} and {110} Planes. *J. Electroanal. Chem. Interfac. Electrochem.* **1979,** *107*, 205-209.

3. Zhang, J.; Kuznetsov, A. M.; Medvedev, I. G.; Chi, Q.; Albrecht, T.; Jensen, P. S.; Ulstrup, J., Single-Molecule Electron Transfer in Electrochemical Environments. *Chem. Rev.* **2008,** *108*, 2737-2791.

4. Ying, E.; Li, D.; Guo, S.; Dong, S.; Wang, J., Synthesis and Bio-Imaging Application of Highly Luminescent Mercaptosuccinic Acid-Coated CdTe Nanocrystals. *PLoS ONE* **2008,** *3*, e2222.

5. Skrabalak, S. E.; Chen, J.; Sun, Y.; Lu, X.; Au, L.; Cobley, C. M.; Xia, Y., Gold Nanocages: Synthesis, Properties, and Applications. *Acc. Chem. Res.* **2008,** *41*, 1587-1595.

6. Regulacio, M. D.; Han, M.-Y., Composition-Tunable Alloyed Semiconductor Nanocrystals. *Acc. Chem. Res.* **2010,** *43*, 621-630.

7. Huang, J.; Wang, D.; Hou, H.; You, T., Electrospun Palladium Nanoparticle-Loaded Carbon Nanofibers and Their Electrocatalytic Activities Towards Hydrogen Peroxide and NADH. *Adv. Funct. Mater.* **2008,** *18*, 441-448.

8. Lu, X.; Zou, G.; Li, J., Hemoglobin Entrapped Within A Layered Spongy Co3O4 Based Nanocomposite Featuring Direct Electron Transfer and Peroxidase Activity. *J. Mater. Chem.* **2007,** *17*, 1427-1432.

9. Wang, J., Nanomaterial-based Electrochemical Biosensors. *Analyst* **2005,** *130*, 421-426.

10. Reilly, C. A.; Aust, S. D., Peroxidase Substrates Stimulate the Oxidation of Hydralazine to Metabolites Which Cause Single-Strand Breaks in DNA. *Chem. Res. Toxicol.* **1997,** *10*, 328-334.

11. Shichiri, M.; Kawamori, R.; Goriya, Y.; Yamasaki, Y.; Nomura, M.; Hakui, N.; Abe, H., Glycaemic Control in Pancreatectomized Pogs with a Wearable Artificial Endocrine Pancreas. *Diabetologia* **1983,** *24*, 179-184.

12. Claremont, D.; Sambrook, E.; Penton, C.; Pickup, J., Subcutaneous Implantation of A Ferrocene-mediated Glucose Sensor in Pigs. *Diabetologia* **1986,** *29*, 817-821.

13. Moussy, F.; Harrison, D. J.; O'Brien, D. W.; Rajotte, R. V., Performance of Subcutaneously Implanted Needle-type Glucose Sensors Employing A Novel Trilayer Coating. *Anal. Chem.* **1993,** *65*, 2072-2077.

14. Zhang, Y.; Wilson, G. S., In Vitro and In Vivo Evaluation of Oxygen Effects on A Glucose Oxidase Based Implantable Glucose Sensor. *Anal. Chim. Acta* **1993,** *281*, 513-520.

15. Lucisano, J. Y.; Gough, D. A., Transient Response of the Two-dimensional Glucose Sensor. *Anal. Chem.* **1988,** *60*, 1272-1281.

16. Zhang, Y.; Hu, Y.; Wilson, G. S.; Moatti-Sirat, D.; Poitout, V.; Reach, G., Elimination of the Acetaminophen Interference in an Implantable Glucose Sensor. *Anal. Chem.* **1994,** *66*, 1183-1188.

17. Pan, S.; Arnold, M. A., Amperometric Internal Enzyme Gas-sensing Probe for Hydrogen Peroxide. *Anal. Chim. Acta* **1993,** *283*, 663-671.

18. Csöregi, E.; Gorton, L.; Marko-Varga, G., Carbon Fibres as Electrode Materials for the Construction of Peroxidase-Modified Amperometric Biosensors. *Anal. Chim. Acta* **1993,** *273*, 59-70.

19. Zhao, J.; Henkens, R. W.; Stonehuerner, J.; O'Daly, J. P.; Crumbliss, A. L., Direct Electron Transfer at Horseradish Peroxidase-Colloidal Gold Modified Electrodes. *J. Electroanal. Chem.* **1992,** *327*, 109-119.

20. Wilson, G. S.; Hu, Y., Enzyme-Based Biosensors for in Vivo Measurements. *Chem. Rev.* **2000,** *100*, 2693-2704.

21. Ahmadalinezhad, A.; Kafi, A. K. M.; Chen, A., Glucose biosensing based on the highly efficient immobilization of glucose oxidase on a Prussian blue modified nanostructured Au surface. *Electrochem. Commun.* **2009,** *11*, 2048-2051.

22. Wang, S.-F.; Shen, L.; Zhang, W.-D.; Tong, Y.-J., Preparation and Mechanical Properties of Chitosan/Carbon Nanotubes Composites. *Biomacromolecules* **2005,** *6*, 3067-3072.

23. Tiwari, A.; Gong, S., Electrochemical Study of Chitosan-SiO2-MWNT Composite Electrodes for the Fabrication of Cholesterol Biosensors. *Electroanalysis* **2008,** *20*, 2119-2126.

Chapter 2

Literature Review

2.1. Introduction

2.1.1. Definitions

A chemical sensor is a device that transforms chemical information, ranging from the concentration of a specific sample component to total composition analysis, into an analytically useful signal. Chemical sensors typically contain two basic components connected in series: a chemical (molecular) recognition system (receptor) and a physico-chemical transducer. Biosensors are chemical sensors in which the recognition system utilizes a biochemical mechanism (Figure 1.1).[1] The biological recognition system translates information from the biochemical domain, usually an analyte concentration, into a chemical or physical output signal with a defined sensitivity. The main purpose of the recognition system is to provide the sensor with a high degree of selectivity for the analyte to be measured. While all biosensors are more or less selective (non-specific) for a particular analyte, some are (by design and construction), only class-specific, since they use certain classes of enzymes, (e.g., phenolic compound biosensors, or whole cells used to measure biological oxygen demand).

For the sensing systems that are present within living organisms, including olfaction, taste, and neurotransmission pathways, actual recognition is performed by cell receptors. Hence, the term receptor or bioreceptor is also often employed to denote the recognition system of a chemical biosensor. These examples are limited to the most common sensing principles, excluding existing laboratory instrumentation systems.

The transducer component of a sensor serves to transfer the signal from the output domain of the recognition system, primarily to the electronic domain. Because of the general significance of the word, a transducer provides bi-directional signal transfer (non-electrical to electrical and vice versa). A transducer is also called a detector, sensor or electrode, however, the term transducer is preferred in order to avoid confusion.

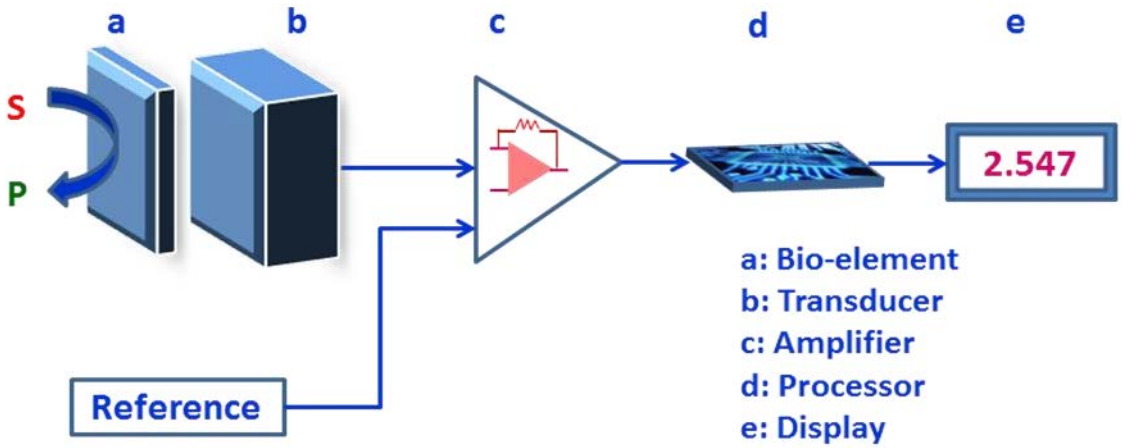

Figure 2.1. Basic elements of a biosensor.

2.2. Classification

2.2.1. Detection methods

2.2.1.1. Optical biosensors

Many optical biosensors based on the phenomenon of surface Plasmon resonance may be considered as evanescent wave techniques. They utilize a property that is inherent to gold and other materials; specifically that a thin layer of gold on a high refractive index glass surface may absorb laser light to produce electron waves (surface plasmons) on the surface of the gold. This

occurs only at a specific angle and wavelength of incident light and is highly dependent on the surface attributes of the gold, such that the binding of a target analyte to a receptor on the gold surface produces a measurable signal.

Surface plasmon resonance sensors operate using a sensor chip that consists of a plastic cassette that supports a glass plate, one side of which is coated with a microscopically thin layer of gold. This is the side that contacts the optical detection apparatus of the instrument. The opposite side is then interfaced with a microfluidic flow system. Contact with the flow system creates channels across which reagents may be passed in solution. This side of the glass sensor chip can be modified in a number of ways to allow for the easy attachment of molecules of interest. Normally it is coated with carboxymethyl dextran or similar compounds.

Light of a fixed wavelength is reflected from the gold side of the chip at the angle of total internal reflection and is detected inside the instrument. This induces the evanescent wave to penetrate through the glass plate and some distance into the liquid that is flowing over the surface.

The refractive index at the flow region of the chip surface has a direct influence on the behaviour of the light that is reflected from the gold region. Binding to the flow region of the chip has an effect on the refractive index and in this way biological interactions may be measured with a high degree of sensitivity when facilitated by a source of energy.

Other evanescent wave biosensors have been commercialised that utilize waveguides where the propagation constant through the waveguide is altered by the absorption of molecules to the waveguide surface. One such example, Dual Polarisation Interferometry uses a buried waveguide as a reference against which the change in propagation constant is measured. Other

configurations such as the Mach-Zehnder have reference arms lithographically defined on a substrate. Higher levels of integration may be achieved using resonator geometries where the resonant frequency of a ring resonator changes when molecules are absorbed.

Other optical biosensors are based primarily on changes in absorbance or fluorescence of an appropriate indicator compound and do not need a total internal reflection geometry. For example, a fully operational prototype device for the detection of casein in milk has been fabricated. The device is based on detecting changes in absorption of a gold layer.[2] A widely used research tool; the microarray, may also be considered a biosensor.

Biosensors often incorporate a genetically modified form of a native protein or enzyme. The protein is configured to detect a specific analyte and the ensuing signal is read by a detection instrument such as a fluorometer or luminometer. An example of a recently developed biosensor is one for detecting cytosolic concentrations of the analyte cAMP (cyclic adenosine monophosphate). cAMP is a second messenger that is involved in cellular signalling, which is in turn triggered by ligand - receptor interactions on the cell membrane.[3] Similar systems have been created to study cellular responses to native ligands or xenobiotics (toxins or small molecule inhibitors). Such "assays" are commonly utilized in drug discovery development by pharmaceutical and biotechnology companies. Most cAMP assays in current use require the lysis of the cells prior to the measurement of cAMP. A live-cell biosensor for cAMP may be used in non-lysed cells with the additional advantage of multiple reads for studying receptor response kinetics.

2.2.1.2. Electrochemical biosensor

Electrochemical biosensors are normally based on the enzymatic catalysis of a reaction that produces or consumes electrons (such enzymes are rightly called redox enzymes). The sensor substrate usually contains three electrodes; a reference electrode, an active electrode and a sink electrode. An auxiliary electrode (also known as a counter electrode) may also be present as an ion source. The target analyte is involved in the reaction that takes place on the active electrode surface, and the ions produced create a potential which is subtracted from that of the reference electrode to provide a signal. We can either measure the current (rate of flow of electrons is now proportional to the analyte concentration) at a fixed potential, or the potential may be measured at zero current (this gives a logarithmic response). Note that the potential of the working or active electrode is space charge sensitive and hence, is often used. Figure 2.2 illustrates the electron transfer mechanism in a typical biosensor. Further, the label-free and direct electrical detection of small peptides and proteins is made possible via their intrinsic charges using biofunctionalized ion-sensitive field-effect transistors.[4]

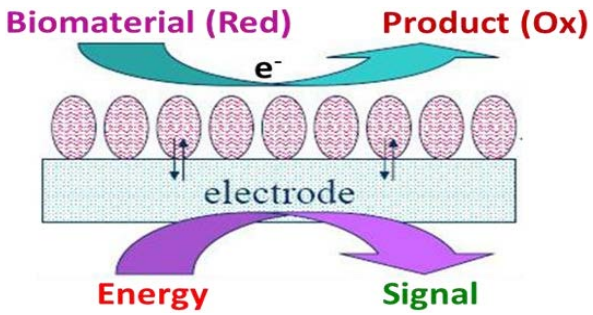

Figure 2.2. Schematic diagram of the electron transfer in a typical biosensor

Another example, in the form of a potentiometric biosensor, works contrary to the current understanding of its ability. Such biosensors are screen printed, conductive polymer coated, open

circuit potential biosensors that are based on conjugated polymeric immunoassays. They contain only two electrodes and are extremely sensitive and robust; enabling the detection of analyte levels that were previously only achievable by HPLC and LC/MS, without rigorous sample preparation. The signal is generated by electrochemical and physical modifications in the conductive polymer layer due to changes that occur at the surface of the sensor. Such alterations may be attributed to ionic strength, pH, hydration and redox reactions. The latter is due to the enzyme label turning over a substrate (IUPAC).

2.2.2. Receptor: Biological recognition element

2.2.2.1. Biocatalytic recognition element

In this instance, the biosensor is based on a reaction that is catalyzed by macromolecules, which are either inherently present in biological environments, previously isolated or manufactured. Thus, the continuous consumption of substrate(s) is achieved by the immobilized biocatalyst that is incorporated into the sensor: transient or steady-state responses are monitored by the integrated detector. Three types of biocatalysts are commonly used:

1. Enzymes (e.g., mono- or multi-enzymes), which are the most common and well developed recognition system;

2. Whole cells (e.g., microorganisms, such as bacteria, fungi, eukaryotic cells or yeast), cell organelles or components thereof (e.g., mitochondria, cell walls);

3. Tissues (e.g., plant or animal tissue layers). Biocatalytic biosensors are the most well known and studied and therefore, have been the most frequently applied to biological matrices since the pioneering work of Clark.[5] One or more analytes; typically named substrates S and S′, react in

the presence of enzyme(s), whole cells or tissue cultures and yield single or multiple products, P and P′, according to the general reaction scheme:

$$S+S' \longrightarrow P+P'$$

There are four strategies that utilize adjacent transducers for monitoring the analyte S consumption by this biocatalysed reaction:

- detection of the co-substrate S′ consumption (e.g., oxygen depleted by oxidase), bacteria or yeast reacting layers, and the corresponding signal decrease from its initial value;
- recycling of P, one of the reaction products (e.g., hydrogen peroxide, H^+, CO_2, NH_3, etc.). Production by oxidoreductase, hydrolase, lyase, etc., and corresponding signal increase;
- detection of the state of the biocatalyst redox active centre, cofactor, prosthetic group evolution in the presence of substrate S, using an immobilized mediator which reacts sufficiently rapidly with the biocatalyst and is easily detected by the transducer; various ferrocene derivatives, as well as quinones, quinoid dyes, Ru or Os complexes in a polymer matrix, have been used;
- direct electron transfer between the active site of a redox enzyme and the electrochemical transducer

The third strategy attempts to eliminate sensor response dependence on the co-substrate, S′ concentration and to decrease the influence of possible interfering species. The first goal is reached only when the reaction rates are much higher for immobilized mediators with biocatalysts than those for co-substrates with biocatalysts.

An alternative approach to the use of such mediators consists in restricting the analyte (substrate) concentration within the reaction layer through an appropriate outer membrane, whose permeability strongly favours co-substrate transport. When multiple enzymes are immobilized within the same reaction layer, a number of strategies for improving biosensor performance may be developed. The following three possibilities have been most frequently proposed:[6-7]

- several enzymes facilitate biological recognition by sequentially converting the product of a series of enzymatic reactions into a final electroactive form: this set-up allows for a much wider range of possible biosensor analytes;

- multiple enzymes applied in series may regenerate the first enzyme co-substrate and a real amplification of the biosensor output signal may be achieved by the efficient regeneration of another co-substrate of the first enzyme;

- multiple enzymes, applied in parallel, may improve biosensor selectivity by decreasing the local concentration of electrochemical interfering substances: this set-up is an alternative to the use of either a permselective membrane or a differential set-up, i.e., subtraction of the output signal generated by the biosensor and by a reference sensor having no biological recognition element.

2.2.2.2. Biocomplexing or bioaffinity recognition element

Biosensor operation is based on the interaction of analytes with macromolecules or organized molecular assemblies that have either been isolated from their original biological environment or engineered.[8] Thus, equilibrium is usually attained and there is no further net consumption of the analyte by the immobilized biocomplexing agent. These equilibrium

responses are monitored by an integrated detector. In some cases, the biocomplexing reaction itself is monitored using a complementary biocatalytic reaction. Steady-state or transient signals are then monitored by the integrated detector.

1. *Antibody-antigen interaction*. The most developed examples of biosensors using biocomplexing receptors are based on immunochemical reactions, i.e. binding of an antigen (Ag) to a specific antibody (Ab). The formation of such Ab-Ag complexes must be detected under conditions where non-specific interactions are minimized. Each Ag determination requires the production of a particular Ab, its isolation and typically, its purification. Several studies have been described that involved the direct monitoring of the Ab-Ag complex formation on Ion Sensitive Field-Effect Transistors (ISFETs). In order to increase the sensitivity of immunosensors, enzyme labels are frequently coupled to Ab or Ag, thus requiring additional chemical synthesis steps. Even in the case of the enzyme-labelled Ab, these biosensors will essentially operate at equilibrium, where the sole function of the enzymatic activity is to quantify the amount of complex produced.

2. *Receptor*:*antagonist*:*agonist*. More recently, attempts have been made in employing ion channels, membrane receptors or binding proteins as molecular recognition systems in conductometric, ISFET, or optical sensors. For example, the transport protein, lactose permease (LP), may be incorporated into liposomal bilayers, thus allowing for the coupling of sugar proton transport with a stoichiometric ratio of 1:1, as demonstrated when the fluorescent pH-probe pyranine is entrapped within these liposomes.[9] These LP-containing liposomes have been incorporated within planar lipid bilayer coatings of an ISFET that is gate sensitive to pH. Preliminary results have shown that these modified ISFETs enable the rapid and reversible detection of lactose in a FIA system. Protein receptor-based biosensors have been recently

developed.[10] The result of the binding of the analyte (termed agonist here), to immobilized channel receptor proteins, is monitored by changes in ion fluxes through these channels.

2.3. Biosensor construction

2.3.1. Immobilization of biological receptors

Since the development of enzyme-based biosensors for glucose (first described by Clark in 1962), in which glucose oxidase was entrapped between two membranes,[5] an impressive volume of literature that describes techniques of immobilization and related biosensor development has appeared. These methods have been extensively reviewed elsewhere.[1, 11] Biological receptors, i.e. enzymes, antibodies, cells or tissues with high biological activity, may be immobilized within a thin layer at the transducer surface by using different procedures. The following protocols are the most generally employed (Figure 3.2):

1. Entrapment behind a membrane: a solution of enzyme, suspension of cells or a slice of tissue is simply confined by an analyte permeable membrane as a thin film, which covers the electrochemical detector;[12]

2. Entrapment of biological receptors within a polymeric matrix such as polyacrylonitrile, agar gel, polyurethane (PU) or poly(vinyl-alcohol) (PVAL) membranes, sol gels or redox hydrogels with redox centers;[13]

3. Entrapment of biological receptors within self-assembled monolayers (SAMs) or bilayer lipid membranes (BLMs);[14]

4. Covalent bonding of receptors onto membranes or surfaces activated by means of bifunctional groups or spacers such as glutaraldehyde, carbodiimide, SAMs or multilayers, avidin-biotin silanization. Several of these activated membranes are commercially available;[15]

5. Bulk modification of an entire electrode material, (e.g., enzyme modified carbon paste or graphite epoxy resin).[16]

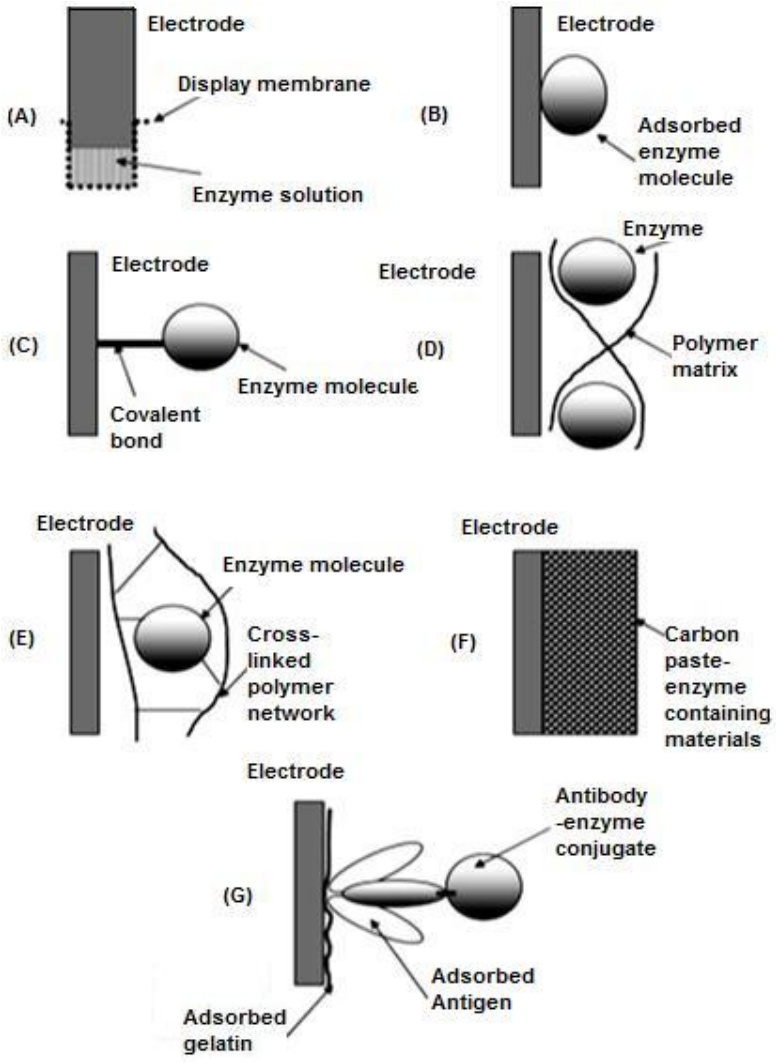

Figure 2.3. Scheme of primary types of enzymatically modified electrodes.[17] (A) Membrane electrode; (B) Modification of the electrode surface through adsorption; (C) Covalent bonding; (D) Gel/polymer entrapment; (E) Entrapment via crosslinking; (F) Entrapment of the enzyme-containing material in a carbon-paste electrode; (G) Antigen-Antibody assembly on an electrode.

Receptors are either individually immobilized or mixed with additional proteins, such as bovine serum albumin (BSA), directly on the transducer surface, or on a polymeric membrane that covers it. In the latter case, pre-activated membranes can be used directly for enzyme or antibody immobilization without the requirement of further chemical modification of the membrane or macromolecule.

Apart from the final example, reticulation and covalent attachment procedures are more complex than those that involve entrapment, but are especially useful in cases where the sensor is so diminutive that the appropriate membrane must be fabricated directly onto the transducer. Under such conditions more stable and reproducible activities may be obtained via covalent attachment.

2.4. Biosensor applications

There are myriad potential applications of biosensors of various classes. The chief prerequisites for a biosensor approach in terms of its value in research and for commercial applications include the identification of a target molecule, the availability of a suitable biological recognition element, and the potential for disposable portable detection systems as preferable to sensitive laboratory-based techniques in particular situations. A number of examples are given below:[14-17]

- Glucose monitoring for diabetes patients (historical market driver).
- Other medical/health-related targets.
- Environmental applications (e.g., detection of pesticides in ecosystems and water resident contaminants).

- Remote sensing of airborne bacteria (e.g., in counter-bioterrorist activities).
- Detection of pathogens.
- Determination of toxic substance levels prior to and following bioremediation.
- Detection and quantification of organophosphates.
- Routine analytical measurement of folic acid, biotin, vitamin B12 and pantothenic acid as an alternative to microbiological assay.
- Determination of drug residues in food, such as antibiotics and growth promoters, particularly in meat products and honey.
- Drug discovery and the evaluation of biological activity of new compounds.
- Protein engineering in biosensors.
- Detection of toxic metabolites such as mycotoxins

2.4.1. Electrochemical glucose biosensor in diabetes management

Diabetes is a rapidly growing problem; the number of people with diabetes increased from 153 million in 1980, to 347 million in 2008.[18] In 2004, an estimated 3.4 million people died as a result of the consequences of high blood sugar. This number is estimated to double by 2030.[19] Diabetes may lead to serious complications such as lower limb amputations, blindness, as well as cardiovascular and kidney disease.

There are three types of diabetes:

1. Type 1 diabetes usually affects the young and occurs when the pancreas no longer produces any (or very little) insulin. Approximately 10% of diabetics have Type 1.

2. Type 2 diabetes commonly affects middle-aged or older patients and occurs when the pancreas does not produce enough insulin or when the body does not use the insulin that is produced effectively. 90% of people with diabetes have Type 2.

3. Gestational diabetes is a temporary condition that occurs during pregnancy. It affects 2–4% of all pregnancies with an increased risk of developing diabetes for both mother and child

Glycaemia and diabetes are on the rise globally and are driven by population growth, ageing and an increasing age-specific prevalence. Effective preventive interventions are essential, and health systems should prepare to sufficiently detect and manage diabetes and its sequel. To attain optimal control, patients must currently monitor their blood glucose levels. This requires a patient to obtain a small sample of blood, usually via a finger prick. Blood is placed onto a sensor test strip that is then read by a handheld electronic reader, which reports the blood glucose concentration. These sensors are based on electrochemical enzymatic measurements with screen-printed electrodes that provide rapid and accurate measurements of blood glucose without the need for laboratory analysis. However, there are limitations to this approach including painful sampling; analyses cannot be performed if the patient is otherwise occupied (e.g., sleeping); and large fluctuations between sampling intervals can be missed.[20] To facilitate the resolution of inherent problems with discrete blood glucose measurement, new commercial products focus on continuous glucose interrogation. Early stage nanotechnology and nanomedical research involving nanosensors and nanomaterials is also focussed on continuous monitoring.

2.4.1.1. Brief history of electrochemical glucose biosensor

The first glucose biosensor was fabricated by entrapping a layer of glucose oxidase (GO_x) within a semipermeable dialysis membrane on an oxygen electrode. The amount of consumed oxygen in the enzyme-catalyzed reaction was proportional to the concentration of glucose:

$$\text{glucose} + O_2 \xrightarrow{GOx} \text{gluconic acid} + H_2O_2 \quad (1)$$

To measure consumed oxygen, a negative potential was applied to the platinum cathode and the reduced form of oxygen was evaluated:

$$O_2 + 4H^+ + 4\,e^- \rightarrow 2H_2O \qquad (2)$$

This discovery prompted further research in field of biosensors. Efforts to develop and improve glucose sensors have been made over the last five decades since Clark and Lyons reported the first enzyme electrode in 1962.[5] Updike and Hicks[21] further developed this principle by using dual oxygen working electrodes (one was coated with enzymes) and measuring the differential current in order to correct for the oxygen background variation in samples. In 1973, Guilbault and Lubrano[22] described an enzyme electrode for the measurement of blood glucose that was based on the amperometric (anodic) monitoring of the hydrogen peroxide product

$$H_2O_2 \rightarrow O_2 + 2H^+ + 2e^- \qquad (3)$$

The resulting biosensor offered good accuracy and precision when tested with 100 µL blood samples. During the 1980‟s, biosensors became a „hot‟ topic; reflecting a growing emphasis on biotechnology. Considerable efforts during this decade focused on the development of mediator-based „second-generation‟ glucose biosensors;[23] the introduction of commercial screen-printed strips for self-monitoring of blood glucose;[24] and use of modified electrodes and

tailored membranes/coatings for enhancing sensor performance.[25] In the 1990s, we witnessed extensive activity directed toward the establishment of electrical communication between the redox center of GO_x and the electrode surface.[26-28] Of particular note is the work of Heller, who introduced the use of a flexible polymer with osmium redox sites.[26] During this period, we also witnessed the development of minimally invasive subcutaneously implantable devices.[29]

Figure 2.4 summarizes various generations of amperometric glucose biosensors based on different mechanisms of electron transfer, including the use of natural secondary substrates, artificial redox mediators, or direct electron transfer. Although substantial progress has been made on the electronic coupling of GO_x, further improvements in the charge transport between its FAD redox center and electrodes are desired.

2.4.1.2. First generation glucose biosensor

First-generation glucose biosensors relied on the use of the natural oxygen co-substrate and generation and the detection of hydrogen peroxide (eqs 1 and 3). The biocatalytic reaction involves reduction of the flavin group (FAD) in the enzyme by reaction with glucose to give the reduced form of the enzyme ($FADH_2$). Then, the flavin may be re-oxidized by molecular oxygen to regenerate the oxidized form of the enzyme GO_x (FAD). Hydrogen peroxide gets reduced as a product of this reaction. Measurements of peroxide formation have the advantage of being simpler, especially when miniaturized devices are concerned.

2.4.1.2.1. Electroactive Interferences

The measurement of hydrogen peroxide at high voltage in a glucose sensor is subject to interference from electroactive species in blood. Electrochemical interferents in blood can cause

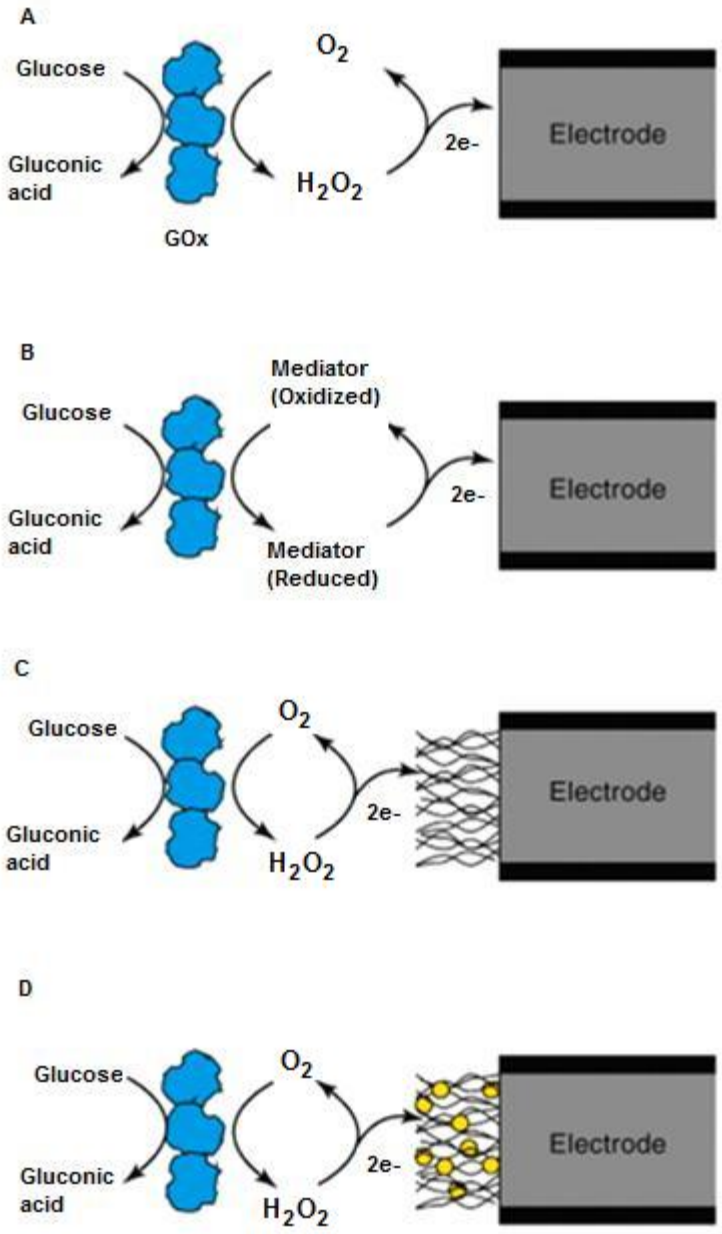

Figure 2.4. Standard GOx-based electrochemical biosensors (A, B) use a GO_x layer to recognize glucose and generate an electrochemical signal. This signal is transferred from the enzyme through O_2 reduction to H_2O_2 (A: first generations sensors) or the reduction of another chemical mediator (B: second generation sensors). Nanomaterials can be incorporated into these sensors to increase surface area, improve catalytic action, modify operating parameters and improve electron transfer from the enzyme to the electrode. This can be accomplished through the use of single types of nanomaterials (C: single-nanomaterial sensors) such as CNTs, or nanocomposites consisting of multiple nanomaterials working together (D: nanocomposite sensors).[30]

a false high glucose reading by donating non-glucose-derived electrons. A list of suggested "standard" interferents, developed by the FDA, is shown in Table 1.1, along with interferent concentrations obtained from the National Center for Clinical Laboratory Standards. (NCCLS Guideline EP7-P, Interference Testing in Clinical Chemistry). Strips are tested at low glucose concentrations, with and without the specified interferents, in order to determine the signal increment due to interferents. From the compounds listed in Table 1.1, those most likely to electrochemically interfere are ascorbate, acetaminophen, and urate. One useful avenue in diminishing electroactive interferences is to employ a permselective coating that minimizes the access of these constituents toward the electrode surface. Different polymers, multilayers, and mixed layers with transport properties based on charge, size, or polarity have thus far been used for blocking coexisting electroactive compounds.[12, 31-34]

Such films also exclude surface-active macromolecules, hence protecting the surface and imparting higher stability. Electropolymerized films, particularly poly(phenylendiamine), polyphenol, and overoxidized polypyrrole, have been shown to be extremely useful in imparting high selectivity (by rejecting interferences based on size exclusion) while confining GO_x onto the surface.[31] The electropolymerization process makes it possible to generate coatings on extremely small surfaces with complex geometries, although the resulting films often have limited stability for in vivo work. Other commonly used coatings include size-exclusion cellulose acetate films,[12] the negatively charged (sulfonated) Nafion or Kodak AQ ionomers,[33] and hydrophobic alkanethiol or lipid layers.[34] Use of overlaid multilayers, which combines the properties of different films, offers additional advantages. For example, the alternate deposition of Nafion and cellulose acetate has been used to eliminate the interference of the neutral acetaminophen and negatively charged ascorbic and uric acids, respectively.[35]

Table 2.1 List of Potential Electrochemical Interferents[a]

interferent	suggested test level (mg/dL)	ref
Acetaminophen	20	1
salicylic acid	50	1
tetracycline	4	1
dopamine	13	1
ephedrine	10	2
ibuprofen	40	1
l-DOPA	5	3
methyl-DOPA	2.5	1
tolazamide	100	2
Tolbutamide	100	1
ascorbic acid	3	1
bilirubin (unconjugated)	20	1
cholesterol	500	1
creatinine	30	1
triglycerides	3000	1
urate	20	1

[a] (1) From NCCLS Document EP7-P; (2) Calculated assuming that the drug, at 10 times the dosage rate, becomes promptly available in 5 L of blood. (3) 10 times the maximum plasma concentration.[36]

Another approach to minimize the interferents effect is to detect the released hydrogen peroxide at the optimal operating potential (+0.0 to -0.20 V vs Ag/AgCl) where contributions from easily oxidizable interfering substances are eliminated.[37] Remarkably high selectivity, coupled with a fast and sensitive response has thus been obtained. In particular, Prussian-Blue (PB; ferric−ferrocyanide) modified electrodes have received considerable attention owing to their very strong and stable electrocatalytic activity.[37-40] Prussian-Blue offers a substantial lowering of the overvoltage for the hydrogen peroxide redox process and hence permits highly selective biosensing of glucose at a very low potential (-0.1 V vs Ag/AgCl). The high catalytic activity of PB leads also to a very high sensitivity toward hydrogen peroxide. Further improvements in the stability and selectivity of PB-based hydrogen peroxide transducers can be

obtained by electropolymerizing a non-conducting poly(1,2-diaminobenzne) permselective coating on top of the PB layer.[39] A glucose nanosensor, based on the co-deposition of PB and GOx on a carbon-fiber nanoelectrode, has also been reported.[40] PB-based carbon inks were developed for fabricating electrocatalytic screen-printed glucose biosensors.[38]

2.4.1.3. Second generation glucose biosensor

Since first generation glucose biosensors rely on the use of oxygen as the physiological electron acceptor, they are subject to errors resulting from fluctuations in oxygen tension and the stoichiometric limitation of oxygen. These errors include changes in sensor response and a reduced upper limit of linearity. Further improvements and solutions to the aforementioned drawbacks may be obtained by replacing the oxygen with a non-physiological (synthetic) electron acceptor that is capable of shuttling electrons from the redox center of the enzyme to the surface of the electrode. The transfer of electrons between the GO_x active site and the electrode surface is the limiting factor in the operation of amperometric glucose biosensors. Glucose oxidase does not directly transfer electrons to conventional electrodes because of a thick protein layer that surrounds its flavin adenine dinucleotide (FAD) redox center, thus introducing an intrinsic barrier to direct electron transfer. Accordingly, different innovative strategies have been suggested for establishing and tailoring the electrical contact between the redox centers of GO_x and electrode surfaces. Use of non-physiological electron acceptors,[41] wired enzyme electrodes, [42] modification of GO_x with electron relays[26] and nanomaterial connectors are some of the approaches. Among them, nanomaterials have been of more interest due to their unique and controllable properties.

2.4.1.3.1. Nanomaterial connectors

A defining characteristic of nanomaterials is that they have at least one structural dimension of the order of 100 nm or less.[43] Nanomaterials and nanosensors offer some significant advantages owing to their small size. High surface area/volume ratios (allowing larger signals, better catalysis and the more rapid movement of analytes through sensors), as well as enhanced optical properties (quantum dot fluorescence, gold nanoparticle quenching, surface-enhanced Raman scattering (SERS)) represent significant benefits over macroscale materials. Researchers have used these properties to improve the accuracy, size, lifetime and usability of sensors for the treatment of diabetes. Nanosensors are finally nearing the stages of commercial and clinical implementation, which will hopefully allow better treatment for patients suffering from diabetes in the future.

The most common application of nanotechnology for sensors in diabetes is the use of nanomaterials to assist the standard enzymatic electrochemical detection of glucose. The incorporation of nanomaterials into these sensors offers a variety of advantages including increased surface area; more efficient electron transfer from enzyme to electrode; and the ability to include additional catalytic steps. Although a detailed discussion of all possible modifications to standard electrodes would be prohibitively long, we highlight recent advances that demonstrate the range of options for nanomaterials in glucose sensors.

Carbon nanotube (CNT) incorporation is a heavily investigated modification to the enzymatic electrode detection of glucose, partly because of the electron transfer capabilities of CNTs as well as their large surface areas. The electrode can be replaced with a highly porous nanofiber onto which glucose oxidase is immobilized.[44] This structure has a much higher

electronic surface area than do bulk metal electrodes and accordingly, may immobilize more enzymes and generate larger signals. Another approach is to modify the nanotubes with an electrochemical mediator such as ferrocene to improve the electron transfer between the enzyme and electrode.[45]

CNTs can be coupled with other nanomaterials or polymers to form nanocomposites for glucose detection. Combining CNTs with additional nanomaterials improves aspects such as catalytic activity. Nanocomposite membranes have recently been fabricated with the layer-by-layer assembly of CNTs and gold nanoparticles.[37, 46] Similar approaches have also coupled CNTs with metal nanoparticles of silver,[47] platinum,[48] as well as non-metals such as silica.[49]

A variety of nanostructured electrodes can improve conventional macrostructured electrodes. Zinc oxide deployed as nanotube arrays[50] has been used for glucose detection. Nanowire arrays fabricated from ruthenium[51] and gold[52] have an increased surface area and improved electrochemical interrogation compared with conventional electrodes. In addition to creating nanoscale features on the surface of the electrode, nanostructures can be generated with nanoparticles. Gold,[37] platinum,[53] and palladium[54] nanoparticles have been used in membranes to enhance electron transfer and increase the surface area of the sensor.

Magnetic nanoparticles, commonly made from iron oxide, have also been used for glucose sensors.[55-56] The magnetic nature of these nanoparticles simplifies the assembly of GO_x-labeled nanoparticles onto the electrode,[55] as well as enabling the formation of nanoparticle comprised conductive wires on the electrode surface.[56] In both of these examples, the nanoparticles were attracted to the electrode surface using magnetic fields, which highlights one advantage in using magnetic nanoparticles in the fabrication of nanoparticle electrode assemblies.

Nanostructured polymers can improve the development of glucose sensors. Hollow spheres of conductive polymers can be used to transfer electrons from GO_x to the electrode.[57] Conductive polymer electrodes can be used in a method similar to other nanostructured surfaces, where GO_x is immobilized directly on the modified electrode. In one example, the electrode surface was covered with highly ordered polyaniline nanotubes, which had GO_x immobilized within the tubes.[58] The use of polymers introduces a range of different electrochemical properties, including operation at varying potentials. The use of different potentials helps to minimize electrochemical interference from common electroactive compounds in blood (e.g., acetaminophen, ascorbic acid and uric acid), which can cause non-specific signals with standard electrochemical detection approaches.

Coupling biological recognition elements with electrochemistry increases the selectivity and sensitivity of sensors and explains both the popularity of this approach and the commercial success of sensors that are based on proteins. Despite these advantages, there are several drawbacks to sensors based on biological recognition, including intrinsically poorer stability in comparison with non-biological systems. As a result of this limitation, many research groups have focused on the development of glucose detection assays that do not rely on a protein for recognition and as a result, could have longer storage lifetimes.

One of the most heavily researched areas in relation to non-enzymatic glucose sensors is the detection of glucose oxidation directly at an electrode. However, this method also has several limitations such as slow reaction kinetics and the need for a large applied potential, which decreases specificity.[59] Nanomaterials have helped to overcome these limitations and thereby

allowed the development of direct oxidation glucose sensors as replacements for biological recognition sensors.

Nanomaterial-based sensors can also be designed to detect glucose through changes in pH or charge, often through a field effect transistor (FET). These devices measure a property of the nanomaterial (such as conductance) that is affected by charges near the surface of the sensor or the pH of the solvent. As the concentration of glucose changes, the charge near the surface or the pH changes either as a result of enzymatic reactions or competitive binding, causing the sensor to register a change in the measured property. This allows for the indirect quantification of glucose concentration, although pH changes in the bulk solution can affect the measured response.

The breakdown of glucose catalyzed by GO_x decreases solution pH by liberating hydrogen ions and generates negative charges by producing the gluconate ion. Risveden and colleagues used a region-selective ion-sensitive field effect transistor (RISFET) to detect gluconate generation to quantify glucose concentrations. The RISFET focuses the gluconate between the sensing electrodes, whereby an increase in current is proportional to the amount of glucose present. The layer-by-layer assembly of CNTs with GO_x allows the change in pH generated by glucose degradation to be monitored by measuring the conductance changes in the CNT layer.[60] Modified nanoparticles can also improve the sensitivity of capacitive electrolyte-insulator-semiconductor (EIS) structures. The use of gold nanoparticles modified with both GO_x and ferrocene improved sensitivity nearly two-fold over nanoparticles modified with only GO_x.[61] In addition to using GO_x to recognize glucose, other proteins such as concanavalin A (ConA), a plant lectin that binds polysaccharide, can be used in FET detection platforms. A CNT-based FET labelled with the polysaccharide dextran has been shown to detect a change in resistance

upon binding, or in the presence of glucose, the displacement of ConA with picomolar detection limits.[62]

2.4.1.4. Third generation glucose biosensor

Ultimately, one would like to eliminate the mediator and develop a reagentless glucose biosensor with a low operating potential, close to that of the redox potential of the enzyme. In this case, the electron is transferred directly from glucose to the electrode via the active site of the enzyme. The absence of mediators, which is the main advantage of new generations of biosensors, may lead to very high selectivity (owing to the very low operating potential). However, as discussed earlier, critical challenges must be overcome for the successful realization of this direct electron-transfer route owing to the spatial separation of the donor−acceptor pair. Efficient direct electron transfer at conventional electrodes has been reported for only a few redox enzymes. There are mixed reports in the literature regarding the direct (mediatorless) electron transfer catalyzed by GO_x.[63] Although several papers claim such direct electron transfer between GO_x and the electrode, only a few provide a sufficient level of proof for such mediatorless detection. Unsuccessful efforts in obtaining direct electron transfer of GO_x at conventional electrodes has led to the exploration of new electrode materials. Optimally designed electrode configuration must ensure that the electron-transfer distance between the immobilized protein and the surface is made as short as possible. One route for creating third-generation amperometric glucose biosensors is to use conducting organic salt electrodes based on charge-transfer complexes such as tetrathiafulvalene-tetracyanoquinodimethane (TTF-TCNQ).[64-65] Different electron-transfer mechanisms at TTF-TCNQ electrodes have been proposed by different authors, and the precise mechanism of GO_x catalysis remains controversial. Khan et al. described a third-generation amperometric glucose sensor based on a stable charge-transfer

complex electrode.[65] The device relied on the growing tree-shaped crystal structure of TTF-TCNQ. The authors claimed that the close proximity and favorable orientation of the enzyme at the crystal surface allowed for the direct oxidation of the enzyme and selective glucose measurements at 0.1 V (vs Ag/AgCl), although they did not furnish convincing evidence for such direct electron transfer. Mediatorless third-generation glucose biosensors based on the GO_x/polypyrrole system were suggested by Yabuki and Koopal.[15, 66] However, the relatively high anodic potential of this system (vs the redox potential of FAD/$FADH_2$, -0.44 V) suggests the possibility of electron transfer mediated by oligomeric pyrroles present on the surface. Recently developed, oxidized boron-doped diamond electrodes have indicated some promise for mediator-free glucose detection based on direct electron transfer.[67]

2.4.1.5. Continuous glucose monitoring

The traditional monitoring of blood glucose uses discrete blood sampling time points during the course of a day. For many diabetics this provides satisfactory data for the control of blood glucose levels. However, current technology for continuous glucose monitoring has some disadvantages that have prevented its widespread adoption for the management of diabetes. All FDA approved devices are implanted sensors, which have a maximum useful lifetime of several days to a week (partially because the immune system responds to the sensor as a foreign body). Because they are implanted in subcutaneous tissue, these sensors do not directly sample blood, and this can lead to a lag time in measurements taken during periods of rapid concentration changes. This lag time has been estimated to be from several minutes to nearly 30 minutes. Additionally, current sensors must be calibrated and checked against standards because they are only approved for tracking trends in blood glucose levels. Finally, current sensors are expensive

and are not always covered by health insurance plans, therefore this technology has not been widely adopted.[30]

2.4.1.5.1. Requirements

The major requirements of clinically accurate in vivo glucose sensors have been discussed in several review articles.[29, 68] The ideal sensor would be one that provides reliable real-time continuous monitoring of all blood glucose variations throughout the day with high selectivity and speed over extended periods under harsh conditions. The challenges for meeting these demands include rejection of the sensor by the body, miniaturization, long-term stability of the enzyme and transducer, oxygen deficit, in vivo calibration, short stabilization times, baseline drift, safety, and convenience. The sensor must be of a very tiny size and proper shape that allows for easy implantation and results in minimal discomfort. Last but not least, is the formulation of workable strategies for powering of an autonomous sensor-transmitter system. Reducing the size of the power source (e.g., biofuel cell, battery) remains a major challenge.

Undesirable interactions between the surface of the implanted device and the biological medium can cause the deterioration of sensor performance upon implantation, and has proved to be the major barrier in the development of reliable in vivo glucose probes. Such adverse effects include the effect of the sensor upon the host environment, as well as the effect of the physiological environment on sensor performance. In blood, the major source of complication arises from the surface fouling of the electrode via proteins and coagulation composites, leding to the risk of thromboembolism. Due to this severe blood-induced biofouling, which suppresses the glucose response, most glucose biosensors lack the capacity for the sustained biocompatibility that is necessary for reliable and prolonged operation in whole blood. The

danger of thrombus formation is another major concern (health risk) that hinders the implementation of sensors that are implanted for access to the blood. Accordingly, the majority of sensors that are being developed for continuous glucose monitoring do not measure blood glucose directly.

Alternative sensing sites, particularly the subcutaneous tissue, have thus received growing attention. The subcutaneous tissue is minimally invasive and its glucose level reflects the glucose concentration of the blood. However, such subcutaneous implantation generates a wound site that experiences an intense localized inflammatory reaction. The inflammatory response that is associated with wound formation is characterized with problems such as scar tissue formation accompanied by the adhesion of bacteria and macrophages, which can distort the glucose concentration in the immediate vicinity of the sensor.[69] The extent of this inflammatory response is dependent upon various factors, including the shape, size, and rigidity of the sensor, as well as its physical and chemical composition.

Recent approaches for the design of more biocompatible in vivo glucose sensors have focused on the preparation of interfaces that resist biofouling. These include the controlled release of nitric oxide (NO),[13, 69] protecting the outer surface with polymeric coatings (such as polyethylene glycols, polyethylene oxides, or the perfluorinated ionomer Nafion) that exhibit low protein adsorption,[70-72] or co-immobilization of the anticoagulant heparin.[73] The former is attributed to the discovery that NO is an effective inhibitor of platelet and bacterial adhesion. Such NO-release glucose sensors were prepared by doping the outer polymeric membrane coating of previously reported needle-type electrochemical sensors with suitable lipophilic diazeniumdiolate species[72] or diazeniumdiolate-modified sol−gel particles.[13] Histological examination of the implant site demonstrated a significant decrease in the inflammatory

response. Similarly, poly(ethylene glycol) (PEG) containing polymers are among the least protein absorbing. Quinn et al. reported on a glucose permeable hydrogel based on crosslinking an eight-armed amine-terminated PEG derivative with a di-succinimidyl ester of a dipropionic acid derivative of PEG.[71] The gel was evaluated as a biocompatible interface between an amperometric glucose microsensor and the subcutaneous tissue of a rat. Very few adherent cells were observed after seven days.

A key issue is the maintenance of calibration over a period of several days. The calibration process should be repeated during implantation to account for variations in sensitivity. A calibration-free operation is the ultimate goal, but this would require a detailed understanding of the sensitivity changes along with highly reproducible devices.

2.4.2. Cholesterol biosensor

The assertion that elevated plasma cholesterol concentrations may lead to an increased chance of developing either atherosclerosis or coronary heart disease (CHD) is now long established[74] and has become a central tenet of the "lipid hypothesis". The need to limit dietary fat and cholesterol intake was recognised by the UK government in the 1992 Health of The Nation Report,[75] and in the United States from the recommendations of the National Research Council.[76] Nevertheless, the role of cholesterol remains controversial. It is not yet clear whether cholesterol is a causal agent for inducing atherosclerosis, or if it is the primary exacerbating factor in the formation of foam cells after initial artery wall injury via some other means. The requirement for the accurate determination of serum cholesterol has, as a consequence, stimulated a large amount of work on the development of methods for its assay that are fast enough for routine assay, whilst simple and reproducible. Serum cholesterol analysis is currently

generally accomplished by using a three-enzyme assay and indicator method as originally devised by Richmond et al.[77] Since ≈70% of the cholesterol present in serum samples is esterified, a typical assay for total serum cholesterol usually begins with the incubation of serum with cholesterol esterase in order to isolate free cholesterol, which is amenable to oxidation with cholesterol oxidase. A peroxidase enzyme subsequently reduces the hydrogen peroxide that is produced when one molecule of cholesterol is oxidized. Oxidation of an indicator molecule in turn reactivates the peroxidase and produces a chromogen, which when measured, facilitates the indirect estimation of total serum cholesterol.

Several versions of this procedure exist[14] and the separation of these steps has been found to give a better test accuracy than a one-step procedure.[78] However, only a few cholesterol biosensors have been successfully commercially launched. One of the reasons for this originates from the optimization of critical parameters, such as enzyme stabilization, quality control and instrumentation design. The cholesterol biosensor must be easy to use, self-testing, fast response and portable, etc. Further, the proper marketing of the product is essential for attracting the attention of potential users. Increased understanding of immobilized bioreagents, improved immobilization techniques and technological advances in microelectronics are likely to speed up the commercialization of a much needed cholesterol biosensor.

2.5. Conclusion and perspectives

Applications of biosensors to address practical problems are related to health, food, or energy supply. A variety of methodologies are envisaged to expand the area of biosensors to additional analytical tasks. For example, the development of new biosensors may be seen as essential to solving the inherent difficulties of a variety of challenging in situ and in vivo

analyses. Although other types of biosensors exist; in all cases, an important challenge that remains is the miniaturization of biosensors, which imparts dual advantages: (i) limits the amount of immobilized enzyme, and (ii) yields tools for direct use and possible implantation in living tissues. The increased integration of biological materials within these patterned structures may be accomplished through the use of nanostructures. Subsequently, very promising pathways toward the development of "ideal" amperometric biosensors have been opened.

References

1. Turner, A. P. F.; Karube, I.; Wilson, G. S., *Biosensors, Fundamentals and Applications*. Oxford University Press: Oxford, 1987.

2. Hiep, H. M.; Endo, T.; Kerman, K.; Chikae, M.; Kim, D.-K.; Yamamura, S.; Takamura, Y.; Tamiya, E., A Localized surface Plasmon Resonance Based Immunosensor for the Detection of Case in Milk *Sci. Technol. Adv. Mater.* **2007,** *8*, 331-338.

3. Fan, F.; Binkowski, B. F.; Butler, B. L.; Stecha, P. F.; Lewis, M. K.; Wood, K. V., Novel Genetically Encoded Biosensors Using Firefly Luciferase. *ACS Chem. Biol.* **2008,** *3*, 346-351.

4. Lud, S. Q.; Nikolaides, M. G.; Haase, I.; Fischer, M.; Bausch, A. R., Field Effect of Screened Charges: Electrical Detection of Peptides and Proteins by a Thin-Film Resistor. *ChemPhysChem* **2006,** *7*, 379-384.

5. Clark, L. C.; Lyons, C., Electrode Systems for Continuous Monitoring in Cardiovascular Surgery. *Annal. NY Acad. Sci.* **1962,** *102*, 29-45.

6. Wollenberger, U.; Schubert, F.; Pfeiffer, D.; Scheller, F. W., Enhancing Biosensor Performance Using Multienzyme Systems. *Trend. Biotechnol.* **1993,** *11*, 255-262.

7. Thevenot, D. R.; Sternberg, R.; Coulet, P. R.; Laurent, J.; Gautheron, D. C., Enzyme Collagen Membrane for Electrochemical Determination of Glucose. *Anal. Chem.* **1979,** *51*, 96-100.

8. Aizawa, M., Principles and Applications of Electrochemical and Optical Biosensors. *Anal. Chim. Acta* **1991,** *250*, 249-256.

9. Kiefer, H.; Klee, B.; John, E.; Stierhof, Y.-D.; Jähnig, F., Biosensors Based on Membrane Transport Proteins. *Biosens. Bioelectron.* **1991,** *6*, 233-237.

10. Sugawara, M.; Hirano, A.; Rehák, M.; Nakanishi, J.; Kawai, K.; Sato, H.; Umezawa, Y., Electrochemical Evaluation of Chemical Selectivity of Glutamate Receptor Ion Channel Proteins with a Multi-Channel Sensor. *Biosens. Bioelectron.* **1997,** *12*, 425-439.

11. Guilbault, G. G., *Handbook of immobilized enzymes*. Marcel Dekker: New York, 1984.

12. Sternberg, R.; Bindra, D. S.; Wilson, G. S.; Thevenot, D. R., Covalent Enzyme Coupling on Cellulose Acetate Membranes for Glucose Sensor Development. *Anal. Chem.* **1988,** *60*, 2781-2786.

13. Shin, J. H.; Marxer, S. M.; Schoenfisch, M. H., Nitric Oxide-Releasing Sol−Gel Particle/Polyurethane Glucose Biosensors. *Analyt. Chem.* **2004,** *76*, 4543-4549.

14. Omodeo, S. F.; Marchesini, S.; Fishman, P. H.; Berra, B., A Sensitive Enzymatic Assay for Determination of Cholesterol in Lipid Extracts. *Anal. Biochem.* **1984,** *142*, 347-350.

15. Koopal, C. G. J.; de Ruiter, B.; Nolte, R. J. M., Amperometric Biosensor Based on Direct Communication between Glucose Oxidase and a Conducting Polymer Inside the Pores of a Filtration Membrane. *J. Chem. Soc. Chem.Commun.* **1991**, 1691-1692.

16. Gorton, L., *Comprehensive Analytical Chemistry Volume XLIV: Biosensors and Modern Biospecific Analytical Techniques*. Elsevier Science: 2005; p 285-327.

17. Lojou, É.; Bianco, P., Application of the Electrochemical Concepts and Techniques to Amperometric Biosensor Devices. *J. Electroceram.* **2006,** *16*, 79-91.

18. Danaei, G.; Finucane, M. M.; Lu, Y.; Singh, G. M.; Cowan, M. J.; Paciorek, C. J.; Lin, J. K.; Farzadfar, F.; Khang, Y.-H.; Stevens, G. A.; Rao, M.; Ali, M. K.; Riley, L. M.; Robinson, C. A.; Ezzati, M., National, Regional, and Global Trends in Fasting Plasma Glucose and Diabetes Prevalence Since 1980: Systematic Analysis of Health Examination Surveys and Epidemiological Studies with 370 Country-Years and 2·7 Million Participants. *Lancet* **2011,** *378*, 31-40.

19. WHO, Diabetes. **August 2011,** *Fact sheet N°312*.

20. Burge, M. R.; Mitchell, S.; Sawyer, A.; Schade, D. S., Continuous Glucose Monitoring: The Future of Diabetes Management. *Diabetes Spectrum* **2008,** *21*.

21. Updike, S. J., Hicks, G.P., The Enzyme Electrode. *Nature* **1967,** *214*, 986-988.

22. Guilbault, G. G.; Lubrano, G. J., An Enzyme Electrode for the Amperometric Determination of Glucose. *Anal. Chim. Acta* **1973,** *64*, 439-455.

23. Cass, A. E. G.; Davis, G.; Francis, G. D.; Hill, H. A. O.; Aston, W. J.; Higgins, I. J.; Plotkin, E. V.; Scott, L. D. L.; Turner, A. P. F., Ferrocene-Mediated Enzyme Electrode for Amperometric Determination of Glucose. *Anal. Chem.* **1984,** *56*, 667-671.

24. Matthews, D. R.; Bown, E.; Watson, A.; Holman, R. R.; Steemson, J.; Hughes, S.; Scott, D., Pen-Sized Digital 30-Second Blood Glucose Meter. *Lancet* **1987,** *329*, 778-779.

25. Murray, R. W.; Ewing, A. G.; Durst, R. A., Chemically Modified Electrodes. Molecular Design for Electroanalysis. *Anal. Chem.* **1987,** *59*, 379A-390A.

26. Degani, Y.; Heller, A., Direct Electrical Communication Between Chemically Modified Enzymes and Metal Electrodes. I. Electron Transfer from Glucose Oxidase to Metal Electrodes via Electron Relays, Bound Covalently to the Enzyme. *J. Phys. Chem.* **1987,** *91*, 1285-1289.

27. Xiao, Y.; Patolsky, F.; Katz, E.; Hainfeld, J. F.; Willner, I., "Plugging into Enzymes": Nanowiring of Redox Enzymes by a Gold Nanoparticle. *Science* **2003,** *299*, 1877-1881.

28. Bartlett, P. N.; Booth, S.; Caruana, D. J.; Kilburn, J. D.; Santamaría, C., Modification of Glucose Oxidase by the Covalent Attachment of a Tetrathiafulvalene Derivative. *Anal.Chem.* **1997,** *69*, 734-742.

29. Reach, G.; Wilson, G. S., Can Continuous Glucose Monitoring be Used for the Treatment of Diabetes? *Anal. Chem.* **1992,** *64*, 381A-386A.

30. Cash, K. J.; Clark, H. A., Nanosensors and Nanomaterials for Monitoring Glucose in Diabetes. *Trend. Mol. Med.* **2010,** *16*, 584-593.

31. Sasso, S. V.; Pierce, R. J.; Walla, R.; Yacynych, A. M., Electropolymerized 1,2-Diaminobenzene As A Means to Prevent Interferences and Fouling and to Stabilize Immobilized Enzyme in Electrochemical Biosensors. *Anal. Chem.* **1990,** *62*, 1111-1117.

32. Malitesta, C.; Palmisano, F.; Torsi, L.; Zambonin, P. G., Glucose Fast-Response Amperometric Sensor Based on Glucose Oxidase Immobilized in an Electropolymerized Poly(o-phenylenediamine) Film. *Anal. Chem.* **1990,** *62*, 2735-2740.

33. Moussy, F.; Jakeway, S.; Harrison, D. J.; Rajotte, R. V., In vitro and in vivo Performance and Lifetime of Perfluorinated Ionomer-Coated Glucose Sensors after High-Temperature Curing. *Anal. Chem.* **1994,** *66*, 3882-3888.

34. Wang, J.; Wu, H., Permselective Lipid Poly(o-phenylenediamine) Coatings for Amperometric Biosensing of Glucose. *Anal. Chim. Acta* **1993,** *283*, 683-688.

35. Zhang, Y.; Hu, Y.; Wilson, G. S.; Moatti-Sirat, D.; Poitout, V.; Reach, G., Elimination of the Acetaminophen Interference in an Implantable Glucose Sensor. *Anal. Chem.* **1994,** *66*, 1183-1188.

36. Bierer, D.; Quebbemann, A., Interference of Levodopa and Its Metabolites with Colorimetry of Uric Acid. *Clin. Chem.* **1981,** *27*, 756-758.

37. Ahmadalinezhad, A.; Kafi, A. K. M.; Chen, A., Glucose Biosensing Based on the Highly Efficient Immobilization of Glucose Oxidase on a Prussian Blue Modified Nanostructured Au Surface. *Electrochem. Commun.* **2009,** *11*, 2048-2051.

38. O'Halloran, M. P.; Pravda, M.; Guilbault, G. G., Prussian Blue Bulk Modified Screen-Printed Electrodes for H_2O_2 Detection and for Biosensors. *Talanta* **2001,** *55*, 605-611.

39. Lukachova, L. V.; Kotel'nikova, E. A.; D'Ottavi, D.; Shkerin, E. A.; Karyakina, E. E.; Moscone, D.; Palleschi, G.; Curulli, A.; Karyakin, A. A., Electrosynthesis of Poly-o-Diaminobenzene on the Prussian Blue Modified Electrodes for Improvement of Hydrogen Peroxide Transducer Characteristics. *Bioelectrochemistry* **2002,** *55*, 145-148.

40. Zhang, X.; Wang, J.; Ogorevc, B.; Spichiger, U. E., Glucose Nanosensor Based on Prussian-Blue Modified Carbon-Fiber Cone Nanoelectrode and an Integrated Reference Electrode. *Electroanalysis* **1999,** *11*, 945-949.

41. Shichiri, M.; Yamasaki, Y.; Kawamori, R.; Hakui, N.; Abe, H., Wearable Artificial Endocrine Pancreas with Needle-Type Glucose Sensor. *Lancet* **1982,** *320*, 1129-1131.

42. Pishko, M. V.; Katakis, I.; Lindquist, S.-E.; Ye, L.; Gregg, B. A.; Heller, A., Direct Electrical Communication between Graphite Electrodes and Surface Adsorbed Glucose Oxidase/Redox Polymer Complexes. *Angew. Chem. Int. Ed. Eng.* **1990,** *29*, 82-84.

43. Chopra, N.; Gavalas, V. G.; Bachas, L. G.; Hinds, B. J., Functional One Dimensional Nanomaterials: Applications in Nanoscale Biosensors. *Anal. Lett.* **2007,** *40*, 2067-2096.

44. Cai, C.; Chen, J., Direct Electron Transfer of Glucose Oxidase Promoted By Carbon Nanotubes. *Anal. Biochem.* **2004,** *332*, 75-83.

45. Qiu, J.-D.; Zhou, W.-M.; Guo, J.; Wang, R.; Liang, R.-P., Amperometric Sensor Based on Ferrocene-Modified Multiwalled Carbon Nanotube Nanocomposites as Electron Mediator for the Determination of Glucose. *Anal. Biochem.* **2009,** *385*, 264-269.

46. Wang, Y.; Wei, W.; Liu, X.; Zeng, X., Carbon Nanotube/chitosan/Gold Nanoparticles-Based Glucose Biosensor Prepared by A Layer-By-Layer Technique. *Mater. Sci. Eng. C* **2009,** *29*, 50-54.

47. Lin, J.; He, C.; Zhao, Y.; Zhang, S., One-Step Synthesis of Silver Nanoparticles/Carbon Nanotubes/Chitosan Film and Its Application in Glucose Biosensor. *Sens. Actuat. B: Chem.* **2009,** *137*, 768-773.

48. Wen, Z.; Ci, S.; Li, J., Pt Nanoparticles Inserting in Carbon Nanotube Arrays: Nanocomposites for Glucose Biosensors. *J. Phys.Chem. C* **2009,** *113*, 13482-13487.

49. Zhang, Y.; Guo, G.; Zhao, F.; Mo, Z.; Xiao, F.; Zeng, B., A Novel Glucose Biosensor Based on Glucose Oxidase Immobilized on AuPt Nanoparticle – Carbon Nanotube – Ionic Liquid Hybrid Coated Electrode. *Electroanalysis* **2010,** *22*, 223-228.

50. Kong, T.; Chen, Y.; Ye, Y.; Zhang, K.; Wang, Z.; Wang, X., An Amperometric Glucose Biosensor Based on the Immobilization of Glucose Oxidase on the ZnO Nanotubes. *Sens. Actuat B: Chem.* **2009,** *138*, 344-350.

51. Chi, B.-Z.; Zeng, Q.; Jiang, J.-H.; Shen, G.-L.; Yu, R.-Q., Synthesis of Ruthenium Purple Nanowire Array for Construction of Sensitive and Selective Biosensors for Glucose Detection. *Sens. Actuat. B: Chem.* **2009,** *140*, 591-596.

52. Liu, Y.; Zhu, Y.; Zeng, Y.; Xu, F., An Effective Amperometric Biosensor Based on Gold Nanoelectrode Arrays. *Nanoscale Res. Lett.* **2008,** *4*, 210 - 215.

53. Li, C.-T., Detection of Block Artifacts for Digital Forensic Analysis Forensics in Telecommunications, Information and Multimedia. Sorell, M., Ed. Springer Berlin Heidelberg: 2009; Vol. 8, pp 173-178.

54. Santhosh, P.; Manesh, K. M.; Uthayakumar, S.; Komathi, S.; Gopalan, A. I.; Lee, K. P., Fabrication of Enzymatic Glucose Biosensor Based on Palladium Nanoparticles Dispersed onto Poly(3,4-ethylenedioxythiophene) Nanofibers. *Bioelectrochemistry* **2009,** *75*, 61-66.

55. Luo, L.; Li, Q.; Xu, Y.; Ding, Y.; Wang, X.; Deng, D.; Xu, Y., Amperometric Glucose Biosensor Based on $NiFe_2O_4$ Nanoparticles and Chitosan. *Sens. Actuat. B: Chem.* **2010,** *145*, 293-298.

56. Jimenez, J.; Sheparovych, R.; Pita, M.; Narvaez Garcia, A.; Dominguez, E.; Minko, S.; Katz, E., Magneto-Induced Self-Assembling of Conductive Nanowires for Biosensor Applications. *J. Phys. Chem. C* **2008,** *112*, 7337-7344.

57. Santhosh, P.; Manesh, K. M.; Uthayakumar, S.; Gopalan, A. I.; Lee, K. P., Hollow Spherical Nanostructured Polydiphenylamine for Direct Electrochemistry and Glucose Biosensor. *Biosens. Bioelectron.* **2009,** *24*, 2008-2014.

58. Wang, Z.; Liu, S.; Wu, P.; Cai, C., Detection of Glucose Based on Direct Electron Transfer Reaction of Glucose Oxidase Immobilized on Highly Ordered Polyaniline Nanotubes. *Anal. Chem.* **2009,** *81*, 1638-1645.

59. Shamsipur, M.; Najafi, M.; Hosseini, M.-R. M., Highly Improved Electrooxidation of Glucose at a Nickel(II) Oxide/Multi-Walled Carbon Nanotube Modified Glassy Carbon Electrode. *Bioelectrochemistry* **2010,** *77*, 120-124.

60. Dongjin, L.; Tianhong, C., Layer-by-Layer Self-Assembled Single-Walled Carbon Nanotubes Based Ion-Sensitive Conductometric Glucose Biosensors. *Sens. J., IEEE* **2009,** *9*, 449-456.

61. Gun, J.; Schöning, M. J.; Abouzar, M. H.; Poghossian, A.; Katz, E., Field-Effect Nanoparticle-Based Glucose Sensor on a Chip: Amplification Effect of Coimmobilized Redox Species. *Electroanalysis* **2008,** *20*, 1748-1753.

62. Cella, L. N.; Chen, W.; Myung, N. V.; Mulchandani, A., Single-Walled Carbon Nanotube-Based Chemiresistive Affinity Biosensors for Small Molecules: Ultrasensitive Glucose Detection. *J. Am. Chem.Soc.* **2010,** *132*, 5024-5026.

63. Ghindilis, A. L.; Atanasov, P.; Wilkins, E., Enzyme-catalyzed Direct Electron Transfer: Fundamentals and Analytical Applications. *Electroanalysis* **1997,** *9*, 661-674.

64. Albery, W. J.; Bartlett, P. N.; Craston, D. H., Amperometric Enzyme Electrodes: Part II. Conducting Salts as Electrode Materials for the Oxidation of Glucose Oxidase. *J. Electroanal. Chem. Interfacial Electrochem.* **1985,** *194*, 223-235.

65. Khan, G. F.; Ohwa, M.; Wernet, W., Design of a Stable Charge Transfer Complex Electrode for a Third-Generation Amperometric Glucose Sensor. *Anal. Chem.* **1996,** *68*, 2939-2945.

66. Yabuki, S.-i.; Shinohara, H.; Aizawa, M., Electro-Conductive Enzyme Membrane. *J. Chem. Soc. Chem.Commun.* **1989**, 945-946.

67. Jing, P.; He, S.; Liang, Z.; Shao, Y., Charge-Transfer Reactions at Liquid/Liquid Interfaces and Their Applications in Bioassays. *Anal. Bioanal. Chem.* **2006,** *385*, 428-432.

68. Wilson, G. S.; Gifford, R., Biosensors for Real-Time In Vivo Measurements. *Biosens. Bioelectron.* **2005,** *20*, 2388-2403.

69. Frost, M.; Meyerhoff, M. E., In Vivo Chemical Sensors: Tackling Biocompatibility. *Anal. Chem.* **2006,** *78*, 7370-7377.

70. Chapman, R. G.; Ostuni, E.; Liang, M. N.; Meluleni, G.; Kim, E.; Yan, L.; Pier, G.; Warren, H. S.; Whitesides, G. M., Polymeric Thin Films That Resist the Adsorption of Proteins and the Adhesion of Bacteria. *Langmuir* **2001,** *17*, 1225-1233.

71. Quinn, C. A. P.; Connor, R. E.; Heller, A., Biocompatible, Glucose-Permeable Hydrogel for In Situ Coating of Implantable Biosensors. *Biomaterials* **1997,** *18*, 1665-1670.

72. Gifford, R.; Batchelor, M. M.; Lee, Y.; Gokulrangan, G.; Meyerhoff, M. E.; Wilson, G. S., Mediation of In Vivo Glucose Sensor Inflammatory Response via Nitric Oxide Release. *J. Biomed. Mater. Res. A* **2005,** *75A*, 755-766.

73. Wang, J.; Chen, L.; Hocevar, S. B.; Ogorevc, B., One-Step Electropolymeric Co-Immobilization of Glucose Oxidase and Heparin for Amperometric Biosensing of Glucose. *Analyst* **2000,** *125*, 1431-1434.

74. Rose, G.; Shipley, M. J., Plasma Lipids and Mortality: A Source of Error. *Lancet* **1980,** *315*, 523-526.

75. Department of Health; Stationery Office; H.M., The Health of The Nation. 1992.

76. NRC, Diet and health implications for reducing chronic disease risk. 1989.

77. Richmond, W., Preparation and Properties of a Bacterial Cholesterol Oxidase from Nocardia sp. and Its Application to Enzyme Assay of Total Cholesterol in Serum. *Clin. Chem.* **1973,** *19*, 1350-1356.

78. Filippova, N.; Rodionov, I.; Ugarova, N. N., The Chemiluminescent Determination of Cholesterol. *Lab Delo* **1991,** *9*, 20-23.

Chapter 3

Materials and Methods

3.1. Introduction

In the previous chapters, we presented an overview of the biosensor, its applications, the issues that the current biosensing systems encountered, along with the objectives of this dissertation. In this chapter, the main experimental methodology and techniques employed in this research project will be described briefly.

3.2. Experimental

3.2.1. Materials

Glucose oxidase (EC 1.1.3.4, Type VII from Aspergillus Niger) and D-glucose were purchased from Sigma and used as received. Chitosan was purchased from Aldrich. $HAuCl_4$ (99.9%), $PdCl_2$ (99.9%), and $Cd(NO_3)_2$ (99.9%) from Alfa Aesar. Ferric chloride ($FeCl_3$) was purchased from Anachemia, and potassium ferricyanide (III) ($K_3Fe(CN)_6$) and ammonium formate (99.995%) from Sigma–Aldrich.

Cholesterol oxidase (from *Streptomyces* species), cholesterol esterase (from hog pancreas), cholesterol, and Triton® X-100 (t-octylphenoxypolyethoxyethanol) were purchased from Sigma, 4-cholesten-3-on from Aldrich, titanium plates (99.2%) from Alfa Aesar and lactic acid from Fluka. Horseradish peroxidase, ascorbic acid, uric acid, lactic acid, sodium phosphate dibasic and sodium phosphate monobasic were used as received from Sigma-Aldrich.

The buckypaper used in this study was produced by the High-Performance Materials Institute of Florida State University with a thickness of 0.035 mm.

Water was purified with the Nanopure® water system (18 MΩ cm) and was used to prepare all solutions and clean all materials. All experiments were performed in a 0.1 M phosphate buffer solution (PBS) with different pH values maintained with K_2HPO_4 and KH_2PO_4.

Various stock concentrations of β-D-glucose and cholesterol were prepared in 0.1M phosphate buffer, pH 7.4 and stored at 4 ºC. Glucose stock solutions were allowed to mutarotate overnight prior to use.

At least five independent trials were carried out to generate each data set obtained in each individual experiment.

3.2.2. Instruments and electrochemical experiments

Surface morphology and composition of the synthesized samples were characterized using scanning electron microscopy (SEM) (JEOL JSM 5900LV) equipped with an energy-dispersive X-ray spectrometer (EDS) (Oxford Links ISIS). Surface elemental compositions based on quantitative EDS analysis were reported in average values of readings taken at five different spots on each sample surface. The X-ray diffraction (XRD) patterns of the as-prepared samples were recorded using a XRD Philips PW 1050-3710 diffractometer with Cu Kα radiation. Field-emission scanning electron microscopy (FE-SEM) (Hitachi, SU-4800), transmission electron microscopy (TEM) (JOEL 2010F) were utilized to characterize the morphology and composition of the buckypaper. FTIR spectra were recorded using a NICOLET 8700 FTIR (Thermo Scientific, USA).

All electrochemical experiments were performed using an electrochemical workstation (CHI660B, CH instrument Inc.), connected with an in-house-built, three-electrode glass cell (30 mL). A platinum coil was used as the counter electrode and was flame-annealed before each

experiment. An Ag/AgCl (saturated KCl) electrode was used as the reference electrode. The fabricated electrodes were used as the working electrode. All measurements were conducted at room temperature (22 ± 2 °C). Figure 3.1. shows the dimention of the working, reference and counter electrodes which were consistent in all of the fabricated biosensors.

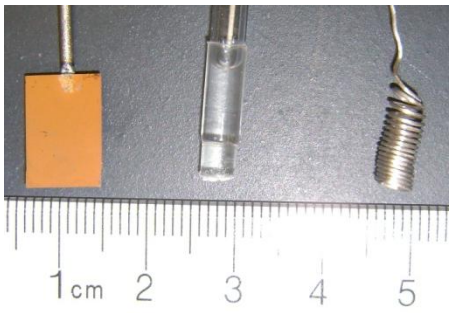

Figure 3.1. A photograph of a typical working, reference and counter electrodes.

3.2.3. Fabrication of electrodes

3.2.3.1. Biosensor fabrication

The titanium (Ti) substrate plates (~1 cm^2) were first degreased in an ultrasonic bath of acetone for 10 min. followed by 10 min. in pure water (18 MΩ). The substrates were then etched in 18% HCl at approximately 85 °C for 30 min.

The gold and palladium/cadmium nanostructure materials were synthesized by a hydrothermal method. In the hydrothermal method, the etched Ti substrates were transferred into Teflon-lined autoclaves, along with a given amount of an aqueous mixture of inorganic metal precursors and a reducing agent. The autoclaves were sealed and heated at 180 ^oC for a given period of time. The Ti plates coated with nanomaterials were dried and annealed under argon at 250 °C for 2 h.

Prussian blue (PB) was deposited onto the nanoporous Au surface by electrodeposition. This was accomplished by immersing the nanoporous Au electrode in a solution containing

$FeCl_3$ + $K_3Fe(CN)_6$ + KCl + HCl and applying a constant potential for a given period of time. Afterwards, the electrode was placed into a supporting electrolyte solution and electrochemically activated by cycling between a given ranges of potential.[1]

The buckypaper was electrochemically activated before use. To activate the buckypaper (BP) surface, cyclic voltammetry was performed in a given range of potential in a phosphate buffer solution (PBS) at pH 7.4 until a steady cyclic voltammogram was obtained, and then a potential of 1.5V was applied for 90s. This step led to the functionalization of the buckypaper with carboxlic groups. The activated surface was thus ready for the immobilization of enzymes.[2]

Titanium dioxide (TiO_2) nanowires were prepared using a H_2O vapor assisted thermal oxidation process in the presence of potassium fluoride (KF). The procedure is described briefly below. Initially, a predetermined volume of KF solution was applied to the surfaces of pre-treated Ti plates (etched in 18% HCl at 85˚C for 15 min), after which the Ti plates were transferred to a ceramic boat. The ceramic boat was next inserted into a quartz tube. After being purged with Argon for 1 h, the gas flow was switched to H_2O vapour. Subsequently, the quartz tube was heated to different temperatures (500-700˚C), which were maintained for various time periods (1-5 h), as required. After thermal treatment, the input gas was switched back to a pure Argon flow until the furnace cooled to room temperature. Finally, the as-synthesized samples were rinsed several times using distilled water to remove any residual salts from the surfaces of the samples.

In order to fabricate the carbon coated TiO_2 nanowires, the as-synthesized TiO_2 nanowire samples were inserted into a quartz tube. After being purged with Argon for 1 h, the gas was switched to ethanol vapor. The quartz tube was then heated to 600 ^oC for different periods of time. Following thermal treatment, the input gas was switched back to pure Argon until the

furnace cooled to room temperature. The electrodes used in this work were carbonized under identical optimized conditions. We followed the same procedure to activate the carbon-modified TiO_2 nanowire surface as we did for buckypaper.[2]

To immobilize the glucose oxidase (GO_x), we applied different methods (chapters 4 & 6).[1-2] briefly, a solution of the mixture of GO_x and chitosan was cast onto the nanomaterials. In another approach a mixeture of GO_x and Nafion® was prepared and the nanomaterial coated substrates dipped into the mixed solution for an optimum amount of time.

We used the multiple enzymes immobilization in cholesterol biosensor preparation. To immobilize the enzymes, a mixture of cholesterol oxidase (ChO_x), horseradish peroxidise (HRP), cholesterol esterase (ChE) and chitosan was cast onto the nanoporous Au electrode substrate.[3] All prepared biosensors were stored at 4 ºC when not in use.

To investigate the selectivity of the biosensors, we tested their response to common interfering species including ascorbic acid (AA), uric acid (UA) and acetamidophenol (AP) at their physiological concentration levels. Chronoamperometry was conducted upon the injection of each of the interference species (0.1 mM AA, 0.1 mM UA and 0.1 mM AP) followed by the glucose injections.

To fabricate enzyme free glucose sensor, glassy carbon electrodes (GC, 3 mm in diameter, CH Instruments) were polished before each experiment with alumina powder, rinsed thoroughly with doubly distilled water and ultrasonicated in 1:1 HNO_3, ethanol and water and allowed to dry at room temperature. Then, a solution of Pd-Cd nanoparticles in Nafion® (0.5% in methanol) were added on GC electrodes.

3.2.2. Real sample analysis

3.2.2.1.Measurements of cholesterol in food and supplements samples

The fabricated cholesterol biosensor was tested using real food samples. The amount of total cholesterol was measured in butter, margarine and fish oil by the fabricated biosensor. The real samples were prepared using the same procedure as the cholesterol standard solution described in chapter 5.[3] The data was collected from five samples for each product.

3.2.2.2. Measurement of glucose in human serum samples

These measurements were performed by chronoampermetry at the potential range of -0.5 to 0.3 V for 100 s in human serum samples. The human serum was derived from male AB plasma (from Sigma). Comparison tests were performed with a commercially available Blood Glucose Monitoring System with the brand name of Ultra2®. The data were collected from five samples for each concentration.

References

1. Ahmadalinezhad, A.; Kafi, A. K. M.; Chen, A., Glucose Biosensing Based on the Highly Efficient Immobilization of Glucose Oxidase on a Prussian Blue Modified Nanostructured Au Surface. *Electrochem. Commun.* **2009,** *11*, 2048-2051.

2. Ahmadalinezhad, A.; Wu, G.; Chen, A., Mediator-free Electrochemical Biosensor Based on Buckypaper with Enhanced Stability and Sensitivity for Glucose Detection. *Biosens. Bioelectron.* **2011,** *DOI: 10.1016/j.bios.2011.09.030*.

3. Ahmadalinezhad, A.; Chen, A., High-Performance Electrochemical Biosensor for the Detection of Total Cholesterol. *Biosens. Bioelectron.* **2011,** *26*, 4508-4513.

Chapter 4

Glucose Biosensing based on the Highly Efficient Immobilization of Glucose Oxidase on a Prussian blue Modified Nanostructured Au Surface*

4.1. Introduction

Certain areas of medical, food and environmental analysis require express and inexpensive monitoring methods, e.g. for glucose in blood and food.[1-3] Regarding its importance, growth in the world glucose monitoring industry is remarkable. There are many different methods to measure glucose concentrations, such as the electromagnetic technique,[4] Fluorescence spectroscopy,[5] fourier transform infrared and near infrared spectroscopy,[6,7] Raman spectroscopy,[8] NMR Spectroscopy,[9] liquid chromatography-mass spectroscopy,[10] laser diode array,[11] high performance liquid chromatography,[12] capillary and microchip electrophoresis,[13-14] polarography,[15] and the electrochemical methods.[16-17] In the area of electrochemical methods, biosensors represent an important subclass of sensors in which an electrode is used as the transduction element, and are highly qualified for meeting the size, cost and power requirement.[18] The development of electrochemical glucose biosensors was progressive in recent years.[19] Enzymatic biosensors performance is based on the electron transfer between enzyme and electrode. Moreover, enzyme-catalyzed reactions are prone to inhibition by molecules that interfere with the formation of product.[20] Indeed, in an enzymatic electrode which is usually prepared by attaching an immobilized enzyme layer to an electrochemical sensor, changes occurring as a result of the enzyme reaction can be monitored either potentiometrically or

* Most of the results presented in this chapter have been published in *Electrochemistry Communications*, **2009**, *11*, 2048.

amperometrically.[21-22] It has been also witnessed that nanoparticles are able to enhance this electron transfer process. In this regard, owing to their large surface area and strong adsorption ability for enzyme immobilization, chemical stability, low inherent toxicity (biocompatibility) and conductivity, gold nanoparticles have attracted particular interest in fabricating biosensors.[23]

Prussian blue, ferric hexacyanoferrate, often provides some sort of activated surface due to its structure which facilitates enzyme immobilisation. In fact, it is an efficient redox mediator for selective detection of H_2O_2 in the presence of oxygen and other interferents.[24-28] Prussian blue can serve as an electrocatalyst by reduction of H_2O_2 and has been applied in the construction of a large number of oxidase enzyme-based glucose biosensors.[29]

Glucose oxidase as an enzyme catalyses the oxidation of β-D-glucose to D-glucono-1,5-lactone and hydrogen peroxide, using molecular oxygen as the electron acceptor. It is a dimeric protein with a molecular weight of 160 kDa, containing one tightly bound ($K = 1\times10^{-10}$) flavin adenine dinucleotide (FAD) per monomer as cofactor. FAD functions as a coenzyme because of its ability to undergo reversible redox reactions.

In this work, a glucose biosensor based on the Gold- Prussian blue nanoparticles is fabricated with immobilization of glucose oxidase onto the surface of the electrode. Due to the mentioned characteristics of gold and Prussian blue, the resulted biosensor displayed high enfficient enzyme immobilization, high sensitivity, low detection limit, good stability and improved lifetime. Details of the preparation and characterization of the fabricated biosensor are described in this study.

4.2. Experimental

4.2.1. Materials

Glucose oxidase (EC 1.1.3.4, Type VII from Aspergillus Niger) and D-glucose were purchased from Sigma and used as received. Chitosan was purchased from Aldrich, and $HAuCl_4$ (99.9%) from Alfa Aesar. Ferric chloride ($FeCl_3$) was purchased from Anachemia, and potassium ferricyanide (III) ($K_3Fe(CN)_6$) and ammonium formate (99.995%) from Sigma–Aldrich. All other reagents were of analytical grade. Water was purified with the Nanopure® water system (18 MΩ cm) and was used to prepare all solutions and clean all materials. All experiments were performed in a 0.1 M phosphate buffer solution (PBS) with different pH values maintained with K_2HPO_4 and KH_2PO_4.

4.2.2. Glucose biosensor fabrication

The Ti substrate plates (1.25 cm × 0.80 cm × 0.5 mm) were first degreased in an ultrasonic bath of acetone for 10 min. followed by 10 min. in pure water (18 MΩ). The substrates were then etched in 18% HCl at approximately 85 °C for 30 min. The etched Ti substrates were transferred into Teflon-lined autoclaves and 10 ml of an aqueous mixture of inorganic metal precursor and a reducing agent was added. 1 M ammonium formate was used as the reducing agent and the metal precursor was 10 mM $HAuCl_4$. The autoclaves were sealed and heated at 180 ^oC for 10 h. The Ti plates coated with Au were dried and annealed under argon at 250 °C for 2 h. After cooling to room temperature, Prussian blue (PB) was deposited onto the nanoporous Au surface by electrodeposition. This was accomplished by immersing the nanoporous Au (NPAu) electrode in a solution containing 2.5 mM $FeCl_3$ + 2.5 mM $K_3Fe(CN)_6$ + 0.1 M KCl + 0.1 M HCl and applying a constant potential of +0.4 V for 4 min. Afterwards, the electrode was placed into a supporting electrolyte solution made of 0.1 M KCl + 0.1 M HCl and electrochemically activated

by cycling between a potential range of −0.05 and +0.4 V at a scan rate of 50 mV s^{-1} for 25 cycles. To immobilize the enzyme GO_x, a solution of the mixture of 20 μL of 9 mg mL^{-1} of GO_x and 10 μL of 2 mg mL^{-1} of chitosan was cast onto the PB modified nanoporous Au electrode (Ti/NPAu/PB/GO_x). Chitosan was used to enhance the stability of the biosensor [30].

For comparison, a glucose biosensor based on a PB modified Au thin film (Ti/Au/PB/GO_x) was also fabricated with the identical procedure. The Au thin film was coated onto the Ti substrate by argon plasma sputtering for 30 s. All prepared enzyme electrodes were stored at 4 °C when not in use.

4.2.3. Biosensor characterization and electrochemical measurements

The morphology and composition of the nanoporous Au materials were characterized by scanning electron microscope (SEM) (JEOL JSM 5900 LV) at an acceleration voltage of 13 kV, and an energy-dispersive X-ray (EDS) spectrometer. The cyclic voltammograms (CVs) were acquired from −0.2 V to +0.3 V at a scan rate of 10 mV/s in 50 ml of 0.1 M pH 7.0 PBS. The amperometric response of the biosensor to glucose was recorded in a stirred PBS at -0.1 V *versus* the Ag/AgCl reference electrode. All electrochemical experiments were performed at room temperature, 20 ± 2 ^{o}C.

4.3. Results and discussion

4.3.1. Characterization of the Ti/Au electrode surface

Figure 4.1A and B present a typical SEM image and EDS spectrum of the Ti/NPAu electrode, respectively, fabricated using the hydrothermal method. The SEM image reveals that nanoporous Au networks were formed and completely covered the substrate. The three-dimensional random porous structures, with diameters of tens to hundreds of nanometers, were formed by the close connection of the Au nanoparticles, with a size range of 50 to 500 nm. Only

Au peaks appear in the EDS spectrum, and no discernible carbon or oxygen signals are seen in the figure, showing that the synthesized Au-nanoporous networks are free of surface organic impurities.

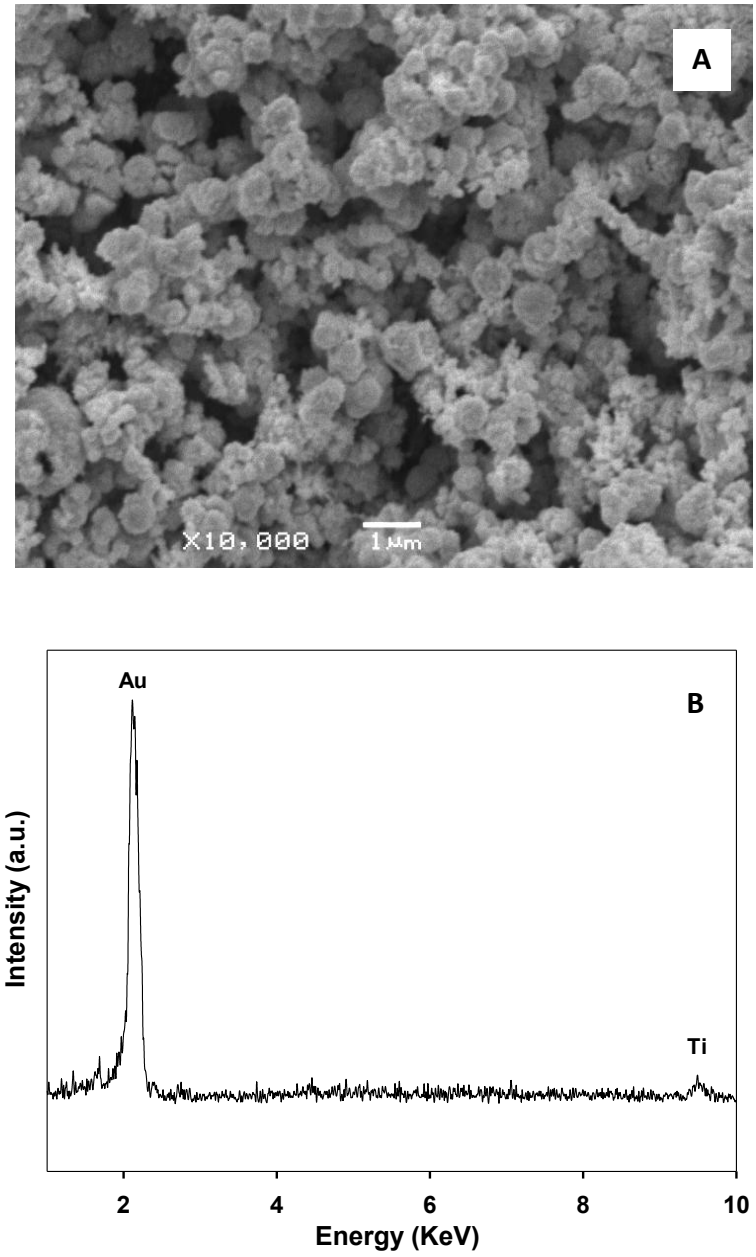

Figure 4.1. The typical SEM image of the nanoporous Au coating (A) and the corresponding EDS spectrum (B).

4.3.2. Electrochemical behaviour of the PB modified Au electrodes

Figure 4.2 displays the cyclic voltammograms of the PB modified Au electrodes recorded in a 0.1 M PBS (pH=7.0) at a scan rate of 10 mV/s. A pair of well-defined oxidation and reduction peaks are observed for the Ti/Au/PB electrode (Plot *a*).

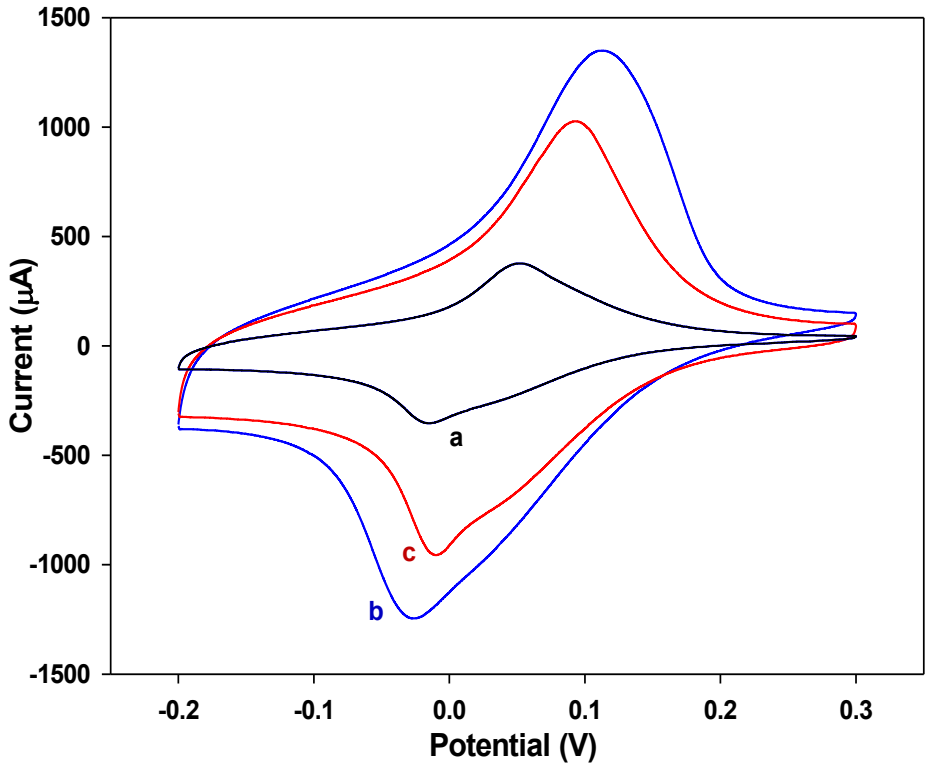

Figure 4.2. Cyclic voltammograms of the Ti/Au/PB electrode (Plot *a*), the Ti/NPAu/PB electrode (Plot *b*) and the Ti/NPAu/PB/GO_x electrode (Plot *c*) recorded in a 0.1 M PBS (pH=7.0) at a scan rate of 10 mV/s.

The anodic and cathodic peak potentials are located at +0.052 V and -0.016 V, respectively. The formal potential E^0 was calculated to be +0.018 V. The redox peaks significantly increase at the Ti/NPAu/PB electrode (Plot *b*), showing that the nanoporous Au

directly grown on the Ti substrate hydrothermally possesses a much higher surface area than the sputtered Au thin film. The oxidation and reduction peaks originate from the redox process of Prussian white ($Fe_4^{3+}[Fe^{2+}(CN)_6]_3$) and Prussian blue ($K_4Fe_4^{3+}[Fe^{2+}(CN)_6]_3$) .[31]

After we immobilized the enzyme GO_x on the Ti/NPAu/PB surface, the redox peaks decreased as seen in Plot *c*. The immobilized GO_x blocks some of the redox reaction sites, indicating the successful immobilization of GO_x on the PB modified nanoporous Au surfaces.

4.3.3. Response of the glucose biosensor

The electrochemical characterization of the biosensor was investigated by cyclic voltammetry.

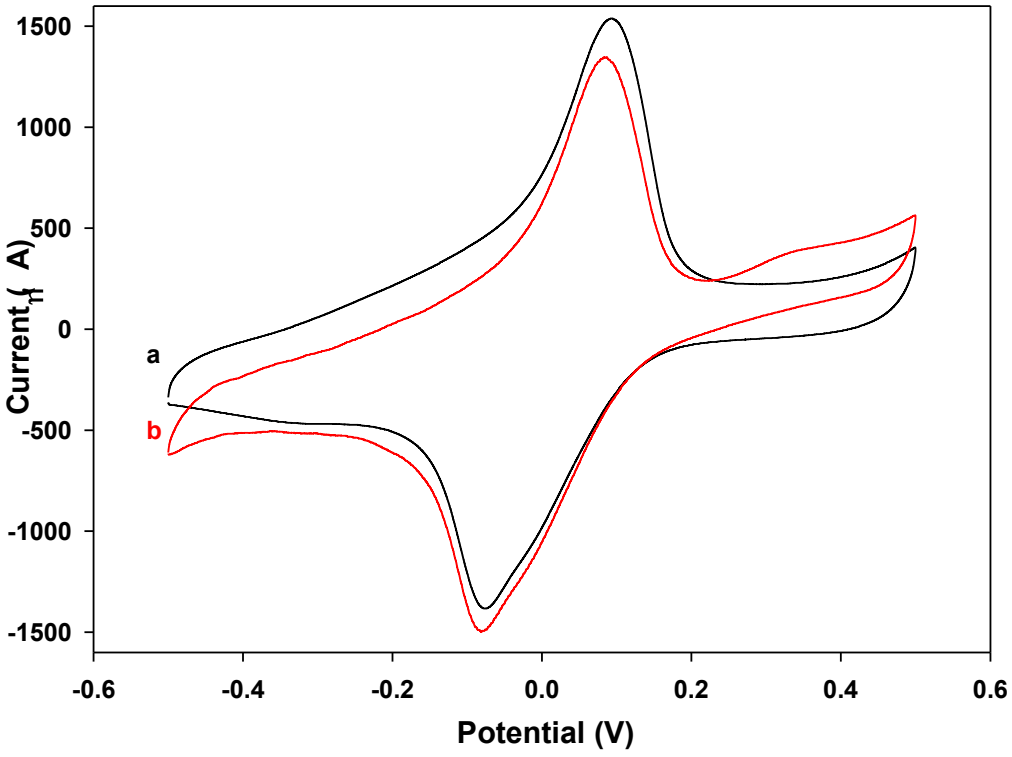

Figure 4.3. Cyclic voltammograms of the Ti/NPAu/PB/GO_x electrode in the absence (a) and in the presence of 1 mM glucose (b) at the scan rate of 20 $mV.s^{-1}$ in 0.1 M PBS (pH 7.0).

Figure 4.3 presents the CV curves recorded in 0.1M PBS (pH=7.0) at a scan rate of 20 mV/s in the absence of glucose (a) and in the presence of 1 mM glucose (b). It is seen that the reduction current increases while the oxidation current decreases, which relates to the oxidation of glucose by GO_x catalysis. The mechanism for the reaction for the detection of glucose can be defined as follows:[32]

$$\text{D-glucose} + O_2 \rightleftharpoons \text{gluconolactone} + H_2O_2 \quad (1)$$

$$K_4Fe_4^{2+}[Fe^{2+}(CN)_6]_3 + 2H_2O_2 \rightleftharpoons Fe^{3+}[Fe^{2+}(CN)_6]_3 + 4OH^- + 4K^+ \quad (2)$$

$$Fe_4^{3+}[Fe^{2+}(CN)_6]_3 + 4e^- + 4K^+ \rightleftharpoons K_4Fe_4^{2+}[Fe^{2+}(CN)_6]_3 \quad (3)$$

The impact of the applied electrode potential and pH of the PBS on the amperometric response of the Ti/NPAu/PB/GO_x electrode to glucose was investigated, revealing the optimized sensing conditions: the applied potential of -0.1 V and pH = 7. Figure 4.4A displays the steady-state amperometric response of (i) the Ti/Au/PB/GOx electrode and (ii) the Ti/NPAu/PB/GO_x biosensor recorded by successively adding glucose into the PBS under the optimized sensing conditions.

For the Ti/NPAu/PB/GO_x biosensor, 95% of the steady-state current was achieved at less than 15 s. The corresponding calibration curves for the two electrodes are shown in Figure 4.4B. The amperometric response of the Ti/NPAu/PB/GO_x biosensor is much higher than that of the Ti/Au/PB/GO_x electrode. A linear relationship of the current to the concentration of glucose was observed between 0 and 2.04 mM with a correlation coefficient of 0.9993 with 17 successive injections of 0.12 mM glucose. The sensitivity of the Ti/NPAu/PB/GO_x biosensor is extremely high, 177 μA/mM. The detection limit is estimated to be 2.5 μM glucose (based on S/N = 3).

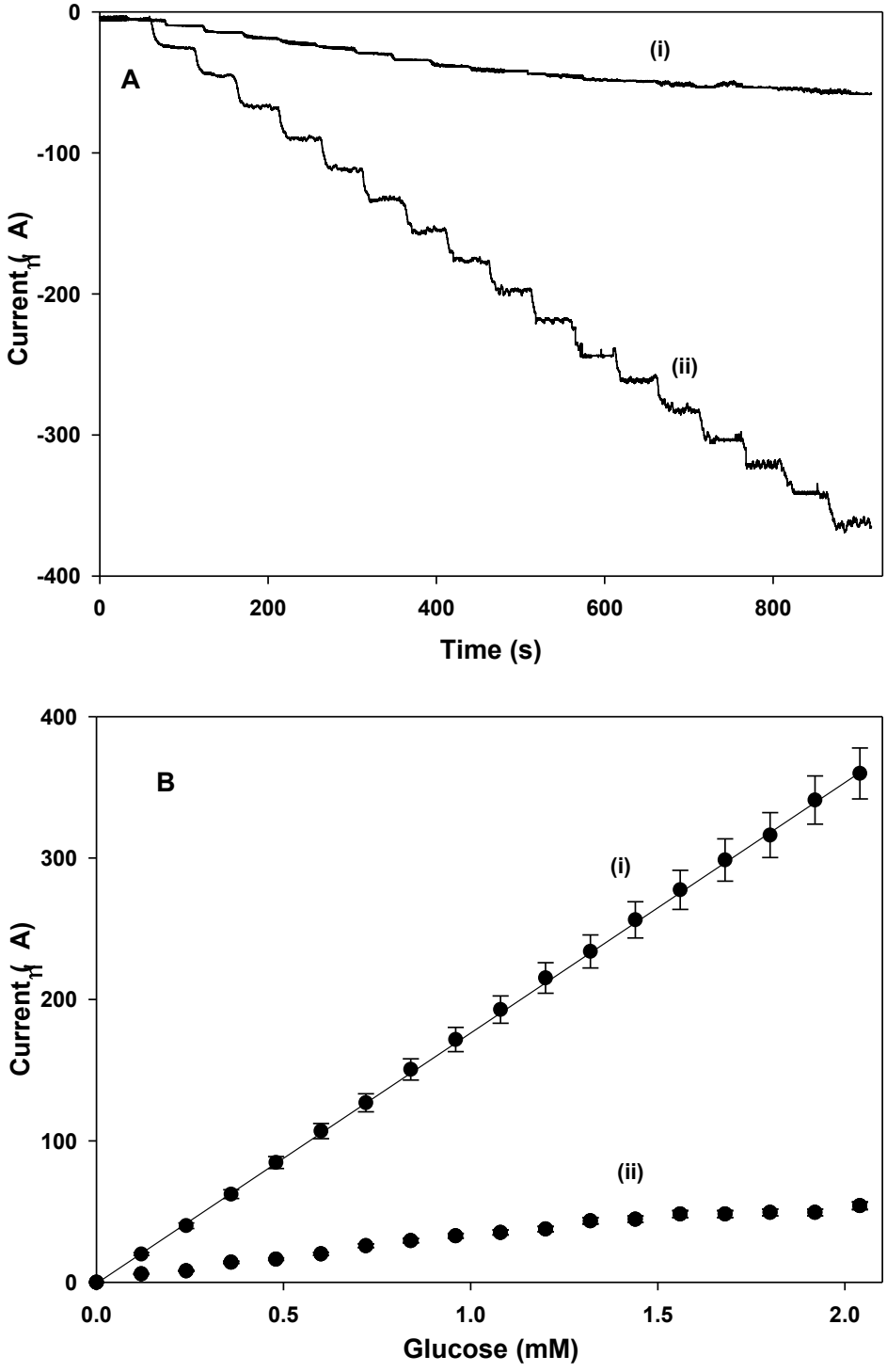

Figure 4.4. (A) Amperometric response to successive additions of 0.12 mM glucose into a 0.1 M pH 7.0 PBS under the applied electrode potential –0.1 V; (B) the corresponding calibration curves for the response of : (i) the Ti/Au/PB/GO_x and (ii) Ti/NPAu/PB/GO_x electrode.

To evaluate the biological activity of the immobilized GO_x, the apparent Michaelis-Menten constant K_m is generally used [22]. According to the Michaelis-Menten equation:

$$I_{max}/I_s = K_m/C+1$$

Where I is the steady-state catalytic current, I_{max} is the maximum current measured under saturated conditions, C refers to the glucose concentration and K_m stands for the apparent Michaelis-Menten constant. This equation allows us to plot the experimental $1/I_s$ *vs.* 1/C to determine K_m. According to our experimental data, K_m was evaluated as 2.1 mM. The value of K_m is much lower than the reported 4.3 mM for gold nanoparticles ,[31] 19 mM for ZnO nanotubes ,[33] and 21.1 mM for microband gold electrodes. [34] The small K_m value indicates that the immobilized GO_x possesses high enzymatic activity and that the fabricated biosensor exhibits a high affinity for glucose. Table 4.1 shows a comparison between the proposed biosensor and the other relevant studies.

Table 4.1 The comparison between the proposed biosensor and the other Prussian blue based glucose biosensors.

Electrode	Detection limit	Linear range	Km	Sensitivity
	μM	mM	mM	$\mu A.mM.cm^{-2}$
AuE/PB/GO_x[32]	3.1	0.06-1.60	N/A	83.8
TiO_2NT/Au/PB/GO_x[35]	5.0	0.015-4.0	N/A	36
PB/CS/Au/GO_x[26]	39.7	0.001-0.4	3.73	81.8
This work	2.5	0.1-2.04	2.1	177

4.3.3. Selectivity and stability of biosensor

We further studied the selectivity of the fabricated Ti/NPAu/PB/GO_x biosensor. The amperometric response of the biosensor to successive additions of common interfering substances and glucose in0.1 M PBS (pH = 7.0) was measured under the applied electrode potential -0.1 V. As shown in Figure 4.5, the biosensor shows no or very little response to ascorbic acid (AA), uric acid (UA), and acetaminophen (AP); in contrast, the biosensor exhibits very strong response to the successive injections of 0.1 mM glucose in the presence of 0.1 mM AA, 0.2 mM UA and 0.1 mM AP, indicating that the glucose biosensor fabricated in this study has a very high anti-interferent ability.

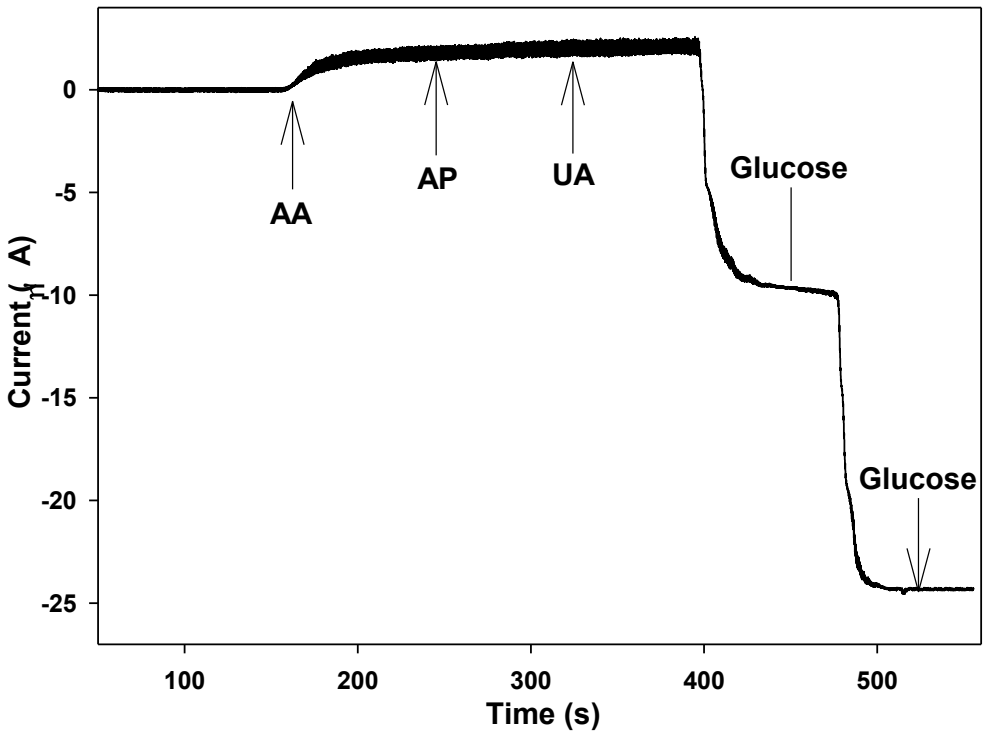

Figure 4.5. Effect of interferents, 0.1 mM ascorbic acid (AA), 0.1 mM acetaminophen and 0.02 mM uric acid (UA), on the response of the Ti/NPAu/PB/GO_x biosensor to successive additions of 0.1 mM glucose.

The reproducibility of the biosensor was also examined by measuring the response towards 1mM glucose in 50 ml pH 7.0 PBS. Four biosensors constructed independently gave a relative standard deviation (R.S.D.) of 4.2%. The long-term stability of the biosensor was evaluated by measuring its performance every week. The biosensor retained around 85% of the initial response after four weeks. After 60 days, the biosensor was still very active, retaining over 70% of the initial response.

4.4. Conclusions

In this chapter, we have demonstrated a novel glucose biosensor based on the highly efficient immobilization of GO_x on a PB modified nanoporous Au surface. The nanoporous Au was directly grown through a facile hydrothermal method and modified by electrodeposited Prussian blue. Our study has shown that the PB modified nanoporous Au substrate provides an excellent matrix for the immobilization of GO_x owing to its large surface area and strong adsorption ability for enzyme binding, high chemical stability, low inherent toxicity and high conductivity. The small K_m value of the Ti/NPAu/PB/GO_x biosensor indicates that the immobilized GO_x possesses high enzymatic activity and that the fabricated biosensor exhibits a high affinity for glucose. Our electrochemical tests show that the fabricated Ti/NPAu/PB/GO_x biosensor exhibits fast amperometric response, a low detection limit (2.5 μM), extremely high sensitivity (177 μA mM^{-1}), good reproducibility, high anti-interferent ability and long-time stability.

References

1. Du, P.; Wu, P.; Cai, C., A Glucose Biosensor Based on Electrocatalytic Oxidation of NADPH at Single-Walled Carbon Nanotubes Functionalized with Poly(Nile Blue A). *J. Electroanal. Chem.* **2008,** *624*, 21-26.

2. Lee, S.-R.; Sawada, K.; Takao, H.; Ishida, M., An Enhanced Glucose Biosensor Using Charge Transfer Techniques. *Biosens. Bioelectron.* **2008,** *24*, 650–656.

3. Antiochia, R.; Gorton, L., Development of A Carbon Nanotube Paste Electrode Osmium Polymer-Mediated Biosensor for Determenation of Glucose in Alcoholic Beverages. *Biosens. Bioelectron.* **2007,** *22*, 2611-2617.

4. Kim, S.; Kim, J.; Babajanyan, A.; Lee, K.; Friedman, B., Noncontact Characterization of Glucose by A Waveguide Microwave Probe. *Curr. Appl.Phys.* **2008,** *9*, 856-860

5. Saxl, T.; Khan, F.; Matthews, D.; Zhi, Z. L.; Ameer-Beg, S.; Rolinski, O.; Pickup, J., Fluorescence Lifetime Spectroscopy and Imaging of Nano-Engineered Glucose Sensor Microcapsules Based on Glucose/Galactose Binding Protein. *Biosens. Bioelectron.* **In Press**.

6. Kajiwara, K.; Fukushima, H.; Kishikawa, H.; Nishida, K.; Hashiguchi, Y.; Sakakida, M.; Uehara, M.; Shichiri, M., Spectroscopic Quantitative-Analysis of Blood Glucose by Fourier-Transform Infrared-Spectroscopy with An Attenuated Total Reflection Prism. *Med. Prog. Technol.* **1992,** *18*, 181-189.

7. Chung, H.; Arnold, M. A.; Rhiel, M.; Murhammer, D. W., Simultaneous Measurements of Glucose, Glutamine, Ammonia, Lactate, and Glutamate in Aqueous Solutions by Near-Infrared Spectroscopy. *Appl. Spect.* **1996,** *50*, 270-276.

8. Yang, L.; Du, C.; Luo, X., Rapid Glucose Detection by Surface Enhanced Raman Scattering Spectroscopy. *J. Nanosci. Nanotech.* **2009,** *9*, 2660-2663.

9. Mendes, A. C.; Caldeira, M. M.; Silva, C.; Burgess, S. C.; Merritt, M. E.; Gomes, F.; Barosa, C.; Delgado, T. C.; Franco, F.; Monteiro, P.; Providencia, L.; Jones, J. G., Hepatic UDP-Glucose C-13 Isotopomers from [U-C-13]glucose: A Simple Analysis by C-13 NMR of Urinary Menthol Glucuronide. *Magnet. Res. Med.* **2006,** *56*, 1121-1125.

10. Hammad, L. A.; Saleh, M. M.; Novotny, M. V.; Mechref, Y., Multiple-Reaction Monitoring Liquid Chromatography Mass Spectrometry for Monosaccharide Compositional Analysis of Glycoproteins. *J. Am. Soc.MS Spect.* **2009,** *In Press*.

11. Nießner, G. S. á. R., New Concept for the Non-Invasive Determination of Physiological Glucose Concentrations Using Modulated Laser Diodes. *Fresen. J. Anal. Chem.* **1996,** *354*, 306-310.

12. Cook, A. P.; MacLeod, T. M.; Appletont, J. D.; Fell, A. F., HPLC Studies on the Degradation Profiles of Glucose 5-Percent Solutions Subjected to Heat Sterilization in A Microprocessor-Controled Autoclave. *J. Clin. Pharm. Therap.* **2009,** *14*, 189-195.

13. Rzygalinski, I.; Pobozy, E.; Drewnowska, R.; Trojanowicz, M., Enzymatic In-Capillary Derivatization for Glucose Determination by Electrophoresis with Spectrophotometric Detection. *Electroanalysis* **2008,** *29*, 1741-1748.

14. Maeda, E.; Kataoka, M.; Hino, M.; Kajimoto, K.; Kaji, N.; Tokeshi, M.; Kido, J.-i.; Shinohara, Y.; Baba, Y., Determination of Human Blood Glucose Levels Using Microchip Electrophoresis. *Electrophoresis* **2007,** *28*, 2927-2933.

15. Lewandowski, J.; Malchesky, P. S.; Krzymien, J.; Szczepanskasadowska, E.; Nalecz, M.; Nose, Y., Application of Pulse-Polarography for Glucose Determination with Electrocatalytic Glucose Sensor. *IEEE Trans. Bio-med. Eng.* **1984,** *31*, 582-582.

16. Gouveia-Caridade, C.; Pauliukaite, R.; Brett, C. M. A., Development of Electrochemical Oxidase Biosensors Based on Carbon Nanotube-Modified Carbon Film Electrodes for Glucose and Ethanol. *Electrochim. Acta* **2008,** *53*, 6732-6739.

17. Miyashita, M.; Ito, N.; Ikeda, S.; Murayama, T.; Oguma, K.; Kimura, J., Development of Urine Glucose Meter Based on Micro-Planer Amperometric Biosensor and Its Clinical Application for Self-Monitoring of Urine Glucose. *Biosens. Bioelectron.* **2009,** *24*, 1336-1340.

18. Hanrahan, G.; Patil, D. G.; Wang, J., Electrochemical Sensors for Environmental Monitoring: Design, Development and Applications. *J. Environ. Mon.* **2004,** *6*, 657-664.

19. Sadik, O. A.; Aluoch, A. O.; Zhou, A., Status of Biomolecular Recognition Using Electrochemical Techniques. *Biosen. Bioelectron.* **2009,** *24*, 2749-2765.

20. Atkins, P.; Paula, J. d., *Physical Chemistry*. 18 ed.; Oxford University Press: New York, 2006; p 841.

21. Guilbault, G. G.; Jr., J. G. M., Urea-Specific Enzyme Electrode. *J. Am. Chem. Soc.* **1969,** *91*, 2164–2165.

22. Shu, F. R.; Wilson, G. S., Rotating Ring-Disk Enzyme Electrode for Surface Catalysis Studies. *Anal. Chem.* **1976,** *48*, 1679-1686.

23. Ofir, Y.; Samanta, B.; Rotello, V. M., Polymer and Biopolymer Mediated Self-Assembly of Gold Nanoparticles. *Chem. Soci. Rev.* **2008,** *37*, 1814-1825.

24. Karyakin, A. A.; Karyakina, E. E., Prussian Blue-based Artificial Peroxidase as A Transducer for Hydrogen Peroxide Detection. Application to Biosensors. *Sens. Actuat. B: Chem.* **1999,** *57*, 268-273.

25. Pchelintsev, N. A.; Vakurova, A.; Millner, P. A., Simultaneous Deposition of Prussian Blue and Creation of An Electrostatic Surface for Rapid Biosensor Construction *Sens. Actuat. B: Chem.* **2009,** *138*, 461-466.

26. Wang, X.; Gu, H.; Yin, F.; Tu, Y., A Glucose Biosensor Based on Prussian Blue/Chitosan Hybrid Film *Biosens. Bioelectron.* **2009,** *24*, 1527-1530.

27. Pan, Q.; Huang, K.; Ni, S.; Yang, F.; He, D., Synthesis of Two-Dimensional Micron-Size Single-Crystalline Prussian Blue Nanosheets by Hydrothermal Methods Assisted by Glucose *Mater. Res. Bul.* **2009,** *44*, 388-392

28. Lin, Y.; Liu, K.; Yu, P.; Xiang, L.; Li, X.; Mao, L., A Facille Electrochemical Method for Simultaneous and On-Line Measurements of Glucose and Lactate in Brain Microdialysate with Prussian Blue as the Electrocatalyst for Reduction of Hydrogen Peroxide. *Anal. Chem.* **2007,** *79*, 9577-9583.

29. Hong, C.; Yuan, R.; Chai, Y.; Zhuo, Y., Amperometric Immunosensor for the Determination of a-1-Fetoprotein Based on Core-Shell-Shell Prussian Blue-BSA-Nanogold Functionalized Interface. *Electroanalysis* **2008,** *20*, 2185-2191.

30. Khan, R.; Dhayal, M., Electrochemical Studies of Novel Chitosan/TiO_2 Bioactive Electrode for Biosensing Application *Electrochem. Commun.* **2008,** *10*, 263-267.

31. Zhang, S.; Wang, N.; Yu, H.; Niu, Y.; Sun, C., Covalent Attachment of Glucose Oxidase to An Au Electrode Modified with Gold Nanoparticles for Use as Glucose Biosensor *Bioelectrochemistry* **2005,** *67*, 15-22.

32. Yin, B.; Yuan, R.; Chai, Y.; Chen, S.; Cao, S.; Xu, Y.; Fu, P., Amperometric Glucose Biosensors Based on Layer-By-Layer Assembly of Chitosan and Glucose Oxidase on the Prussian Blue-Modified Gold Electrode. *Biotechnol. lett.* **2008,** *30*, 317-322.

33. Kong, T.; Chen, Y.; Ye, Y.; Zhang, K.; ZhenxingWang; XiaopingWang, An Amperometric Glucose Biosensor Based on the Immobilization of Glucose Oxidase on the ZnO Nanotubes. *Sens. Actuat. B: Chem.* **2009,** *138*, 344-350.

34. Ju, H.; Zhou, D.; Xiao, Y.; Chen, H., Amperometric Biosensor for Glucose Based on a Nanometer-Sized Microband Gold Electrode Coimmobilized with Glucose Oxidase and Poly(o-phenylenediamide). *Electroanalysis* **1998,** *10*, 541-545.

35. Benvenuto, P.; Kafi, A. K. M.; Chen, A., High performance glucose biosensor based on the immobilization of glucose oxidase onto modified titania nanotube arrays. *J. Electroanal. Chem.* **2009,** *627*, 76-81.

Chapter 5

High Performance Electrochemical Biosensor for the Detection of Cholesterol*

5.1. Introduction

Cholesterol is made by the liver as well as being part of a healthy dietary intake of fats. Cholesterol and triglycerides are important building blocks in the structure of cells and are used in making hormones and vitamin D, and producing energy. However, having a high total cholesterol (the sum of free cholesterol and cholesterol esters) level, particularly those of the low density lipoprotein type, can cause blood vessel damage and resulting diseases such as coronary heart disease and peripheral vascular disease. High cholesterol has also been linked to nephrosis, diabetes mellitus, myxedema and jaundice. On the other hand, a low cholesterol level may result in hyperthyroidism, anemia and maladsorption.[1] Most recent studies have shown that high cholesterol can affect macrophages which are part of the innate immune system that typically gobble up pathogens and clear away dead cells.[2] The desired total plasma cholesterol for an individual is less than 5.2 mM (200 mg/dl), with a high level being considered as greater than 6.2mM (240 mg/dl).[1] Thus, the industrial and clinical determination of cholesterol is of great interest.[3-5]

Electrochemical biosensors offer several distinct advantages. These devices are uniquely qualified for meeting the small size, inexpensive, low volume and power requirements of decentralized testing and show great promise for a wide range of biomedical and environmental applications.[6] In the development of electrochemical biosensor, facilitation of the electron

* Most of the results presented in this chapter have been published in *Biosensors and Bioelectronics*, **2011**, *26*, 4508.

transfer between the enzyme and the electrode is a great challenge because of the deeply embedded redox-active center of the metalloenzyme. On one hand, great efforts have been made to enhance the electron transfer in sensor design by using mediators, promoters or other special materials such as peroxidases for the construction of enzyme-based biosensors.[6-8] On the other hand, with the use of nanomaterials, higher sensitivity and the intimate attachment of enzymes are achievable due to the nanomaterials' high surface roughness as well as their unique physical, electronic and chemical properties. Applications of nanostructured materials have been attracting great attention in the development of high-performance electrochemical biosensors. Among them, gold nanomaterials have gained particular interest due to their ease of synthesis and functionalization, high chemical stability, low inherent toxicity (biocompatibility), and tunable optical and electronic properties.[9-10] It has been reported that the above mentioned properties of Au nanomaterials can effectively facilitate the electron transfer in the design of an electrochemical biosensor.[11-13] Few biosensors have been reported for cholesterol determination compared with those reported for glucose; thus, developing biosensors based on gold nanostructures for the detection of total cholesterol may have a significant impact on both the clinical diagnostics and the food industry.

To develop the electrochemical cholesterol biosensor, Aravamudhan et al. attached the enzymes to the surface of aligned-gold nanowires through direct physical adsorption.[3] Their studies showed the fabricated biosensor with the sensitivity of 0.85 $\mu A.mM^{-1}$ and the Michaelis-Menten constant of 17.1 mM. To improve the sensitivity, Gopalan et al. recently reported on the fabrication of a biosensor for the detection of free cholesterol by combining the advantageous features of MWNT (multi-walled carbon nanotubes), Au nanoparticles, chitosan and ionic liquid.[14] Chitosan, a polysaccharide composed mainly of β-(1,4)- linked 2-deoxy-2-amino-D-

glucopyranose units, is the deacetylated product of chitin, poly (N-acetyl-D-glucosamine). Chitosan has been used for the fabrication of biosensing devices because of its biocompatibility, biodegradability, multiple functional groups, as well as its solubility in acidic aqueous medium.[12, 15-16]

Given the huge medical implications, the industrial and clinical determination of cholesterol is increasingly important. Since 70% of cholesterol exists in ester form and 30% as free form in a blood sample, detection of the total cholesterol is desirable. In the present work, for the first time, we co-immobilized three enzymes, cholesterol oxidase (ChO_x), cholesterol esterase (ChE) and horseradish peroxidase (HRP), on the nanoporous Au networks with the aid of chitosan for the detection of the total cholesterol. The nanoporous Au networks were directly grown on a titanium (Ti) substrate using the hydrothermal method. The fabricated biosensor was free of any other promoters or special materials toxic to the environment and human. Our electrochemical measurements show that the fabricated cholesterol biosensor has high sensitivity, a very low Michaelis-Menten constant, a wide linear range, low detection limit, high selectivity and excellent stability. The cholesterol biosensor developed in this study was further tested using real food samples, indicating the promising applications in both clinical diagnostics and the food industry.

5.2. Experimental

5.2.1. Materials

Cholesterol oxidase (from *Streptomyces* species), cholesterol esterase (from hog pancreas), cholesterol, glucose, and Triton® X-100 (t-octylphenoxypolyethoxyethanol) were purchased from Sigma, 4-cholesten-3-on from Aldrich, titanium plates (1.25 cm × 0.8 cm × 0.5 mm, 99.2%) from Alfa Aesar and lactic acid from Fluka. Horseradish peroxidase, ascorbic acid, uric

acid, lactic acid, sodium phosphate dibasic and sodium phosphate monobasic were used as received from Sigma-Aldrich. Nanopure water (18.2 MΩ cm) was used to prepare all solutions. All other chemicals were analytical grade and were used as received from commercial sources. A stock solution of cholesterol was prepared by dissolving cholesterol in isopropanol, then adding Triton X-100 and finally the phosphate buffer (pH 7.4) in a volume ratio of 10: 4: 86.

5.2.2. Preparation of the cholesterol biosensor

The hydrothermal method used in fabricating the nanoporous gold networks is similar to the previous studies.[17-19] Briefly, titanium plates (1.25 cm×0.8 cm) were washed in acetone, followed by Nanopure water, and then etched in a solution of 18% wt hydrochloric acid at 85 °C for 10 min to remove the oxide layer and roughen the Ti surface. The etched Ti substrates were transferred into Teflon-lined autoclaves containing 10 mL of an aqueous mixture of inorganic metal precursor and a reducing agent. A 1.0 M ammonium formate solution was used as the reducing agent and the metal precursor was $HAuCl_4$. The autoclaves were sealed and heated at 180 ºC for 10 h. The Ti plates coated with Au were dried and annealed under argon at 250 ºC for 2 h. After final rinsing with pure water, the Ti plates coated with nanoporous gold were ready for further surface analysis and for the immobilization of enzymes. To immobilize the enzymes, a mixture of 20 µL of 2 mg mL^{-1} of cholesterol oxidase (ChO_x), 10 µL of 2 mg mL^{-1} horseradish peroxidase (HRP), 10 µL of 2 mg mL^{-1} of cholesterol esterase (ChE) and 10 µL of 2 mg mL^{-1} of chitosan was cast onto the nanoporous Au electrode (Ti/NPAu/ChO_x-HRP-ChE). Chitosan was used as a glue to enhance the stability of the biosensor.[20-21] All prepared biosensors were stored at 4 ºC when not in use.

5.2.3. Instruments and Electrochemical Experiments

Surface morphology and composition of the synthesized samples were characterized using scanning electron microscopy (SEM) (JEOL JSM 5900LV) equipped with an energy-dispersive X-ray spectrometer (EDS) (Oxford Links ISIS). Surface elemental compositions based on quantitative EDS analysis were reported in average values of readings taken at five different spots on each sample surface. All electrochemical experiments were performed using an electrochemical workstation (CHI660B, CH instrument Inc.), connected with an in-house-built, three-electrode glass cell (30 mL). A platinum coil was used as a counter electrode and was flame-annealed before each experiment. An Ag/AgCl (saturated KCl) electrode was used as the reference electrode. The fabricated Ti/NPAu/ChO_x-HRP-ChE electrodes were used as the working electrode. All potentials reported in this paper are referred to the Ag/AgCl (saturated KCl) reference electrode. Cyclic voltammetric measurements of cholesterol were carried out in a 0.1 M phosphate buffer solution (pH 7.4) at selected potential ranges. All measurements were conducted in a 30 mL solution and at room temperature (22 ± 2 °C).

5.3. Results and discussion

5.3.1. Surface morphological studies

Figure 5.1A and B present a typical SEM image at ×15,000 magnification and EDS spectrum of the nanoporous gold (Ti/NPAu) electrode, respectively, fabricated using the hydrothermal method. The SEM image shows that nanoporous gold structure was formed and completely covered the substrate and that the thickness of the nanoporous gold layer was around 0.4 μm. The diameter of the formed randomly porous structures varies from tens to hundreds of nanometers. Only Au and Ti peaks appear in the EDS spectrum, and no discernible carbon or

oxygen signals are seen in the figure, showing that the synthesized nanoporous Au is free of surface organic impurities.

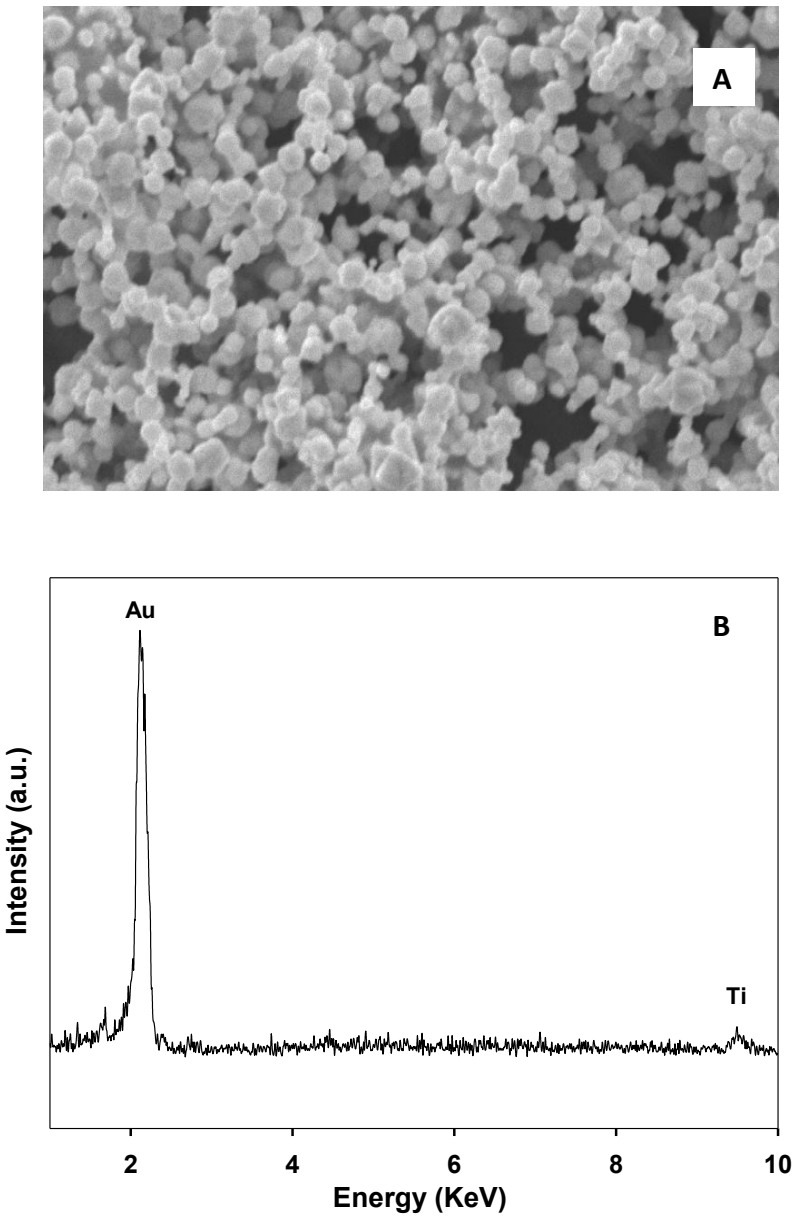

Figure 5.1. SEM image of the nanoporous Au directly grown on a titanium substrate and the corresponding EDS spectrum.

The XRD pattern of the as-synthesized Ti/NPAu surface is shown in Figure 5.2. All diffraction peaks originate from the Au film and the Ti substrate. The lattice constant calculated from the pattern was 4.079 Å, consistent with the literature a = 4.078 Å (Joint Committee on Powder Diffraction Standards file no. 04-0784). The XRD analysis reveals that the agglomerated structure observed by SEM has an average crystallite size of 22 nm. As seen in the experimental section, only inorganic metal precursors and diluted reducing agent were

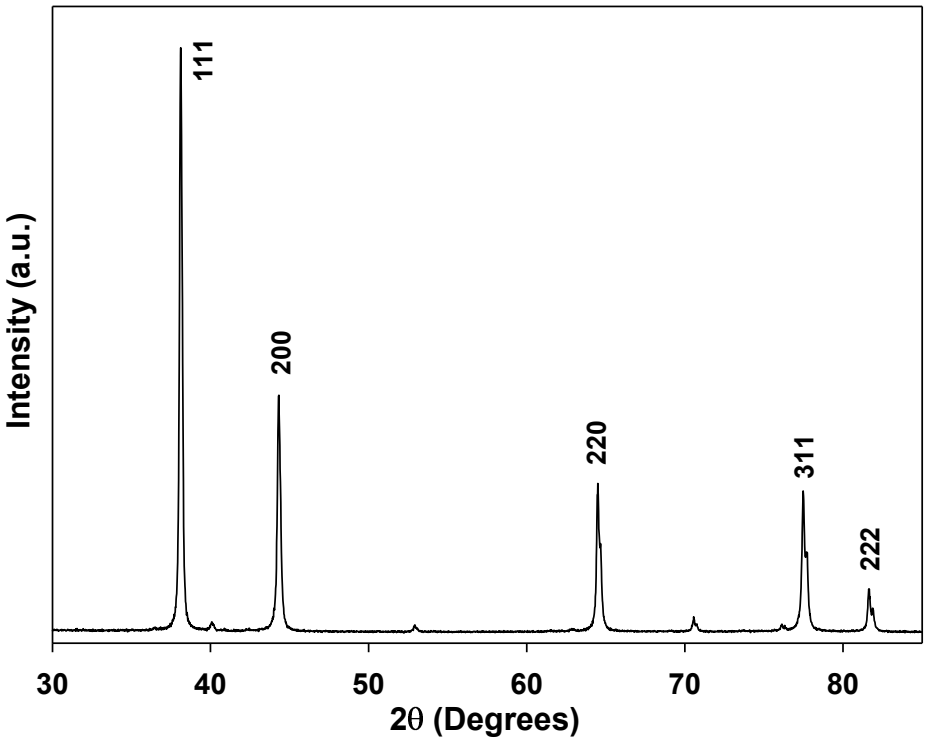

Figure 5.2. (A) (B). (C) XRD spectrum recorded from the synthesized nanoporous Au.

involved in the direct growth of nanoporous Au on the Ti substrate. The above results show that the one-step hydrothermal reduction process is an environmentally friendly approach and does not require any further separation and purification of the formed nanoporous Au with a large surface area, which is ready for the immobilization of enzymes. The surface roughness of

nanoporous Au was calculated by integrating the Au oxide reduction peak area obtained from the cyclic voltammogram in 50 mM H_2SO_4, then, dividing by the geometrical surface area. The surface roughness for nanoporous Au was 5.9.

5.3.2. Electrochemical characterization

The electrochemical responses of the Ti/AuNPs/ChO_x-HRP-ChE electrodes were studied by cyclic voltammetry (CV). Figure 5.3A shows the bioelectrocatalytic behaviour of the enzyme electrode recorded in a phosphate buffer solution (pH 7.4) in the potential range of -0.8 to 0.4 V at different scan rates. For instance, at the scan rate of 50 mV s^{-1}, the cathodic and anodic peaks appear at -0.36 and -0.047 V, respectively. The formal potential, E^0=1/2 ($E_{p,a}$ + $E_{p,c}$), was calculated to be -0.203V (vs. Ag/AgCl) and the electroactive enzyme amount, Γ =Q/nFA, (Where Q is the integrated charge which is calculated based on the peak area under the I-E curve, n is the electron number transferred, F the faraday constant, and A is the geometric surface area of the working electrode) is 2.1×10^{-9} mol.cm^{-2}. This is higher than the experimental values 7.52×10^{-10} and 4.7×10^{-10} mol.cm^{-2} [22-23] for the monolayer of flavoenzymes reported in literature. The higher value can be ascribed to the efficient immobilization of the enzymes on the nanoporous gold surface with high conductivity and a large surface area.

As seen in Figure 5.3B, both the anodic and cathodic peak currents increase linearly with the scan rates, indicating that the pair of redox waves originates from the surface confined molecules. The anodic and cathodic peak potentials also change as a function of the scan rate (10 – 300 mV s^{-1}). With increasing the scan rate, the oxidation peak shifts to more positive potentials, while the reduction peak shifts to more negative potentials. The anodic and cathodic peak potentials are linearly dependent on the logarithm of the scan rates (ν) when $\Delta E_p > 200/n$ where n is the number of electron transferred. This is in agreement with Laviron theory.[24-25]

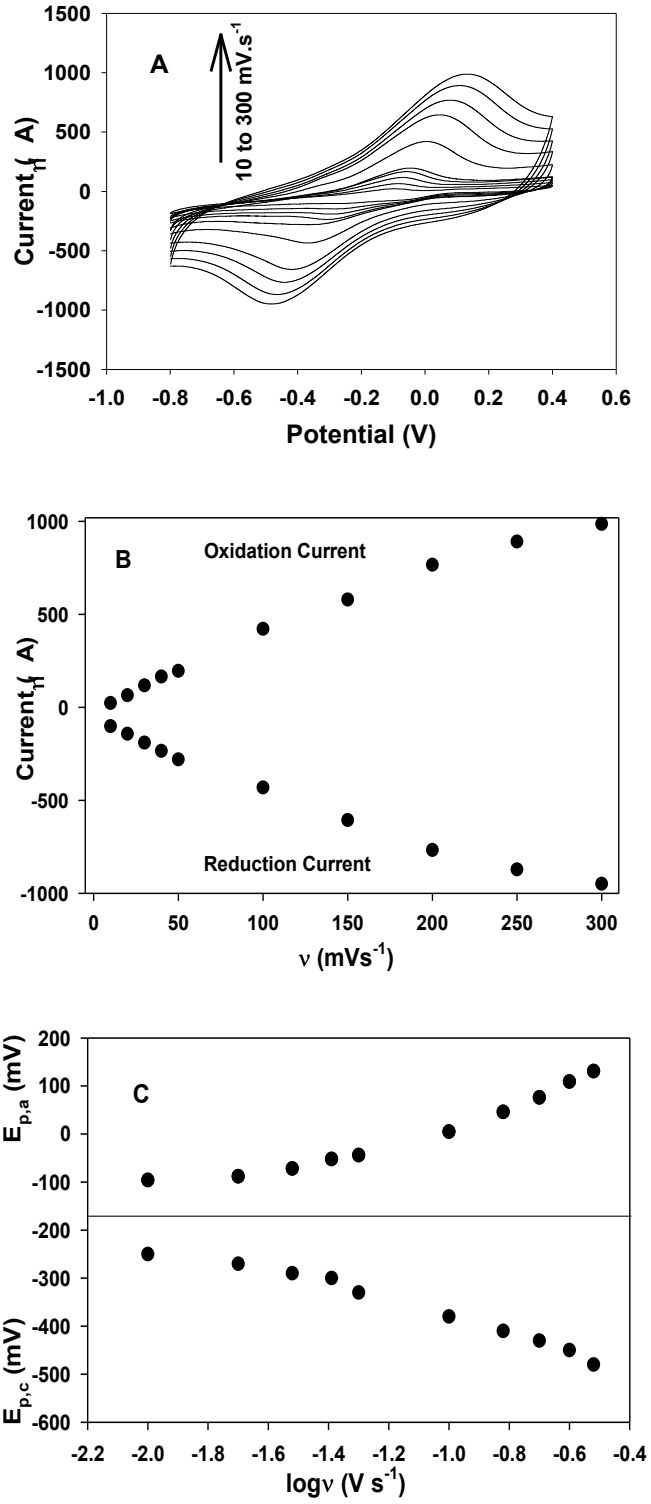

Figure 5.3. (A) Cyclic voltammamograms of the Ti/AuNPs/ChO_x-HRP-ChE electrode at different scan rates (10, 20, 30, 40, 50, 100, 150, 200, 250, 300 mVs^{-1}) in a phosphate buffer (pH 7.4). (B) Plot of anodic and cathodic peak currents *vs.* scan rates. (C) Variation of peak potentials *vs.* the logarithm of the scan rates.

The plots of E_p versus log ν are displayed in Figure 5.3C, yielding two straight lines with slopes of -2.3RT/αnF and 2.3RT/(1−α)nF for the cathodic and anodic peaks, respectively. Thus, experimental α was estimated to be 0.36.

The effect of pH on the performance of the Ti/NPAu/ChO_x-HRP-ChE electrodes was investigated in 0.1M phosphate buffer solutions with the pH varied from 4.0 to 9.0 at the scan rate of 50 mV/s. The current response was found to be maximum at pH 7-8, indicating that the biosensor is more active at this pH range and the immobilized enzymes retain their natural structure and do not denature. Thus, all the performance tests of the biosensor were conducted at pH 7.4 to simulate the physiological condition.

Figure 5.4A presents the two CV curves of the Ti/NPAu/ChO_x-HRP-ChE electrode recorded in a phosphate buffer solution (pH 7.4) in the absence of cholesterol (dashed line) and in the presence of 300 $mg.dl^{-1}$ cholesterol (solid line). Comparison of the two CV curves shows that the addition of cholesterol decreased the anodic current and significantly increased the cathodic current, revealing the strong response of the Ti/AuNPs/ChO_x-HRP-ChE electrode to cholesterol. As seen in Figure 5.4B, the reduction peak current increased strongly with the increase of the concentration of cholesterol, illustrating a typical electrocatalytic reduction process of H_2O_2 produced by the enzymatic reaction of cholesterol with cholesterol oxidase on the biosensor surface area as the following mechanism:[26]

$$\text{Cholesterol} + O_2 \xrightarrow{ChO_x} \text{Cholest-4-en-3-one} + H_2O_2 \qquad (1)$$

$$\text{Cholesterol ester} + H_2O \xrightarrow{ChE} \text{Cholesterol} + \text{Fatty acids} \qquad (1^*)$$

Cholesterol oxidase is an alcohol dehydrogenase/oxidase flavoprotein that catalyzes the dehydrogenation of C(3)-OH of a cholesterol molecule to yield the corresponding carbonyl

product. During the reductive half-reaction, the oxidized FAD (flavin adenine dinucleotide) cofactor accepts a hydride from the substrate and, in the ensuing oxidative half-reaction, the reduced flavin transfers the redox equivalents to molecular oxygen yielding hydrogen peroxide. Interestingly, the carbonyl species can also catalyze the isomerization of cholest-5-en-3-one (the product of the redox reaction) to cholest-4-en-3-one [26]. While the immobilized ChO_x catalyzes the oxidation of cholesterol, the ChE catalyzes the hydrolysis of esterase-esterified cholesterol, thus allowing us to determine the total cholesterol.

To sense the formed H_2O_2 in Equation 1 electrochemically, either a reducing or oxidising agent is required. Peroxidases such as HRP are ubiquitous oxidative heme-containing enzymes with which, in an early step in the catalytic cycle, H_2O_2 binds to the heme in the Fe(III) state. This binding causes the heterolytic cleavage of the oxygen-oxygen bond of H_2O_2.[27]

$$H_2O_2 + \text{HRP(Fe(III))} \rightarrow \text{Compound I(Fe(IV)=O)} + H_2O \quad (2)$$

$$\text{Compound I(Fe(IV)=O)} \rightarrow \text{Compound II(Fe(IV)=O)} \quad (3)$$

$$\text{Compound II(Fe(IV)=O)} \rightarrow \text{HRP(Fe(III))} + H_2O \quad (4)$$

A water molecule is released during this reaction with the concomitant two-electron oxidation of the heme to form an intermediate (compound I) comprising a ferryl species (Fe(IV)=O) and a porphyrin radical cation.[28] Compound I is then converted back to the resting enzyme via two successive single-electron transfers from the reducing substrate molecules. The first reduction of the porphyrin radical cation yields a second enzyme intermediate, compound II,

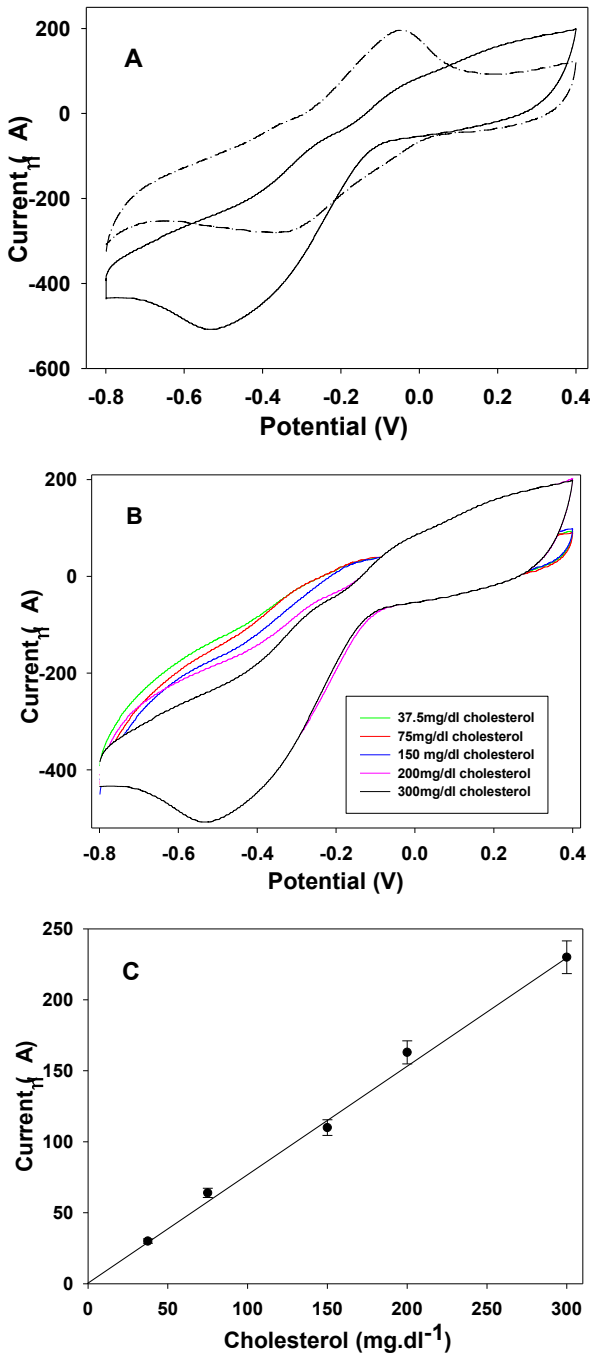

Figure 5.4. (A) Cyclic voltammetric response of the Ti/AuNPs/ChO_x-HRP-ChE electrode measured a phosphate buffer (pH 7.4) in the absence (dashed line) and presence (solid line) of cholesterol 300mg.dl^{-1}, (B and C) Cyclic voltammograms and calibration curve of the biosensor upon addition of different concentrations of cholesterol in phosphate buffer (pH 7.4). Potehtial scan rate: 50 mV s^{-1}.

which retains the heme in the ferryl (Fe(IV)=O) state.[29] Compound II oxidizes an additional equivalent of substrate, generating ferric enzyme and the corresponding substrate free radical.[8]

As seen in Figure 5.4C, the cyclic voltammetric response of the Ti/NPAu/ChO_x-HRP-ChE biosensor to different concentrations of cholesterol solutions shows a linear dynamic range of up to 300 $mg.dl^{-1}$ and sensitivity of 29.33 $\mu A.mM^{-1}.cm^{-2}$. Five biosensors constructed independently gave a relative standard deviation (R.S.D.) of 5.0%. The limit of detection of the biosensor was calculated to be 1 $mg.dl^{-1}$. Since the desired total plasma cholesterol for an individual is less than 5.2 mM (200 $mg.dl^{-1}$), with a high level being considered as greater than 6.2mM (240 $mg.dl^{-1}$), the fabricated biosensor covers a wide range of cholesterol concentration, promising for the clinical diagnostics of total cholesterol.

The apparent Michaelis-Menten constant (K_M^{app}), which gives an indication of the enzyme–substrate kinetics, can be estimated from the Lineweaver–Burk equation:[30]

$$1/I_{ss} = (K_M^{app}/I_{max})\ (1/C) + 1/I_{max} \qquad (5)$$

where I_{ss} is the steady state current, I_{max} is the current measured for the enzymatic product when electrode surface is saturated and C is the concentration of cholesterol. From the Lineweaver–Burk equation, the apparent Michaelis-Menten constant of the Ti/NPAu/ChOx-HRP-ChE biosensor was calculated to be 0.64 mM, which is much lower than the cholesterol biosensors reported in literature (Table 5.1). The small K_M^{app} value indicates that the immobilized enzymes possess high enzymatic activity and that the fabricated biosensor exhibits a high affinity for cholesterol.

Table 5.1 Comparison of the performances of various types of gold-based cholesterol biosensors.

Electrode	K_m mM	Sensitivity μA mM^{-1}	Linearity mM	Durability
DTSP-Au/ChO_x[31]	N/A	0.054	0.2 -2.1	40 days, 77%
(MWNTs)-Au/PPD-ChO_x[32]	7.17	0.559	0.5-6	N/A
MWNT(SH)–Au/Chi–IL/ChO_x[14]	N/A	0.2	0.5-5	20 days, 80%
Au Nanowire/ChOx-ChE[26]	17.1	0.85	0.01-0.060	10 days, 75%
This work	0.64	29.33	0.97-7.8	60 days, 95%

ChO_x: Cholesterol oxidase, ChEt & ChE: Cholesterol esterase, DTSP: dithiobissuccinimidyl propionate, Au: Gold, MWNT: Multi-wall carbon nanotubes, Chi: Chitosan, IL: Ionic liquid, NPAu: Nanoporous gold, HRP: Horseradish peroxidase , PPD: poly(o-phenylenediamine)

5.3.3. Selectivity and long-term stability of the biosensor

We further tested the selectivity of the Ti/NPAu/ChOx-HRP-ChE biosensor using four common interfering species. Figure 5.5 presents the response of the Ti/NPAu/ChOx-HRP-ChE biosensor to 0.1mM ascorbic acid, 5mM lactic acid, 5mM glucose, 0.1mM uric acid and 5.2mM cholesterol in 0.1 M PBS (pH 7.4). The biosensor produces negligible current signals for lactic acid and uric acid, a small response to ascorbic acid and glucose, but a very strong response to cholesterol.

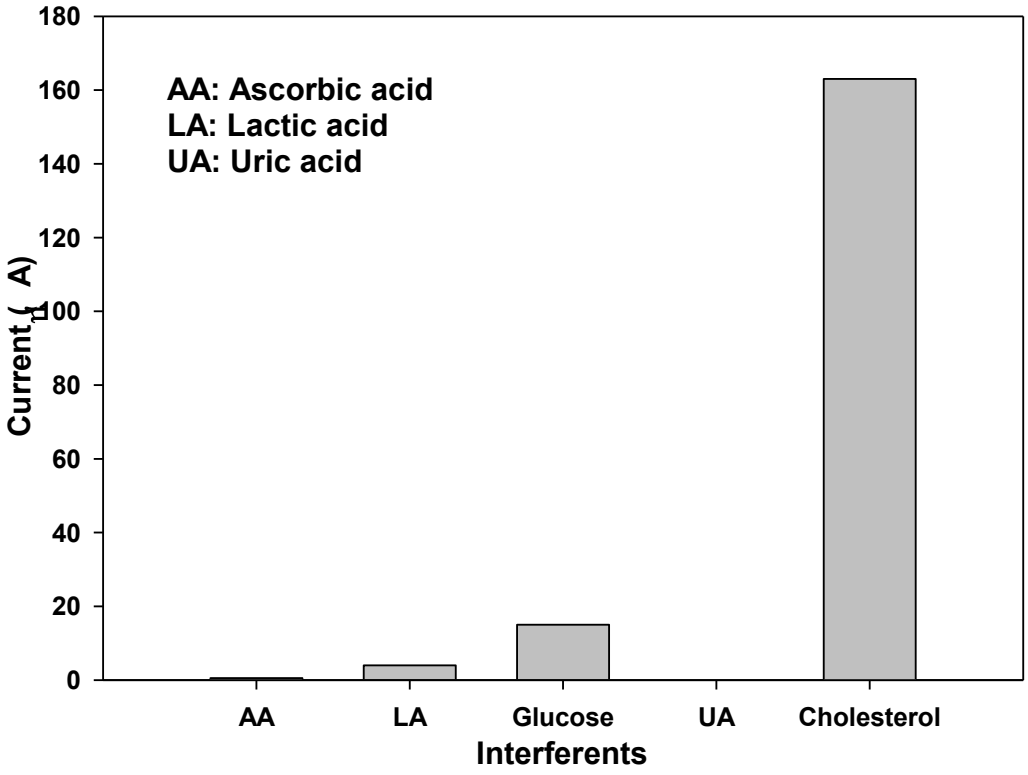

Figure 5.5. Selectivity response of the Ti/NPAu/ChO_x-HRP-ChE electrode after the addition of ascorbic acid (0.1 mM), lactic acid (5 mM) , glucose (5 mM), uric acid (0.1 mM) and finally cholesterol (5.2 mM) into phosphate buffer (pH 7.4) individually (background current was subtracted).

The stability of the Ti/NPAu/ChOx-HRP-ChE biosensor was tested by measurement of a 200 mg dl^{-1} standard cholesterol solution for 60 days. The tests were carried out once a week. During this period, the biosensors were stored in a phosphate buffer solution at 4ºC. The biosensor exhibited 95% of the initial current response after the 60-day period. The high stability can be attributed to the use of chitosan and the nanoporous Au networks. Since chitosan in an aqueous solvent is protonated and positively charged, it can be strongly adsorbed onto the nanoporous gold networks. The resulting interaction between gold-chitosan increases the retention of enzymes on the surface. In addition, gold nanostructures can strongly adsorb

enzymes and prevent the leakage of the immobilized enzymes [33]. The high sensitivity and high stability of the fabricated biosensor indicate that the nanoporous Au network structure along with chitosan provides an excellent microenvironment for the immobilization of the enzymes.

5.3.4. Real Sample Analysis

The developed Ti/NPAu/ChOx-HRP-ChE biosensor was further tested using real food samples butter, margarine and fish oil. The real samples were prepared using the same procedure as the cholesterol standard solution. The Margarine sample, which contains only vegetable fat, showed a small signal.

As seen in Table 5.2, the amount of total cholesterol found in butter, margarine and fish oil was 2.35, 0.69 and 45.82 mg, respectively. This is in good agreement with the amount of the total cholesterol listed on the product labels (2.4, 0 and 46 mg for Organic butter, NoName margarine and Naturaceutical Science Institute fish oil, respectively).

Table 5.2 Cholesterol detection of real samples by the Ti/AuNPs/ChO_x-HRP-ChE biosensor.

Samples	AuNPs biosensor (mg)	Product label (mg)	Brand
Margarine	0.69 ±0.05	0	NoName
Organic Butter	2.35±0.03	2.4	Harmonie
Fish oil	45.82±0.06	46	Naturaceutical Science Institute

All these results show that the fabricated cholesterol biosensor offers a great potential of application in cholesterol quality control of food products.

5.4. Conclusions

We have successfully fabricated a novel high-performance cholesterol biosensor by co-immobilizing cholesterol oxidase, cholesterol esterase and horseradish peroxidase on the nanoporous gold networks. The immobilized cholesterol oxidase effectively catalyzes the oxidation of cholesterol while the cholesterol esterase catalyzes the hydrolysis of esterase-esterified cholesterol, thus allowing the determination of the total cholesterol. Meanwhile, the immobilized horseradish peroxidase facilitates the detection of the H_2O_2 generated by the catalytic conversion of cholesterol to cholest-4-en-3-one. The developed Ti/NPAu/ChOx-HRP-ChE biosensor showed highly anti-interferents behaviour as tested toward common interfering species such as ascorbic acid, uric acid, lactic acid and glucose. A very low Michaelis-Menten constant indicates a very high activity of the immobilized enzymes. Under the physiological condition (pH 7.4), the designed biosensor exhibited reliable cyclic voltammetric responses, high sensitivity, a wide linear range up to 300 $mg.dl^{-1}$ and very high stability. The developed biosensor was also successfully used to measure the total cholesterol in real food samples. The high-performance along with the ease of fabrication and low costs makes the new Ti/NPAu/ChOx-HRP-ChE biosensor promising for the detection of total cholesterol in both clinical diagnostics and the food industry.

References

1. National Cholesterol Education Program. *Arch. Intern. Med.* **1988,** *148*, 36.

2. Becker, L.; Gharib, S. A.; Irwin, A. D.; Wijsman, E.; Vaisar, T.; Oram, J. F.; Heinecke, J. W., A Macrophage Sterol-Responsive Network Linked to Atherogenesis. *Cell Metabolism* **2010,** *11*, 125-135.

3. Aravamudhan, S.; Kumar, A.; Mohapatra, S.; Bhansali, S., Sensitive Estimation of Total cholesterol in Blood Using Au Nanowires Based Micro-Fluidic Platform. *Biosens. Bioelectron.* **2007,** *22*, 2289-2294.

4. Brahim, S.; Narinesingh, D.; Guiseppi-Elie, A., Amperometric Determination of Cholesterol in Serum Using A Biosensor of Cholesterol Oxidase Contained within A Polypyrrole–Hydrogel Membrane. *Anal. Chim. Acta* **2001,** *448*, 27-36.

5. Adanyi, N.; Varadi, M., Development of Organic Phase Amperometric Biosensor for Measuring Cholesterol in Food Samples. *Eur. Food Res. Technol.* **2003,** *218*, 99-104.

6. Wang, J., Nanomaterial-Based Electrochemical Biosensors. *Analyst* **2005,** *130*, 421-426.

7. Lu, X.; Zou, G.; Li, J., Hemoglobin Entrapped within A Layered Spongy Co_3O_4 Based Nanocomposite Featuring Direct Electron Transfer and Peroxidase Activity. *J. Mater. Chem.* **2007,** *17*, 1427-1432.

8. Reilly, C. A.; Aust, S. D., Peroxidase Substrates Stimulate the Oxidation of Hydralazine to Metabolites Which Cause Single-Strand Breaks in DNA. *Chem. Res. Toxicol.* **1997,** *10*, 328-334.

9. Ofir, Y.; Samanta, B.; Rotello, V. M., Polymer and Biopolymer Mediated Self-Assembly of Gold Nanoparticles. *Chem. Soc. Rev.* **2008,** *37*, 1814-1825.

10. Eustis, S.; El-Sayed, M. A., Why Gold Nanoparticles Are More Precious Than Pretty Gold: Noble Metal Surface Plasmon Resonance and Its Enhancement of the Radiative and Nonradiative Properties of Nanocrystals of Different Shapes. *Chem. Soc. Rev.* **2006,** *35*, 209-217.

11. Sperling, R. A.; Gil, P. R.; Zhang, F.; Zanella, M.; Parak, W. J., Biological Applications of Gold Nanoparticles. *Chem. Soc. Rev.* **2008,** *37*, 1896-1908.

12. Ahmadalinezhad, A.; Kafi, A. K. M.; Chen, A., Glucose Biosensing Based on the Highly Efficient Immobilization of Glucose Oxidase on A Prussian Blue Modified Nanostructured Au Surface. *Electrochem. Commun.* **2009,** *11*, 2048-2051.

13. Kafi, A. K. M.; Ahmadalinezhad, A.; Wang, J.; Thomas, D. F.; Chen, A., Direct Growth of Nanoporous Au and Its Application in Electrochemical Biosensing. *Biosens. Bioelectron.* **2010,** *25*, 2458-2463.

14. Gopalan, A. I.; Lee, K.-P.; Ragupathy, D., Development of A Stable Cholesterol Biosensor Based on Multi-Walled Carbon Nanotubes-Gold Nanoparticles Composite Covered with A Layer of Chitosan-Room-Temperature Ionic Liquid Network. *Biosens. Bioelectron.* **2009,** *24*, 2211-2217.

15. Wang, S.-F.; Shen, L.; Zhang, W.-D.; Tong, Y.-J., Preparation and Mechanical Properties of Chitosan/Carbon Nanotubes Composites. *Biomacromolecules* **2005,** *6*, 3067-3072.

16. Tiwari, A.; Gong, S., Electrochemical Study of Chitosan-SiO2-MWNT Composite Electrodes for the Fabrication of Cholesterol Biosensors. *Electroanalysis* **2008,** *20*, 2119-2126.

17. Peng, X.; Koczkur, K.; Nigro, S.; Chen, A., Fabrication and Electrochemical Properties of Novel Nanoporous Platinum Network Electrodes. *Chem. Com.* **2004,** *24*, 2872-2873.

18. Koczkur, K.; Yi, Q.; Chen, A., Nanoporous Pt-Ru Networks and Their Electrocatalytical Properties. *Adv. Mater.* **2007,** *19*, 2648-2652.

19. Wang, J.; Thomas, D. F.; Chen, A., Nonenzymatic Electrochemical Glucose Sensor Based on Nanoporous PtPb Networks. *Anal. Chem.* **2008,** *80*, 997-1004.

20. Khan, R.; Dhayal, M., Electrochemical Studies of Novel Chitosan/TiO_2 Bioactive Electrode for Biosensing Application *Electrochem. Commun.* **2008,** *10*, 263-267.

21. Kafi, A. K. M.; Chen, A., A Novel Amperometric Biosensor for the Detection of Nitrophenol. *Talanta* **2009,** *79*, 97-102.

22. Deng, C.; Chen, J.; Nie, Z.; Si, S., A Sensitive and Stable Biosensor Based on the Direct Electrochemistry of Glucose Oxidase Assembled Layer-By-Layer at the Multiwall Carbon Nanotube-Modified Electrode. *Biosens. Bioelectron.* **2010,** *26*, 213-219.

23. Deng, S.; Jian, G.; Lei, J.; Hu, Z.; Ju, H., A Glucose Biosensor Based on Direct Electrochemistry of Glucose Oxidase Immobilized on Nitrogen-Doped Carbon Nanotubes. *Biosens. Bioelectron.* **2009,** *25*, 373-377.

24. Laviron, E., General Expression of the Linear Potential Sweep Voltammogram in the Case of Diffusionless Electrochemical Systems. *J. Electroanal. Chem.* **1979,** *101*, 19-28.

25. Zhang, L.; Jiang, X.; Wang, E.; Dong, S., Attachment of Gold Nanoparticles to Glassy Carbon Electrode and Its Application for the Direct Electrochemistry and Electrocatalytic Behavior of Hemoglobin. *Biosens. Bioelectron.* **2005,** *21*, 337-345.

26. Aravamudhan, S.; Ramgir, N. S.; Bhansali, S., Electrochemical Biosensor for Targeted Detection in Blood Using Aligned Au Nanowires *Sens. Actuators B* **2007,** *127*, 29-35.

27. Rodriguez-Lopez, J. N.; Lowe, D. J.; Hernandez-Ruiz, J.; Hiner, A. N. P.; Garcia-Canovas, F.; Thorneley, R. N. F., Mechanism of Reaction of Hydrogen Peroxide with Horseradish

Peroxidase: Identification of Intermediates in the Catalytic Cycle. *J. Am. Chem. Soc.* **2001,** *123*, 11838-11847.

28. Courteix, A.; Bergelt, A., Horseradish Peroxidase-Catalyzed Hydroxylation of Phenol: I. Thermodynamic Analysis. *Enzyme Microb. Technol.* **1995,** *17*, 1087-1093.

29. Dunford, H. B.; Stillman, J. S., On the Function and Mechanism of Action of Peroxidases. *Coord. Chem. Rev.* **1976,** *19*, 187-251.

30. Kamin, R. A.; Wilson, G. S., Rotating Ring-Disk Enzyme Electrode for Biocatalysis Kinetic Studies and Characterization of the Immobilized Enzyme Layer. *Anal. Chem.* **1980,** *52*, 1198-1205.

31. Parra, A.; Casero, E.; Pariente, F.; Vázquez, L.; Lorenzo, E., Bioanalytical Device Based on Cholesterol Oxidase-Bonded SAM-Modified Electrodes. *Anal. Bioanal. Chem.* **2007,** *388*, 1059–1067.

32. Guo, M.; Chen, J.; Li, J.; Nie, L.; Yao, S., Carbon Nanotubes-Based Amperometric Cholesterol Biosensor Fabricated Through Layer-by-Layer Technique. *Electroanalysis* **2004,** *16*, 1992-1998.

33. Luo, X.-L.; Xu, J.-J.; Du, Y.; Chen, H.-Y., A Glucose Giosensor Based on Chitosan-Glucose Oxidase-Gold Nanoparticles Biocomposite Formed by One-Step Electrodeposition. *Anal. Biochem.* **2004,** *334*, 284-289.

Chapter 6

Mediator-Free Electrochemical Biosensor Based on Buckypaper with Enhanced Stability and Sensitivity for Glucose Detection*

6.1. Intuduction

Buckypapers are thin membranes (10-50 μm) of carbon nanotube (CNT) networks which are classified as smart nanomaterials owing to their remarkable structural, mechanical, electrochemical, piezoresistive and physical properties.[1] Since the discovery of CNTs in 1991,[2] tremendous efforts have been made to modify the characteristics of CNTs both chemically[3-6] and physically[7] toward the development of thin films of CNTs. Among the two types of CNTs, single-wall carbon nanotubes (SWNTs) and multi-wall carbon nanotubes (MWNTs), SWNTs consist of a single fullerene-structured graphite sheet, which is rolled seamlessly to form a nanotube.[2] SWNTs have a strong tendency to form bundles and aggregate due to their inherently high surface areas and strong Van der Waals interactions. In addition, SWNT networks exhibit higher conductivity than MWNTs.[8] In addition, mechanical deformation and chemical functionalization can improve interconnectivity of CNTs.[4] In this regard, polymerization has been widely used in the synthesis of homogenous and compressed CNT films.[9-10] Park et al. attempted an in situ polymerization method with the aim of dispersing as-pristine SWNT bundles into polyimide with the aid of sonication.[11] Two challenges were encountered: the dispersion issue and the rapidly increasing viscosity of the polymer. This chemical modification may also destroy the pristine structure of the SWNTs, resulting in a decrease of the maximum modulus

* Most of the results presented in this chapter have been published in *Biosensors and Bioelectronics*, **2011**, *30*, 287.

and strength by 15% .[12] Hence, to adapt CNT powder in the formation of substrates for certain applications such as biosensors, a variety of conductive supporting chemical matrices have been explored.[13-22] Another approach was the introduction of functionalities such as carboxylic groups into the side walls of CNTs. For most of the aforementioned CNT-based sensors, glassy carbon was used as a conductive substrate; however, the fabrication suffered from the necessity of complex reagents, homogeneity and a multiple step preparation process which, in turn, lowered the activity and stability of the resulting sensors.

It has been reported that CNTs in conjunction with a mediator or at a fairly high operating electrode potential have an enhanced effect on the electrocatalytic activity of glucose oxidase (GO_x) for the oxidation of glucose.[14-15, 23-26] However, mediated biosensors are subjected to a low selectivity and high toxicity. These drawbacks limit their in vivo applications. On the other hand, at a high potential, common electroactive species such as ascorbic acid, uric acid and acetamidophenol may act as interfering agents. Several strategies have been employed to minimize the effects of this interference. Polymeric membranes and metal-based compounds have been utilized.[17, 27-30] Effective but nonsufficient rejection of interferents has been reported in most cases. Moreover, multiple preparation steps and manipulation lower the sensor activity and increase its complexity. Such detection relies on the tuning of the operating potential to the optimal region of 0.0 to -0.20 V vs Ag/AgCl to effectively detect hydrogen peroxide released from the reaction of GO_x and glucose using peroxidases.[27] Although a few mediator-free bi-enzyme glucose sensors based on CNTs have been reported in the literature,[31-34] the narrow linear dynamic range, low sensitivity and stability hamper their medical diagnostic application.

In this study, we have designed a mediator-free glucose sensor based on buckypaper. To the best of our knowledge, this is the first time that titanium interfaced buckypaper has been

explored in the design of an electrochemical biosensor. The glucose sensor fabricated with the scheme proposed in this study exhibited high sensitivity, stability, selectivity and reproducibility. The robust buckypaper-based platform presented in this study is anticipated to open the door for the design of high-performance electrochemical biosensors for medical diagnostics and environmental monitoring.

6.2. Experimental

6.2.1. Materials

The buckypaper used in this study was produced by the High-Performance Materials Institute of Florida State University with a thickness of 0.035 mm. Glucose oxidase (EC 1.1.3.4, Type VII from Aspergillus niger) and β-D-glucose were purchased from Sigma and were used as received. Chitosan was purchased from Aldrich and titanium foils (99.2%) from Alfa Aesar. Horseradish peroxidase (HRP), potassium ferricyanide ($K_3Fe(CN)_6$), ascorbic acid, uric acid, 3-acetamidophenol were purchased from Sigma–Aldrich. All other reagents were of analytical grade. Water was purified with the Nanopure® water system (18 MΩ.cm) and was used in the preparation of all solutions. Various stock concentrations of β-D-glucose were prepared in 0.1 M phosphate buffer, pH 7.4 and stored at 4 ºC. Glucose stock solutions were allowed to mutarotate overnight prior to use.

6.2.2. Instrumentation and electrochemical measurements

Field-emission scanning electron microscopy (FE-SEM) (Hitachi, SU-4800), transmission electron microscopy (TEM) (JOEL 2010F) and energy dispersive x-ray spectrometry (EDS) were utilized to characterize the morphology and composition of the buckypaper. FTIR spectra were recorded using a NICOLET 8700 FTIR (Thermo Scientific, USA). Cyclic voltammetry

(CV) and amperometric measurements were performed using an electrochemical workstation (CHI660, CH Instrument Inc., USA) connected with an in-house-built, three-electrode glass cell (30 mL). A platinum coil was used as a counter electrode and was flame-annealed prior to each experiment. Ag/AgCl (3 M KCl) was used as a reference electrode. The constructed hybrid titanium/buckypaper-based biosensors were employed as working electrodes. All measurements were conducted at room temperature (22 ± 2 °C).

6.2.3. Biosensor preparation

The detailed procedure of the biosensor fabrication is illustrated in Scheme 6.1.

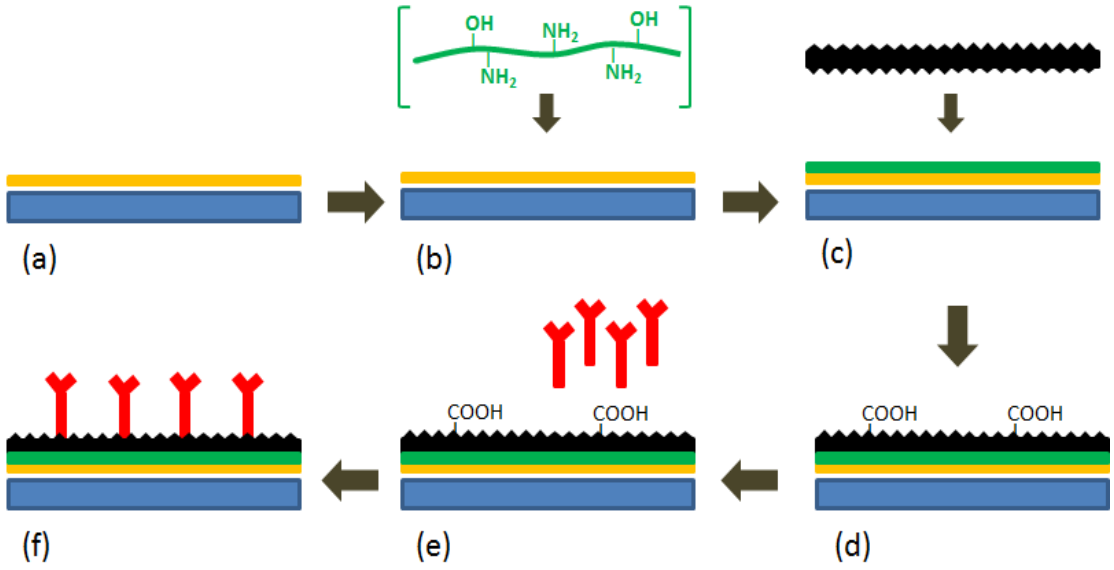

Scheme 6.1. Schematic diagram for the preparation of the buckypaper-based electrochemical biosensor. (a) a titanium plate sputtered with a thin layer of gold; (b) gold interaction with chitosan; (c) attachment of buckypaper to the gold surface by chitosan; (d) activation of buckypaper ; (e) immobilization of enzymes; (f) the fabricated biosensor.

Titanium plates (1.25 cm × 0.8 cm × 0.5 mm) were ultrasonically cleaned in acetone, ethanol and water. To provide a mechanical support for the buckypaper and to enhance the

conductivity, a titanium plate was coated with an Au thin film sputtered by argon plasma for 30 s (Scheme 6.1a). After rinsing with pure water, a section of buckypaper was attached to the gold coated titanium plate with the aid of 5μL of 2 $mg.mL^{-1}$ chitosan (Scheme 6.1b & c).

In order to engender this structure with utility as a glucose biosensor, the buckypaper was electrochemically activated. To activate the buckypaper (BP) surface, cyclic voltammetry was performed in the range of -0.8 to 0.4 V at a scan rate of 10 $mV.s^{-1}$ in phosphate buffer solution (PBS) at pH 7.4 until a steady cyclic voltammogram was obtained, and then a potential of 1.5 V was applied for 90 s. This step led to the functionalization of the buckypaper with carboxlic groups (Scheme 6.1d). The activated surface was thus ready for the immobilization of enzymes. To immobilize the enzymes, a mixed solution of 20 μL of 5 $mg.mL^{-1}$ GO_x, 10 μL of 2 $mg.mL^{-1}$ HRP and 10 μL of 2 $mg.mL^{-1}$ chitosan was cast onto the buckypaper (Scheme 6.1e and f). All prepared biosensors (Ti/Au/BP/GO_x-HRP) were stored at 4 ºC in 0.1 M PBS at pH 7.4 when not in use.

6.3. Results and discussion

6.3.1. Surface morphological studies

The morphology and composition of the buckypaper were characterized using FESEM, TEM and EDS. Figure 6.1A shows a photograph of the buckypaper used in this study. It is a very thin film. A typical FESEM image is presented in Figure 6.1B, which reveals that the SWNTs were arranged in bundles, forming networks. A high magnification TEM image of the buckypaper is displayed in Figure 6.2A, showing that the nanotubes were aggregated in a rope structure; the diameter of an individual SWNT was less than 4 nm. The volume density of buckypaper represents a high specific surface area, desirable for the immobilization of enzymes.

Figure 6.2B shows the EDS spectrum of the buckypaper. Only carbon and oxygen peaks were observed with no other discernable peaks, indicating the absence of impurities such as heavy metals.

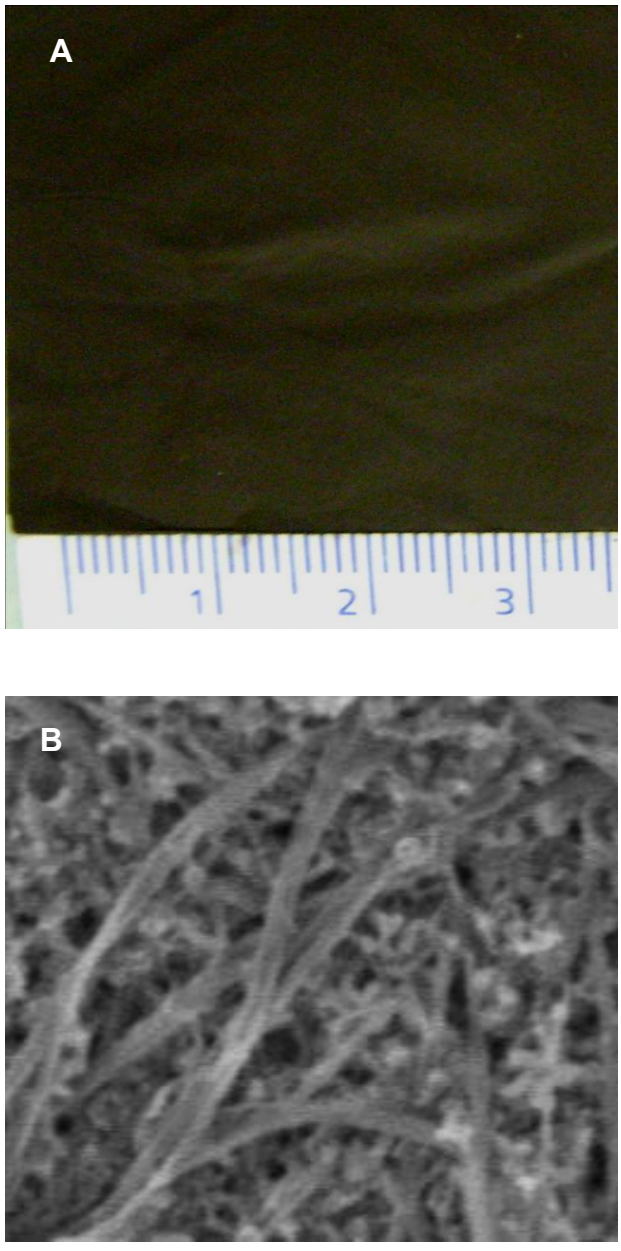

Figure 6.1. (a) A photograph; (b) FESEM image of the buckypaper

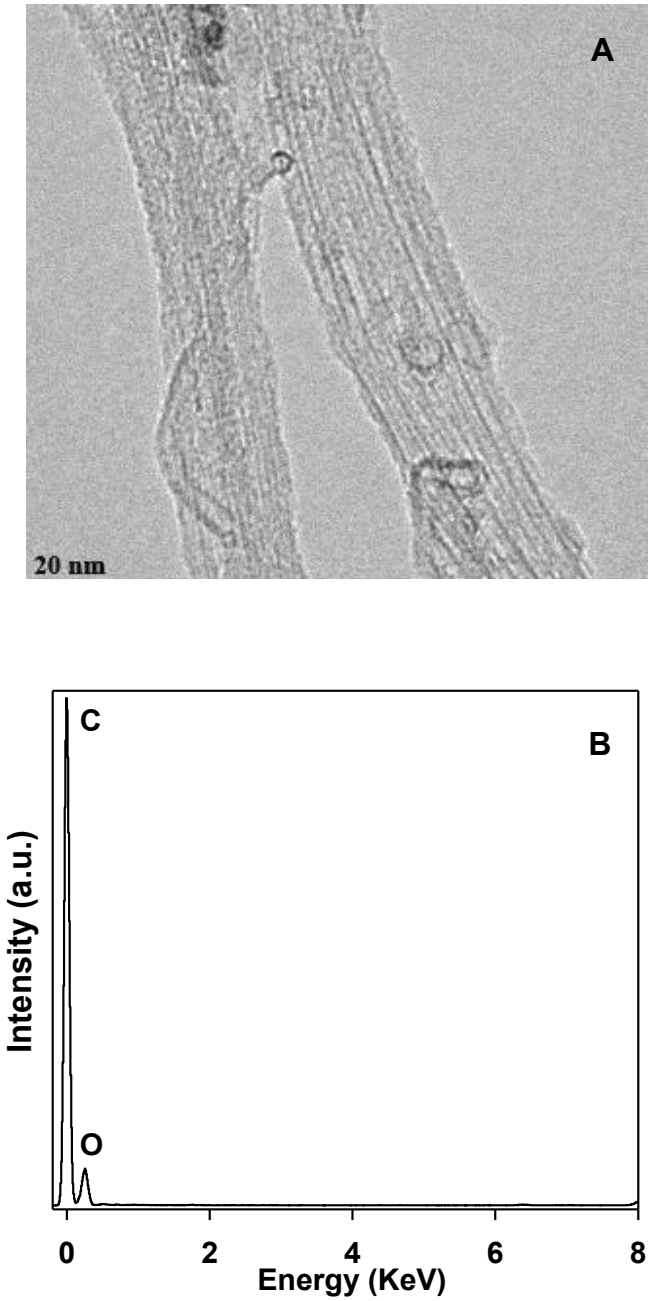

Figure 6.2. (A) TEM image; and (B) the corresponding EDS spectrum of the buckypaper.

6.3.2. Electrochemical characterization

The cyclic voltammograms of the Ti/BP, Ti/Au/BP, and Ti/Au/BP/GOx-HRP electrodes recorded in 0.1M $K_3Fe(CN)_6$ + 0.1M KCl + 0.1M PBS (pH 7.4) at a scan rate of 50 $mV.s^{-1}$ are presented in Figure 6.3. The well-defined oxidation and reduction peaks are observable due to the Fe^{3+}/Fe^{2+} redox couple. In the absence of the Au thin film, the oxidation peak appeared at 0.46V, while the reduction peak was observed at around -0.36V vs Ag/AgCl. The peak-to-peak separation (ΔE_p) was 0.82V for the Ti/BP electrode. While in the presence of the sputtered Au thin film (Ti/Au/BP electrode), ΔE_p decreases to 0.47V. In addition, the peak current increased by approximately 40%. All these results show that the sputtered gold thin film significantly enhanced the electrical communication between the buckyppaer and the titanium substrate. After the immobilization of the enzymes GO_x and HRP, both ΔE_p and peak current (I_p) slightly decreased. The electrochemical active surface area of the Ti/Au/BP and Ti/Au/BP/GOx-HRP electrodes may be calculated via the Randles-Sevcik equation:[35]

$$I_p = 2.69\times10^5 A D^{1/2} n^{3/2} \upsilon^{1/2} C$$

where n is the number of electrons that participate in the redox reaction, A is the area of the electrode (cm^2), D is the diffusion coefficient of the probe molecule in the bulk solution ($cm^2.s^{-1}$), C is the concentration of the $K_3Fe(CN)_6$ in the bulk solution ($mol.cm^{-3}$) , and υ is the scan rate ($V.s^{-1}$). The electroactive surface area of the Ti/Au/BP and Ti/Au/BP/GOx-HRP electrodes is thus estimated to be 1.85 and 1.75 cm^2, respectively. The slightly decrease in the electroactive surface area subsequent to the immobilization of the enzymes can be attributed to the blockage of some redox sites by GO_x and HRP, indicating that the immobilization did not diminish electron transfer between the redox species and the electrode substrate.

To investigate whether GO_x immobilized on the activated buckypaper retains its bio-electrocatalytic activity for the oxidation of glucose, control experiments were conducted for the Ti/Au/PB, Ti/Au/PB/HRP and Ti/Au/BP/HRP-GO_x electrodes.

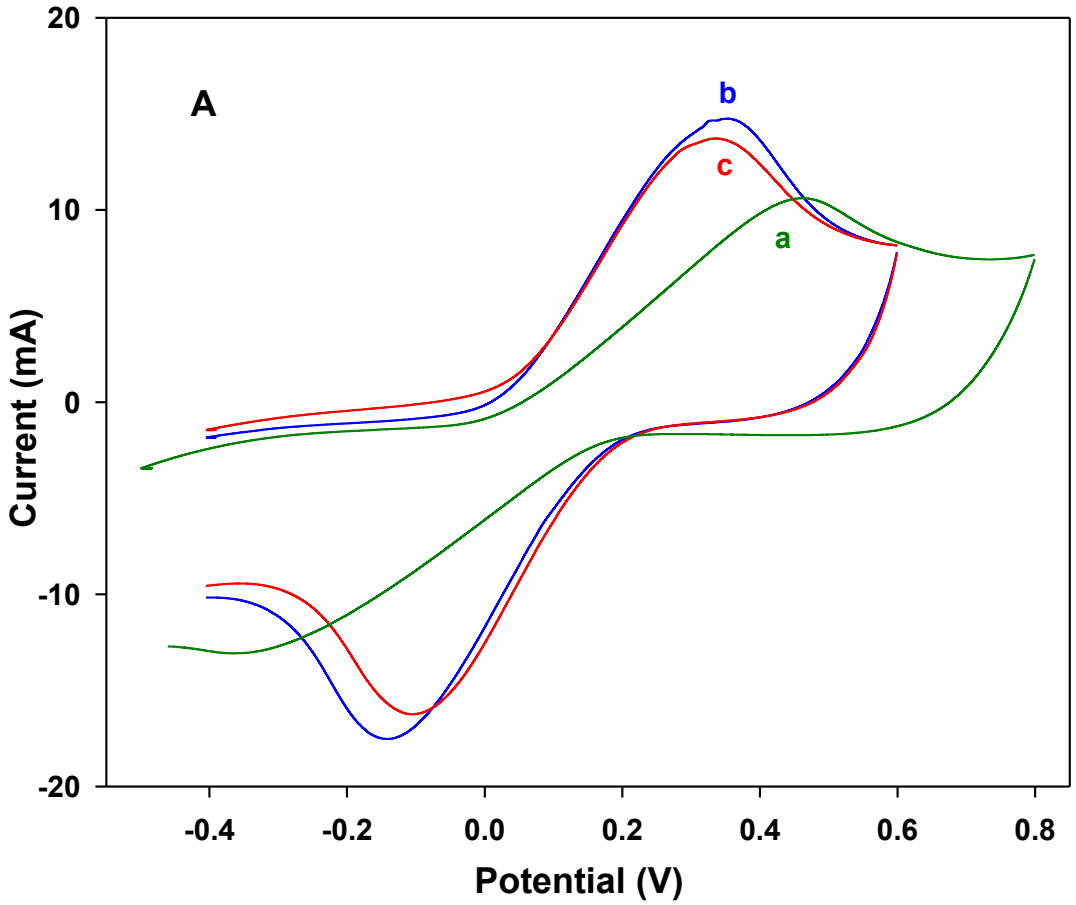

Figure 6.3. Cyclic voltammograms of Ti/BP (a), Ti/Au/BP (b), and Ti/Au/BP/GOx-HRP (c) electrodes at a scan rate of 50 $mV.s^{-1}$ in 0.1 M $K_3Fe(CN)_6$ + 0.1 M KCl + 0.1 M PBS solution pH 7.4.

As seen in the CV curves (Figure 6.4) recorded in 0.1 M PBS (pH 7.4), a pair of well-defined peaks centered at -0.19 and -0.5 V were observed for the Ti/Au/PB electrode, which can

be attributed to the surface functionalities of the activated buckypaper. The well-defined peaks disappeared after the immobilization of HRP with the aid of chitosan due to the interactions between the functional groups of the activated buckypaper with chitosan. In contrast, a pair of well-defined redox peaks located at -0.09 and -0.35 V appeared after the co-immobilization of HRP and GO_x with the aid of chitosan, showing the direct electrochemistry of the GO_x immobilized on the buckypaper.

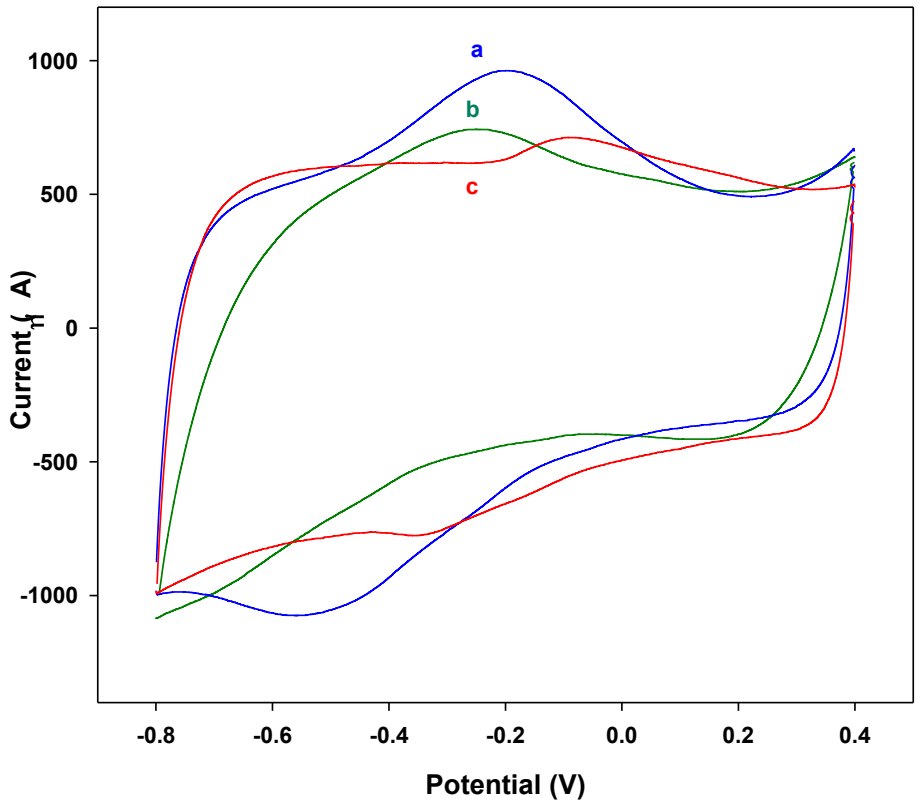

Figure 6.4. Cyclic voltammograms of Ti/Au/BP (a), Ti/Au/BP/HRP (b), and Ti/Au/BP/GOx-HRP (c) electrodes in PBS pH 7.4.

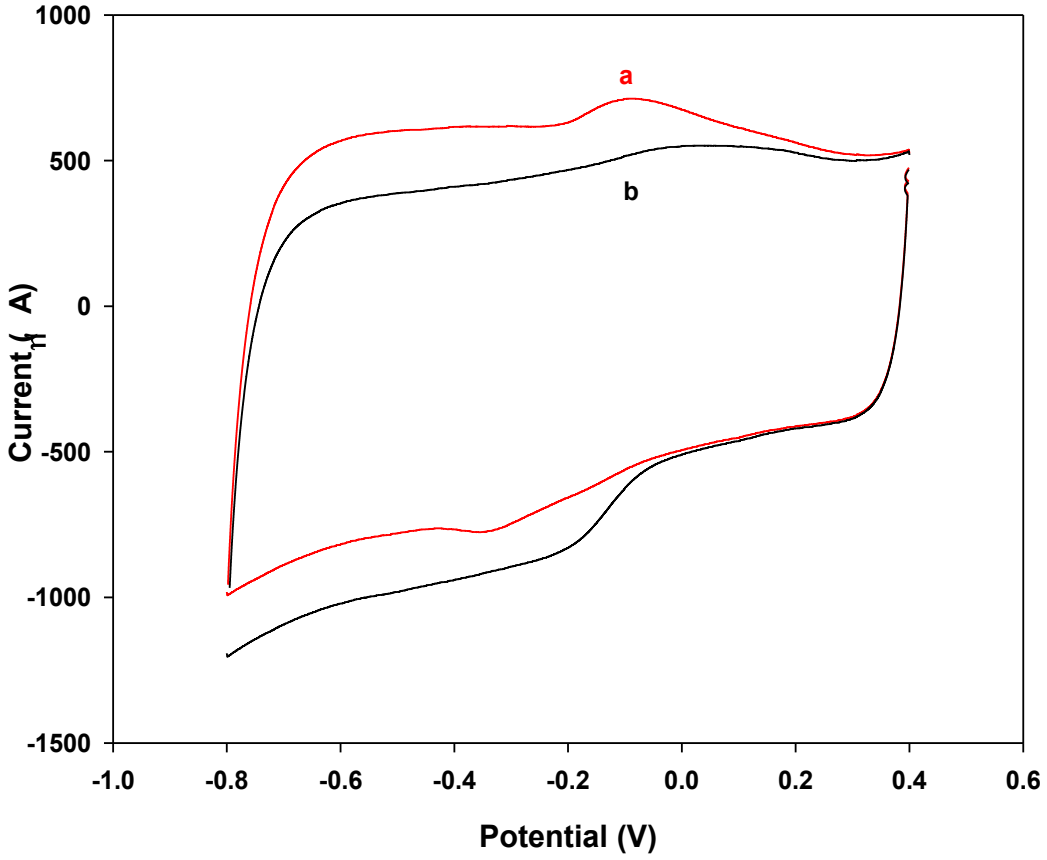

Figure 6.5. Cyclic voltammograms of Ti/Au/BP/GOx-HRP electrode before (a) and after (b) injection of 10 mM glucose at the scan rate of 10 $mV.s^{-1}$ in PBS pH 7.4.

The formal potential, E^0=1/2 (E_{pa} + E_{pc}), was calculated to be -0.22V. This indicates that the activated buckypaper improves the contact between the electrode surface and GO_x and decreases the overpotential required for the FAD/$FADH_2$ redox reaction.[36] The effect of the scan rate on the cyclic voltammograms of the Ti/Au/BP/GO_x-HRP electrode was studied in the range of 5 to 50 $mV.s^{-1}$ in 0.1M PBS. A pair of symmetric and well-defined redox peaks were obtained with a linear relationship between the current and scan rate, indicating that the redox process of the immobilized GO_x is a surface-controlled redox reaction rather than diffusion-controlled reaction.

The amount of the electroactive enzymes, Γ =Q/nFA, (where Q is the charge, n is the electron transfer number, F is the faraday constant, and A is the geometric area of the working electrode) was calculated to be 3.65×10^{-9} mol.cm^{-2}. This value is much higher than the theoretical value for a monolayer of GO_x (2.86×10^{-12} mol cm^{-2})[37] and a monolayer of HRP (8.5×10^{-12} mol cm^{-2})[38] and experimental values (7.52×10^{-10} mol cm^{-2} for GOx and 2.1×10^{-11} mol cm^{-2} for HRP) reported in the literature,[16, 39-41] indicating that the enzymes immobilized on the buckypaper effectively participated in the electron transfer.

We further studied the response of the Ti/Au/BP/GO_x-HRP electrode to glucose. As shown in Figure 6.5, upon addition of 10mM glucose, the oxidation peak current decreased while the reduction current significantly increased, showing a strong response to glucose. This can be attributed to the reduction of H_2O_2 generated by the oxidation of glucose by the immobilized GO_x as per the following equations:[15, 42-43]

$$\beta\text{-D-glucose} + GO_x\text{-FAD} \longrightarrow \delta\text{-D-gluconolactone} + GO_x\text{-FADH}_2 \quad (1)$$

$$GO_x\text{-FADH}_2 + O_2 \longrightarrow GO_x\text{-FAD} + H_2O_2 \quad (2)$$

$$HRP(Fe^{3+}) + H_2O_2 \longrightarrow CompoundI(Fe^{4+} = O) + H_2O \quad (3)$$

$$CompoundI(Fe^{4+} = O) + e^- + H^+ \longrightarrow CompoundII \quad (4)$$

$$CompoundII + e^- + H^+ \longrightarrow HRP(Fe^{3+}) + H_2O \quad (5)$$

GO_x, as a glycoprotein, oxidizes glucose to gluconolactone and hydrogen peroxide in the presence of oxygen. On the other hand, HRP, as an oxidative heme-containing enzyme, cleaves the O-O bond of hydrogen peroxide. Compound I is an intermediate comprising a ferryl species and a porphyrin radical cation; while Compound II is the second intermediate from the first reduction of the porphyrin radical cation, which retains the heme in the ferryl state.

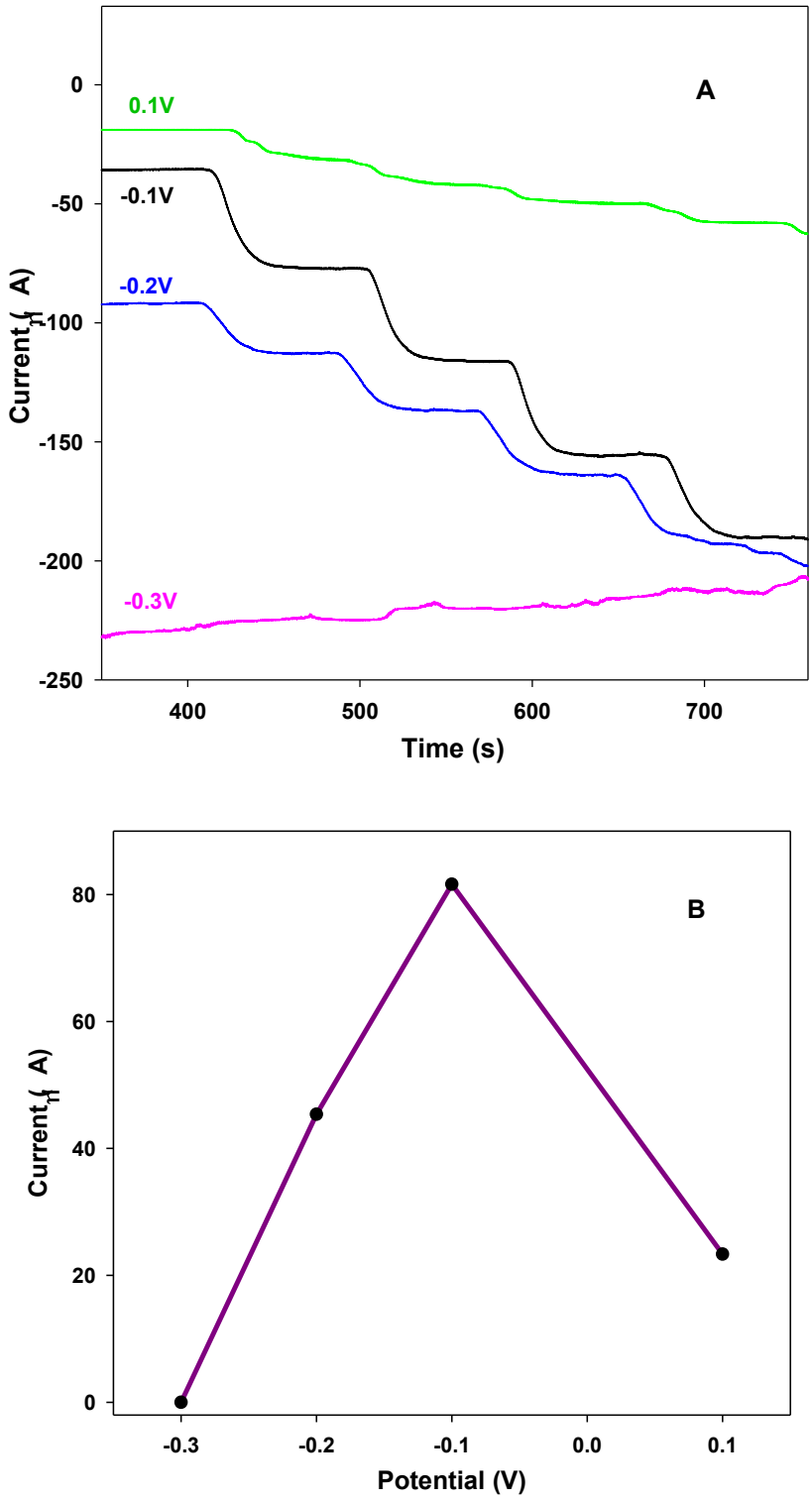

Figure 6.6 Amperometric response of the Ti/Au/BP/GOx-HRP electrode upon addition of 1mM glucose at different potentials (A), and the corresponding current change for 4mM glucose (B) in PBS at pH 7.4.

To achieve a maximum current response, the detection of glucose under optimized applied potential is necessary. Figure 6.6A shows the responses of the Ti/Au/BP/GO_x-HRP biosensor upon the successive addition of 2 mM glucose at different potentials. At 0.1V a small current response was observed. The cathodic current response to glucose significantly increased when the potential was lowered to -0.1V. By further lowering the electrode potential to -0.2 or -0.3 V, the current response decreased. Figure 6.6B compares the corresponding current response to 4mM glucose at different potentials, showing that -0.1V is the optimum potential for the Ti/Au/BP/GO_x-HRP biosensor.

The amperometric response of the Ti/Au/BP/GO_x-HRP biosensor at the optimized potential under the physiological pH 7.4 upon the successive addition of 1 mM glucose is shown in Figure 6.7A. For comparison, the amperometric response of the Ti/Au/BP electrode is also included in Figure 6.7A. No obvious current response was observed at the non-enzymatic electrode, while a strong response was achieved by the enzymatic electrode. Figure 6.7B shows the corresponding current *vs.* glucose concentration plot for the biosensor. A linear relationship with a correlation coefficient R^2 of 0.993 was obtained in the glucose range of over 9 mM, which effectively covers the normal physiological glucose range (3-7 mM). The sensitivity and the detection limit of the fabricated biosensor are thus estimated to be 20 $\mu A.mM^{-1}.cm^{-2}$ and 0.01 mM, respectively.

To examine the ability of the biosensor to detect low concentrations of glucose, the amperometric study was further conducted with the injection of 0.25 mM glucose under the same experimental conditions. As shown in Figure 6.8A, a strong response to each injection was observed.

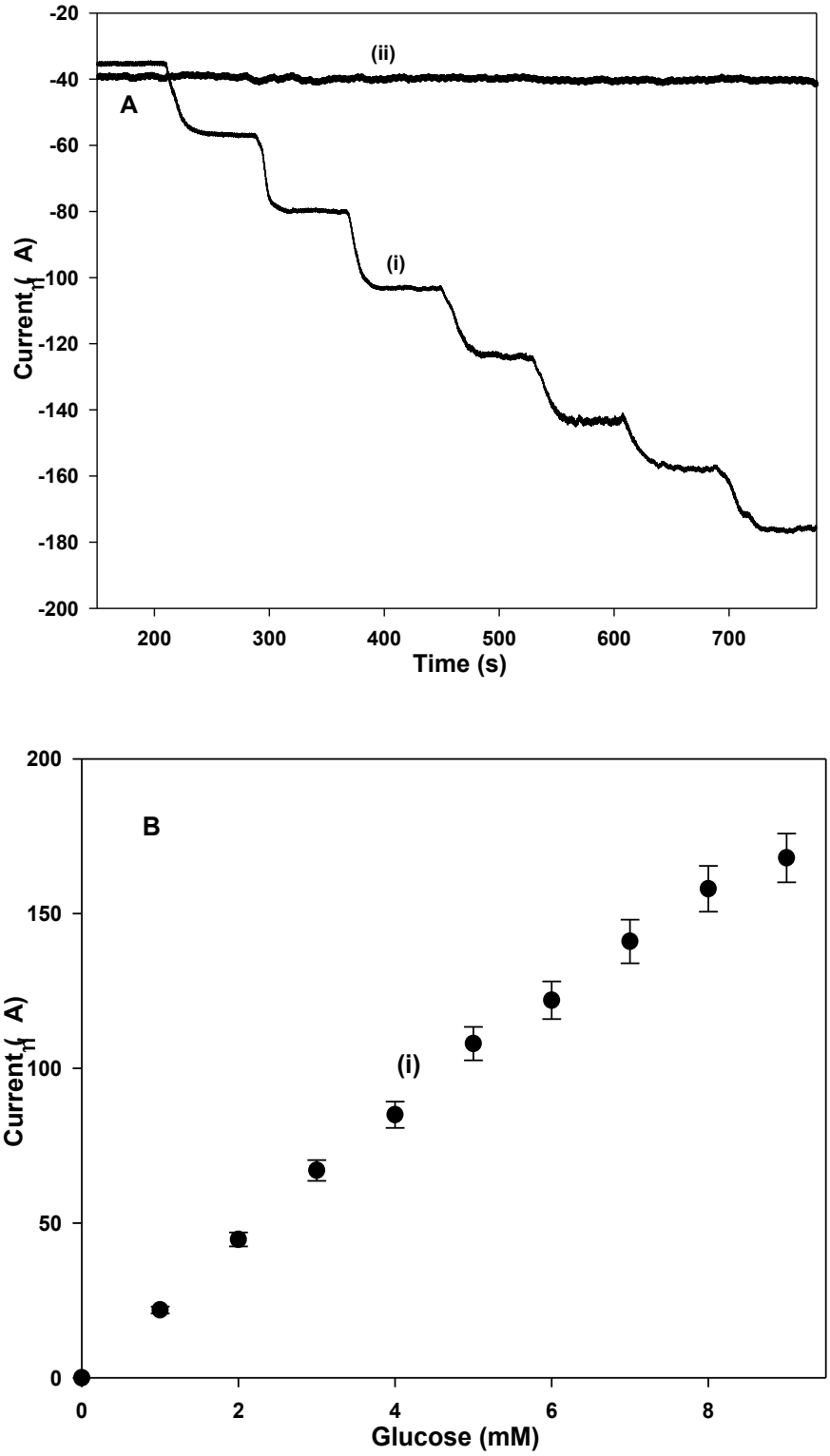

Figure 6.7. Amperometric response and calibration curve of the Ti/Au/BP/GOx-HRP (i) and Ti/Au/BP (ii) electrodes upon addition of 1 mM glucose (A and B).

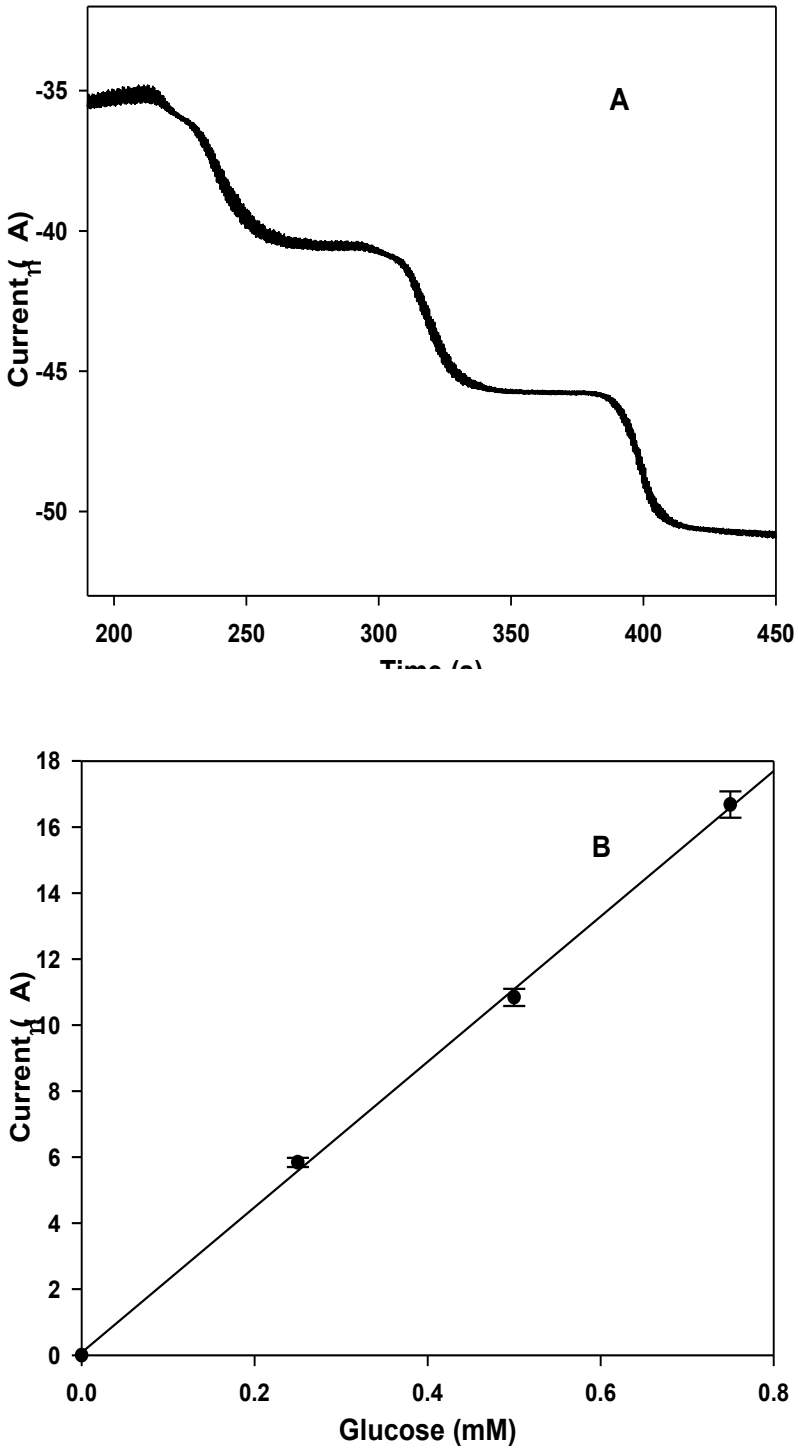

Figure 6.8. Amperometric response and calibration curve of the Ti/Au/BP/GOx-HRP upon addition of 0.25 mM (C and D) at -0.1V in PBS pH 7.4.

A linear relationship with a correlation coefficient R^2 of 0.993 (Figure 6.8B) was obtained in the range of 0-0.75 mM glucose. The calculated sensitivity is as high as the one determined from Figure 6.7B for the 1 mM successive injection, further showing that the biosensor is very sensitive to glucose.

To evaluate the efficiency of the immobilized enzymes, the apparent Michaelis-Menten constant, K_M^{app} can be determined using the following "Lineweaver-Burk" type equation:

$$1/I_{ss} = (K_M^{app}/I_{max})\ (1/C) + 1/I_{max}$$

where I_{max} and I_{ss} are the currents measured for enzymatic product detection under conditions of substrate saturation and steady state, respectively, for a given substrate concentration C.[44-45] This equation allows us to plot the experimental I_{max}/I_s *vs.* 1/C to determine K_M^{app} from the slope of the resultant linear plot. The value of $K_M^{app}$was obtained to be 4.67 mM for the fabricated biosensor. This low K_M^{app}value reflects the efficient enzyme immobilization process proposed in this study.

6.3.3. Selectivity of the biosensor

To investigate the selectivity of the Ti/Au/BP/GO_x-HRP biosensor, we tested its response to the common interfering species including ascorbic acid (AA), uric acid (UA) and acetamidophenol (AP).

As shown in Figure 6.9, there is no salient current response upon the addition of the interferents at their physiological level, 0.1 mM AA, 0.1 mM UA and 0.1 mM AP. In contrast, a strong response to the successive injection of 1 mM glucose was observed in the presence of all the three common interfering species, showing that the Ti/Au/BP/GO_x-HRP biosensor allows for the highly selective quantification of glucose without the usage of membranes or metal particles.

6.3.4. Stability of the biosensor

The stability of the fabricated biosensor was further investigated. The biosensor was tested once a week in a stirring cell during the electrochemical measurements. It was stored in 0.1 M PBS (pH 7.4) at 4 ºC when not in use. Figure 6.10A presents the amperometric response of the Ti/Au/BP/GO_x-HRP biosensor at the beginning (red line) and after 80 days (black line) upon addition of 1.2 mM glucose at -0.1 V in 0.1 M PBS (pH 7.4), revealing that the biosensor retained 94% of its initial current response after such a long period of time.

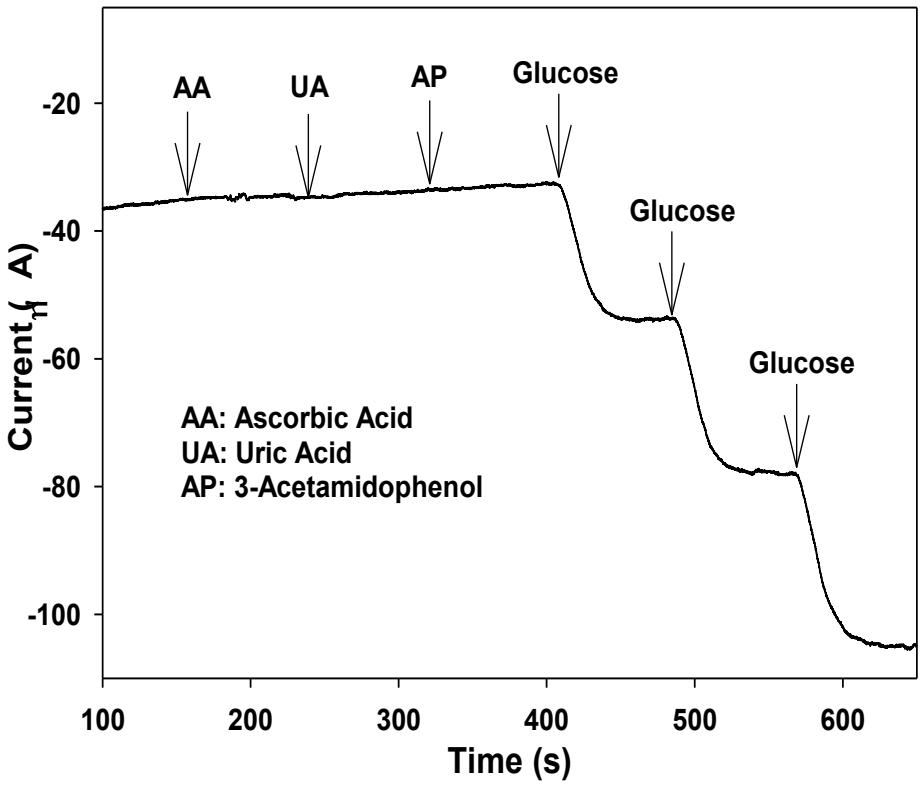

Figure 6.9. Amperometric response of the Ti/Au/BP/GOx-HRP electrode upon successive addition of 1mM glucose in the presence of interferents AA (ascorbic acid), UA (uric acid), AP (3-Acetamidopheol) at -0.1 V in PBS pH 7.4.

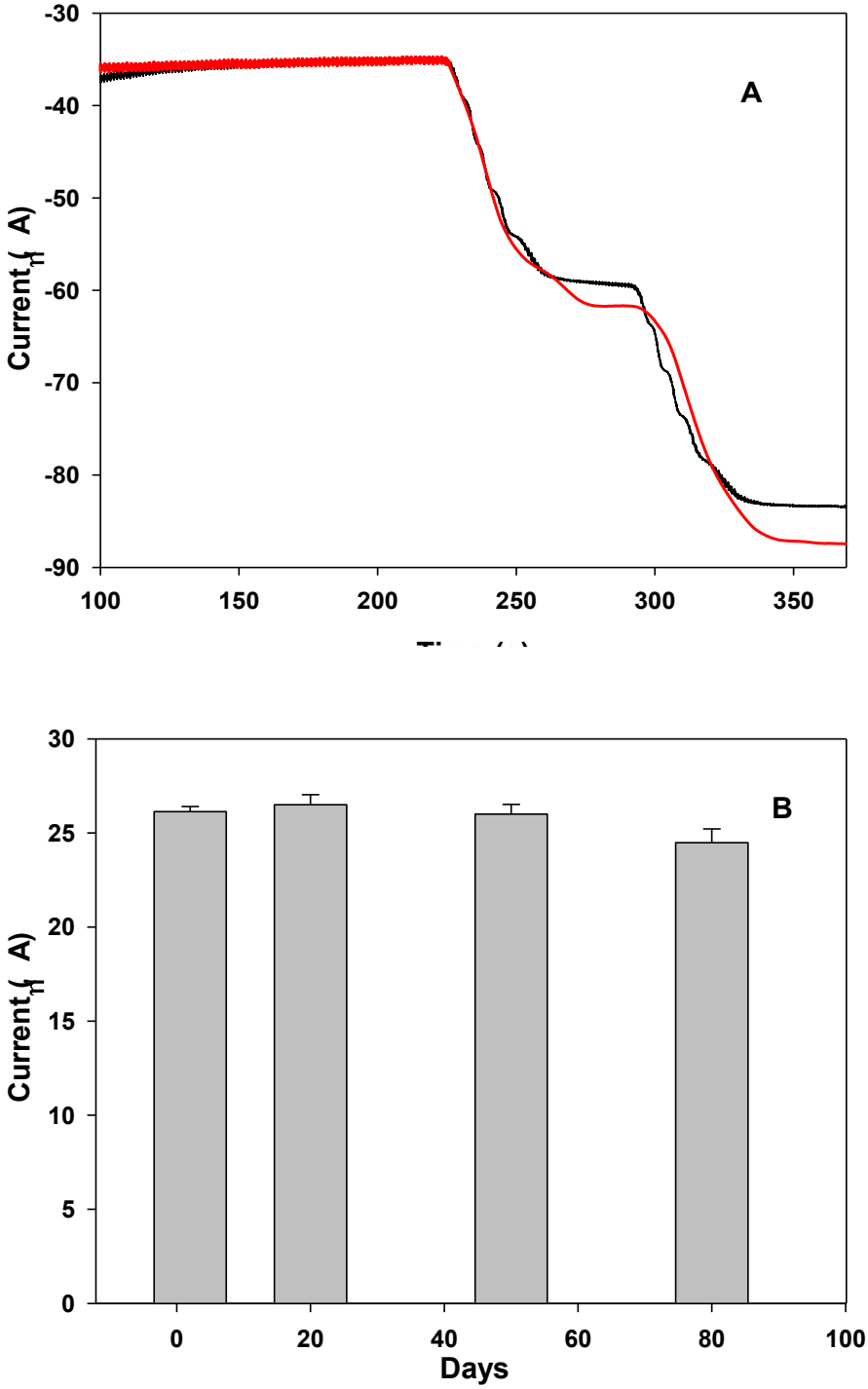

Figure 6.10. (A) Amperometric response of the Ti/Au/BP/GOx-HRP electrode initially (red line) and after a period of 80 days (black line) upon addition of 1.2 mM glucose at -0.1 V in PBS pH 7.4. (B) Comparison of the current response of the Ti/Au/BP/GOx-HRP electrode to 1.2 mM glucose during the 80-day stability tests.

Three biosensors were prepared and tested for their stability. Figure 6.10B presents the amperometric response of the biosensors versus time. The relative standard deviation (RSD) of their response to glucose was 3.0%. Over 98% of their initial current response was retained during the first 50 days. The reproducibility of the biosensor for the current response was also tested, showing that the RSD was 3.5% for 10 successive measurements of 1mM glucose at -0.1V in 0.1M PBS (pH 7.4).

We further compared the performance of the biosensor developed in this study with that of the various CNT-based glucose biosensors reported in the literature. As seen in Table 6.1, the mediator-free biosensor developed in this study possesses remarkable properties in terms of linear dynamic range and stability compared to the other mediator-based and mediator-less biosensors. During the 80-day stability tests, the biosensors were washed each time and the temperature was changed regularly between 4 ^{o}C and room temperature. The long lifetime shows that the Ti/Au/BP/GO_x-HRP biosensor fabricated by the innovative procedure proposed in this study possesses high thermal stability and excellent mechanical strength. This can be attributed to the efficient immobilization of the enzymes along with the unique physical and chemical properties of the activated buckypaper. The interaction between the Au thin film sputtered on the Ti substrate and the buckypaper with the aid of chitosan is so strong that it is almost impossible to remove the buckypaper from the substrate without breaking the buckypaper film. Chitosan contains primary amines, hydroxyl and acetyl groups which under weakly acidic conditions are protonated. These charged functional groups on chitosan molecules might induce strong adsorption of chitosan onto the surface of Au in the way similar to the modification of Au surface with charged alkanethiols.[46] To decipher the significant role of the activated buckypaper in the fabrication of the biosensor with high stability, we carried out FTIR analysis. Figure 6.11

Table 6.1 Comparison of the performance of different carbon nanotube-based glucose biosensors.

Electrode modifier	Detection Limit (μM)	Linear Range (mM)	Stability % (day)	Detection Potential (V)
(Au-Pt)NPs/CNT/Au/GOx[18]	400	0.5-17.5	75 (25)	0.6
GCE/PB/MWNT/GOx[25]	12.7	0.0-8.0	85 (14)	0.0
GCE/CNT-PtNPs/GOx[6]	0.5	0.5×10^{-3}-5.0	N/A	0.55
PDDA/GOx/PDDA/CNT/GCE[49]	7.0	15×10^{-3}-6.0	90 (30)	-0.1
MWNT/Nafion/GCE/GOx[17]	4.0	25×10^{-3}-2	N/A	0.7
GCE/CNT-CHIT-GDI-GDH[50]	3.0	5×10^{-3}-0.3×10^{-3}	80 (4)	0.4
SWNTs/Nafion/GCE/FMCA[24]	6.0	0.0-6.0	N/A	0.3
GC/CNT/HRP-GOx/Nafion[31]	0.5	0.025-0.4	97 (7)	0.0
Au/SWNT/GOD-HRP/PPy[32]	90	0.030-2.43	67 (14)	-0.1
HRP-GOxCNT/PAMAM[33]	2.5	0.004-1.2	N/A	-0.34
GOD–HRP–Cys–SG/GNP/ITO[34]	10	0.02-3.2	80 (5)	-0.1
Proposed biosensor	10	0.0-9.0	94 (>80)	-0.1

GCE: glassy carbon electrode, GOx: glucose oxidase, MWNTs: multi-walled carbon nanotubes, PB: Prussian blue, PDDA: polydiallyldimethylammonium chloride, SWNTs: single-walled carbon nanotubes, Au: gold, PtNPs: Platinum nanoparticles, CNT: carbon nanotubes, CHIT: chitosan, GDI: glutaric dialdehyde, GDH: glucose dehy-drogenase; FMCA: ferrocene monocarboxylic acid; PPy: polypyrrole; PAMAM: poly(amidoamine); Cys: L-Cysteine; SG: sol-gel; ITO: indium tin oxide; N/A: not available.

presents the FTIR spectra of the activated buckypaper (a), chitosan immobilized on the activated buckypaper (b), and chitosan (c). For the activated buckypaper (Figure 6.11a), several strong peaks were observed. The peaks located at 1719 and 1652 cm^{-1} can be assigned to the C=O stretching vibration of -COOH and $-COO^-$ groups, respectively, which were generated during the electrochemical treatment. The peaks at 1597, 1505 and 1448 cm^{-1} could be attributed to the C=C aromatic vibration[23, 47-48] reports.

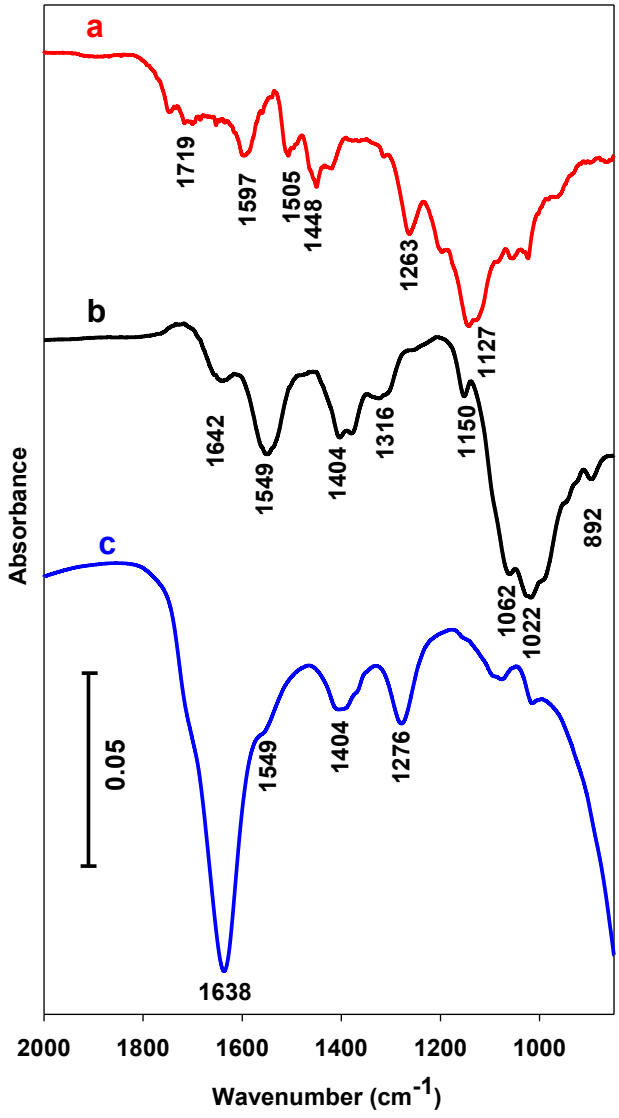

Figure 6.11. FT-IR spectra of activated buckypaper (a), chitosan on the activated buckypaper (b), and chitosan (c).

The FTIR spectrum of chitosan (Figure 6.11c) contains the C-N stretching at 1404 cm^{-1} and NH_2 bending vibration modes at ~1549 and 1638 cm^{-1}. The upshift in this region observed in the spectrum of the chitosan-buckypaper indicates a strong interaction between the –COOH and –NH_2 groups and the formation of –NHCO- (Figure 6.11b). The very strong peaks at 1022 and 1062 cm^{-1} are the typical stretching vibration of the C-O bond. The peak at 1638 cm^{-1} in the spectrum of chitosan which can be related to the N-H of amide (I) group, almost disappeared in the spectrum of chitosan-buckypaper. The spectrum of the activated buckypaper shows strong peaks at 1200 and 1263 cm^{-1} which can be attributed to C-O aliphatic group and C-O of carboxylic acids, respectively. These two peaks also disappeared in the spectrum of chitosan-buckypaper. Two bands of the glucopyranose rings appeared at ca. 892 and 1150 cm^{-1}, implying the attachment of chitosan to the activated buckypaper. These results confirm the functionalization of the buckypaper with chitosan, which has strong interactions with nucleophilic substitutions by primary and secondary amines that exist in abundance on the surface of the glycoprotein. Therefore, the interconnectivity of physically aggregated CNTs in the buckypaper, its compatibility and strong interactions with chitosan on one hand and chitosan interaction with the enzymes on the other hand may significantly enhance the interfacial adhesion and mechanical strength of the biosensor.

6.4. Conclusion

In summary, we have fabricated a mediator-free glucose biosensor based on the co-immobilization of GO_x and HRP on the activated buckypaper. Direct electrochemistry of GO_x on the buckypaper was observed. The glucose biosensor showed a high sensitivity, low detection

limit (0.01mM), fairly wide linear dynamic range (0-9 mM), long life-time (over 80 days) and high selectivity in the presence of common interferent species under the physiological condition. These properties of the buckypaper-based biosensor, coupled with the biocompatibility of its components are important factors which could be attractive for real-time in vivo glucose monitoring and lead to a substantial improvement in the management of diabetes. The facile and robust buckypaper-based platform proposed in this study opens many opportunities for the development of high-performance electrochemical biosensors for medical diagnostics and environmental monitoring.

References

1. Kang, I.; Schulz, M. J.; Kim, J. H.; Shanov, V.; Shi, D., A Carbon Nanotube Strain Sensor for Structural Health Monitoring. *Smart Mater. Struct.* **2006,** *15*, 737-748.
2. Iijima, S., Helical Microtubules of Graphitic Carbon. *Nature* **1991,** *354*, 56 - 58.
3. Zhu, W.; Zheng, J. P.; Liang, R.; Wang, B.; Zhang, C.; Walsh, S.; Au, G.; Plichta, E. J., Highly-Efficient Buckypaper-Based Electrodes For PEMFC. *ESC Trans.* **2008,** *16*, 1615-1626.
4. Meng, C.; Liu, C.; Fan, S., Flexible Carbon Nanotube/Polyaniline Paper-Like Films and their Enhanced Electrochemical Properties. *Electrochem. Commun.* **2009,** *11* 186-189.
5. Kwon, K. Y.; Yang, S. B.; Kong, B.-S.; Kim, J.; Jung, H.-T., High-Performance Biosensors Based on Enzyme Precipitate Coating in Gold Nanoparticle-Conjugated Single-Walled Carbon Nanotube Network Films. *Carbon* **2010,** *48*, 4504-4509.
6. Hrapovic, S.; Liu, Y.; Male, K. B.; Luong, J. H. T., Electrochemical Biosensing Platforms Using Platinum Nanoparticles and Carbon Nanotubes. *Anal. Chem.* **2004,** *76*, 1083-1088.

7. Wang, Z.; Liang, Z.; Wang, B.; Zhang, C.; Kramer, L., Processing and Property Investigation of Single-Walled Carbon Nanotube (SWNT) Buckypaper/Epoxy Resin Matrix Nanocomposites. *Composites: A* **2004,** *35*, 1225-1232.

8. Collins, P.; Zettl, A.; Bando, H.; Thess, A.; Smalley, R., Nanotube Nanodevice. *Science* **1997,** *278*, 100-103.

9. Ma, Y.; Cheung, W.; Wei, D.; Bogozi, A.; Chiu, P. L.; Wang, L.; Pontoriero, F.; Mendelsohn, R.; He, H., Improved Conductivity of Carbon Nanotube Networks by In Situ Polymerization of a Thin Skin of Conducting Polymer. *ACS Nano* **2008,** *2*, 1197-1204.

10. Zengin, H.; Zhou, W.; .Jin, J.; Czerw, R.; Smith, J. D. W.; Echegoyen, L.; Carroll, D. L.; Foulger, S. H.; Ballato, J., Carbon Nanotube Doped Polyaniline. *Adv. Mater.* **2002,** *14*, 1480–1483.

11. Park, C.; Ounaies, Z.; Watson, K.; Crooks, R.; Smith, J. J.; Lowther, S.; Connell, J.; Siochi, E.; Harrison, J.; Clair, S. T., Dispersion of Single Wall Carbon Nanotubes by In Situ Polymerization Under Sonication. *Chem. Phys. Lett.* **2002,** *364*, 303.

12. Garg, A.; Sinnott, S., Effect of Chemical Functionalization on the Mechanical Properties of Carbon Nanotubes. *Chem. Phys. Lett.* **1998,** *295*, 273.

13. Rubianes, M. D.; Rivas, G. A., Carbon Nanotubes Paste Electrode. *Electrochem. Commun.* **2009,** *5*, 689-694.

14. Rakhi, R. B.; Sethupathi, K.; Ramaprabhu, S., A Glucose Biosensor Based on Deposition of Glucose Oxidase onto Crystalline Gold Nanoparticle Modified Carbon Nanotube Electrode. *J. Phys. Chem. B* **2009,** *113*, 3190-3194.

15. Liu, Y.; Wang, M.; Zhao, F.; Xu, Z.; Dong, S., The Direct Electron Transfer of Glucose Oxidase and Glucose Biosensor Based on Carbon Nanotubes/Chitosan Matrix. *Biosens. Bioelectron.* **2005,** *21*, 984-988.

16. Deng, C.; Chen, J.; Nie, Z.; Si, S., A Sensitive and Stable Biosensor Based on the Direct Electrochemistry of Glucose Oxidase Assembled Layer-By-Layer at the Multiwall Carbon Nanotube-Modified Electrode. *Biosens. Bioelectron.* **2010,** *26*, 213-219.

17. Tsai, Y.-C.; Li, S.-C.; Chen, J.-M., Cast Thin Film Biosensor Design Based on a Nafion Backbone, a Multiwalled Carbon Nanotube Conduit, and a Glucose Oxidase Function. *Langmuir* **2005,** *21*, 3653-3658.

18. Chu, X.; Dua, D.; Shen, G.; Yu, R., Amperometric Glucose Biosensor Based on Electrodeposition of Platinum nanoparticles onto Covalently Immobilized Carbon Nanotube Electrode. *Talanta* **2007,** *71*, 2040-2047.

19. Wang, J.; Liu, G.; Jan, M. R., Ultrasensitive Electrical Biosensing of Proteins and DNA: Carbon-Nanotube Derived Amplification of the Recognition and Transduction Events. *J. Am. Chem. Soc.* **2004,** *126*, 3010-3011.

20. Azamian, B. R.; Davis, J. J.; Coleman, K. S.; Bagshaw, C. B.; Green, M. L. H., Bioelectrochemical Single-Walled Carbon Nanotubes. *J. Am. Chem. Soc.* **2002,** *124*, 12664-12665.

21. Li, F.; Wang, Z.; Shan, C.; Song, J.; Han, D.; Niu, L., Preparation of Gold Nanoparticles/Functionalized Multiwalled Carbon Nanotube Nanocomposites and its Glucose Biosensing Application. *Biosens. Bioelectron.* **2009,** *24*, 1765-1770.

22. Li, F.; Song, J.; Li, F.; Wang, X.; Zhang, Q.; Han, D.; Ivaska, A.; Niu, L., Direct Electrochemistry of Glucose Oxidase and Biosensing for Glucose Based on Carbon Nanotubes@SnO_2-Au Composite. *Biosens. Bioelectron.* **2009,** *25*, 883-888.

23. Cai, C.; Chen, J., Direct Electron Transfer of Glucose Oxidase Promoted by Carbon Nanotubes. *Anal. Biochem.* **2004,** *332*, 75-83.

24. Liu, X.; Shi, L.; Niu, W.; Li, H.; Xu, G., Amperometric Glucose Biosensor Based on Single-Walled Carbon Nanohorns. *Biosens. Bioelectron.* **2008,** *23*, 1887-1890.

25. Zhu, L.; Zhai, J.; Guo, Y.; Tian, C.; Yang, R., Amperometric Glucose Biosensors Based on Integration of Glucose Oxidase onto Prussian Blue/Carbon Nanotubes Nanocomposite Electrodes. *Electroanalysis* **2006,** *18*, 1842-1846.

26. Deng, L.; Wang, Y.; Shang, L.; Wen, D.; Wang, F.; Dong, S., A Sensitive NADH and Glucose Biosensor Tuned by Visible Light Based on Thionine Bridged Carbon Nanotubes and Gold Nanoparticles Multilayer. *Biosens. Bioelectron.* **2008,** *24*, 951-957.

27. Wang, J., Electrochemical Glucose Biosensors. *Chem. Rev.* **2008,** *108*, 814-825.

28. Ahmadalinezhad, A.; Kafi, A. K. M.; Chen, A., Glucose Biosensing Based on the Highly Efficient Immobilization of Glucose Oxidase on a Prussian Blue Modified Nanostructured Au Surface. *Electrochem. Commun.* **2009,** *11*, 2048-2051.

29. Newman, J. D.; White, S. F.; Tothill, I. E.; Tumer, A. P. F., Catalytic Materials, Membranes, and Fabrication Technologies Suitable for the Construction of Amperometric Biosensors. *Anal. Chem.* **1995,** *67*, 4594.

30. Benvenuto, P.; Kafi, A. K. M.; Chen, A., High Performance Glucose Biosensor Based on the Immobilization of Glucose Oxidase onto Modified Titania Nanotube Arrays. *J. Electroanal. Chem.* **2009,** *627*, 76-81.

31. Yao, Y.-L.; Shiu, K.-K., A Mediator-Free Bienzyme Amperometric Biosensor Based on Horseradish Peroxidase and Glucose Oxidase Immobilized on Carbon Nanotube Modified Electrode. *Electroanalysis* **2008,** *20*, 2090-2095.

32. Zhu, L.; Yang, R.; Zhai, J.; Tian, C., Bienzymatic Glucose Biosensor Based on Co-Immobilization of Peroxidase and Glucose Oxidase on a Carbon Nanotubes Electrode. *Biosens. Bioelectron.* **2007,** *23*, 528-535.

33. Zeng, Y.-L.; Huang, Y.-F.; Jiang, J.-H.; Zhang, X.-B.; Tang, C.-R.; Shen, G.-L.; Yu, R.-Q., Functionalization of Multi-Walled Carbon Nanotubes with Poly(amidoamine) Dendrimer for Mediator-Free Glucose Biosensor. *Electrochem. Commun.* **2007,** *9*, 185-190.

34. Gu, M.; Wang, J.; Tu, Y.; Di, J., Fabrication of Reagentless Glucose Biosensors: A Comparison of Mono-Enzyme GOD and Bienzyme GOD-HRP Systems. *Sensor Actuat. B: Chem.* **2010,** *148*, 486-491.

35. Bard, A. J.; Faulkner, L. R., *Electrochemical Methods-Fundamentals and Applications*. John Wiley and Sons: New York, 2000.

36. Wang, J.; Li, M.; Shi, Z.; Li, N.; Gu, Z., Direct Electrochemistry of Cytochrome C at a Glassy Carbon Electrode Modified with Single-Wall Carbon Nanotubes. *Anal. Chem.* **2002,** *74*, 1993-1997.

37. Jin-Zhong, X.; Jun-Jie, Z.; Qiang, W.; Zheng, H.; Hong-Yuan, C., Direct Electron Transfer Between Glucose Oxidase and Multi-walled Carbon Nanotubes. *Chin. J. Chem.* **2003,** *21*, 1088-1091.

38. Liu, G.; Gooding, J. J., An Interface Comprising Molecular Wires and Poly(ethylene glycol) Spacer Units Self-Assembled on Carbon Electrodes for Studies of Protein Electrochemistry. *Langmuir* **2006,** *22*, 7421-7430.

39. Huang, Y.; Zhang, W.; Han Xiao, G. L., An Electrochemical Investigation of Glucose Oxidase at a CdS Nanoparticles Modified Electrode. *Biosens. Bioelectron.* **2005,** *21*, 817-821.

40. Deng, S.; Jian, G.; Lei, J.; Hu, Z.; Ju, H., A Glucose Biosensor Based on Direct Electrochemistry of Glucose Oxidase Immobilized on Nitrogen-Doped Carbon Nanotubes. *Biosens. Bioelectron.* **2009,** *25*, 373-377.

41. Zhao, X.; Mai, Z.; Kang, X.; Zou, X., Direct Electrochemistry and Electrocatalysis of Horseradish Peroxidase Based on Clay-Chitosan-Gold Nanoparticle Nanocomposite. *Biosens. Bioelectron.* **2008,** *23*, 1032-1038.

42. Rodriguez-Lopez, J. N.; Lowe, D. J.; Hernandez-Ruiz, J.; Hiner, A. N. P.; Garcia-Canovas, F.; Thorneley, R. N. F., Mechanism of Reaction of Hydrogen Peroxide with Horseradish Peroxidase: Identification of Intermediates in the Catalytic Cycle. *J. Am. Chem. Soc.* **2001,** *123*, 11838-11847.

43. Reilly, C. A.; Aust, S. D., Peroxidase Substrates Stimulate the Oxidation of Hydralazine to Metabolites Which Cause Single-Strand Breaks in DNA. *Chem. Res. Toxicol.* **1997,** *10*, 328-334.

44. Kamin, R. A.; Wilson, G. S., Rotating Ring-Disk Enzyme Electrode for Biocatalysis Kinetic Studies and Characterization of the Immobilized Enzyme Layer. *Anal Chem* **1980,** *52*, 1198-1205.

45. Shu, F. R.; Wilson, G. S., Rotating Ring-Disk Enzyme Electrode for Surface Catalysis Studies. *Anal. Chem.* **1976,** *48*, 1679-1686.

46. Hu, K.; Bard, A. J., In Situ Monitoring of Kinetics of Charged Thiol Adsorption on Gold Using an Atomic Force Microscope. *Langmuir* **1998,** *14*, 4790-4794.

47. Chen, J.; Hamon, M. A.; Hu, H.; Chen, Y.; Rao, A. M.; Eklund, P. C.; Haddon, R. C., Solution Properties of Single-Walled Carbon Nanotubes. *Science* **1998,** *282*, 95-98.

48. Ortiz, R.; Mfirquez, O. P.; Mfirquez, j.; Guti&rez, C., FTIR Spectroscopy Study of the Electrochemical Reduction of CO_2 on Various Metal Electrodes in Methanol. *J. Electroanal. Chem.* **1995,** *390*, 99-107.

49. Liu, G.; Lin, Y., Amperometric Glucose Biosensor Based on Self-Assembling Glucose Oxidase on Carbon Nanotubes. *Electrochem. Commun.* **2006,** *8*, 251-256.

50. Zhang, M.; Smith, A.; Gorski, W., Carbon Nanotube-Chitosan System for Electrochemical Sensing Based on Dehydrogenase Enzymes. *Anal. Chem.* **2004,** *76*, 5045-5050.

Chapter 7

Controllable Growth of Titanium Dioxide Nanowire and its Size Effect on Electrochemical Biosensing*

7.1. Introduction

Over the past few decades, the development of bioactive and biocompatible materials has attracted much interest for a variety of prospective technological applications encompassing sensors,[1-3] drug delivery,[4] and chromatographic supports.[5] Such efforts aim to achieve miniaturized and cost effective devices with enhanced sensitivity and recognition limits for the detection of biomolecules. Proteins, as bio-recognition elements, are potentially capable of interacting with specific biomolecules and differentiating them electrochemically, while redox-active sites of proteins encounter an intrinsic barrier to direct electron transfer. This barrier emerges from the spatial configuration of protein components that surround and insulate the redox center.[6-7] Accordingly, various innovative strategies have been proposed and investigated with the aim of enabling electron transfer at the redox centers of proteins. Among them, the chemical modification of proteins,[8] protein wiring,[9-10] artificial mediators,[11-12] and nanostructured materials[13-15] have been extensively studied.

In the development of biosensors, nanostructure materials are particularly attractive due to their intrinsically high surface area, intimate and specific attachment of protein, and biocompatibility.[16-17] These biophysical attributes are likely to be contingent on the size, geometries, and composition of the nanostructures. The concept of utilizing inorganic, receptor

*Most of the results presented in this chapter have been submitted to a Peer-Reviewed Journal.

or ligand-modified nanowires and nanotubes for specific detection has been extended in various directions such as the real-time monitoring of biological and chemical species.[1, 3, 18] Inorganic nanotubes and nanowires may typically be prepared using two approaches: namely "top-down" and "bottom-up". It is desirable to precisely control the sizes and shapes of formed nanomaterials; however, it is often a challenge to achieve.

Among all inorganic nanomaterials, titanium dioxide (TiO_2), as a transition-metal oxide, has been extensively studied.[19-20] Exceptional biocompatibility and unique optical and electronic properties are some of the distinguishing features of TiO_2 that make it a promising substrate in protein-based assays.[13, 15, 21] Most recently, an optical interferometric biosensor based on TiO_2 nanotube arrays demonstrated the sensing of rabbit immunoglubin.

The synthesis of TiO_2 nanostructures is achievable using various top-down and bottom-up strategies, including sol-gel methods,[2, 13] template-assisted methods,[22] hydrothermal approaches,[23-24] ultrasound irradiation[25] and electrochemical means.[26] In addition, the composition, structure, and dimension of TiO_2 can be further tuned to optimize the performance of the TiO_2-based biosensors. Although TiO_2 has been explored in optical and electrochemical biosensing,[15, 27] to the best of our knowledge, there is no report to date that explicitly examines the effects of the dimensions and geometries of nanostructured TiO_2 on the performance of direct electron transfer with biomolecules. As a semiconductor, TiO_2 itself has low conductivity. Our recent study has shown that carbon nanomaterials possess high conductivity and that carbon based biosensors exhibit considerable longevity.[28] In this study, we hypothesized that the large surface area and biocompatibility of TiO_2 nanowires in conjunction with the high conductivity and easy functionalization of a carbon thin layer might allow for the effective immobilization of proteins such as enzymes to develop high-performance biosensors. These hybrid TiO_2 nanowires

may represent an efficient approach for „plugging" an electrode into an enzyme. Thus, the objective of this study is to explore whether it might be possible to facilitate the direct electrochemical detection of glucose using carbonized titanium oxide nanowires with a specific dimension.

7.2. Experimental

7.2.1. Materials

The buckypaper used in this study was produced by the High-Performance Materials Institute of Florida State University with a thickness of 0.035 mm. Glucose oxidase (EC 1.1.3.4, Type VII from Aspergillus niger) and β-D-glucose were purchased from Sigma and were used as received. Chitosan was purchased from Aldrich and titanium foils (99.2%) from Alfa Aesar. Horseradish peroxidase (HRP), potassium ferricyanide (K3Fe(CN)6), ascorbic acid, uric acid, 3-acetamidophenol were purchased from Sigma–Aldrich. All other reagents were of analytical grade. Water was purified with the Nanopure® water system (18 MΩ.cm) and was used in the preparation of all solutions. Various stock concentrations of β-D-glucose were prepared in 0.1M phosphate buffer, pH 7.4 and stored at 4 ºC. Glucose stock solutions were allowed to mutarotate overnight prior to use.

7.2.2. Synthesis and modification of TiO_2 nanowires

TiO_2 nanowires were prepared using a H_2O vapor assisted thermal oxidation process in the presence of potassium fluoride (KF). The procedure is described briefly below. Titanium plates (1.25 cm × 0.8 cm × 0.5 mm) (99.2%, Alfa Aesar), were ultrasonically cleaned in acetone, ethanol and water. Initially, a predetermined volume of KF solution was applied to the surfaces of pre-treated Ti plates (etched in 18% HCl at 85 ^{o}C for 15 min), after which the Ti plates were

transferred to a ceramic boat. The ceramic boat was next inserted into a quartz tube. After being purged with Argon for 1 h, the gas flow was switched to H_2O vapor. Subsequently, the quartz tube was heated to different temperatures (600 and 650 ^oC), which were maintained for 3 h. After thermal treatment, the input gas was switched back to a pure Argon flow until the furnace cooled to room temperature. Finally, the as-synthesized samples were rinsed several times using distilled water to remove any residual salts from the surfaces of the samples.

In order to fabricate the carbon coated TiO_2 nanowires, the as-synthesized TiO_2 nanowire samples were inserted into a quartz tube. After being purged with Argon for 1 h, the gas was switched to ethanol vapor. The quartz tube was then heated to 600 ^oC for 3 h. Following thermal treatment, the input gas was switched back to pure Argon until the furnace cooled to room temperature. The electrodes used in this work were carbonized under identical optimized conditions.

7.2.3. Structure characterization

The as-synthesized TiO_2 nanowires and carbon coated TiO_2 nanowires were characterized using scanning electron microscopy (JEOL JSM 5900LV) equipped with an energy dispersive X-ray spectrometer (Oxford Links ISIS operated at 20 kV) and transmission electron microscopy (JEOL 2010 microscope).

7.2.4. Biosensor preparation

In order to engender TiO_2 nanowires with the utility as a glucose biosensor, the electrodes were electrochemically activated. To activate the carbon-modified TiO_2 nanowire surface, cyclic voltammetry was performed in the range of -0.8 to 0.6 V at a scan rate of 10 $mV.s^{-1}$ in 0.1 M phosphate buffer solution (pH 7.4) until steady-state current-voltage was obtained, after which a

potential of 1.5 V was applied to the electrode for 90 s. The activated surface was then ready for the immobilization of glucose oxidase. To immobilize the enzyme, the electrodes were dipped into a solution of 5 $mg.mL^{-1}$ GO_x (EC 1.1.3.4, Type VII from Aspergillus niger) containing 0.01% Nafion. The adsorption of GO_x on the nanowires was confirmed by monitoring the attenuation of the electrochemical signal obtained in 0.1 M phosphate buffer solution (pH 7.4). All prepared biosensors were stored at 4 ˚C in 0.1 M phosphate buffer solution at pH 7.4 when not in use. All reagents were of analytical grade. Water was purified with the Nanopure® water system (18 MΩ.cm) and was used in the preparation of all solutions. Stock solutions of β-D-glucose were prepared in 0.1 M phosphate buffer at pH 7.4 and stored at 4 ˚C. Glucose stock solutions were allowed to mutarotate overnight prior to use.

7.2.5. Electrochemical measurement

Cyclic voltammetry and amperometric measurements were performed using an electrochemical workstation (CHI660, CH Instrument Inc., USA) connected with an in-house-built, three-electrode glass cell (30 mL). A platinum coil was used as the counter electrode and was flame-annealed prior to each experiment. Ag/AgCl (3 M KCl) was used as the reference electrode. The constructed biosensors were employed as the working electrodes. Cyclic voltammetry was conducted before and after carbonization in a solution of 20 mM $K_3Fe(CN)_6$ + 0.1 M KCl in 0.1 M phosphate buffer (pH 7.4) at a scan rate of 20 $mV.s^{-1}$. All measurements were conducted at room temperature (22 ± 2 °C).

7.2.6. TiO_2 nanowire based biosensing experiment

Electrochemical signals were measured through cyclic voltammetry prior to and following GO_x immobilization, as well as upon injection of glucose in a 0.1 M phosphate buffer (pH 7.4) at

a scan rate 20 $mV.s^{-1}$. The detection limit was calculated through S/N=3. At least five independent trials were used to generate each data set described in the above article. In order to evaluate the electron rate coefficient and constant, CVs were conducted at a scan rate range of 5 to 500 $mV.s^{-1}$ in the buffer solution (pH 7.4). To investigate the selectivity of the biosensor, we tested its response to common interfering species including ascorbic acid (AA), uric acid (UA) and acetamidophenol (AP) at their physiological concentration levels.

7.2.7. Human serum glucose measurement

These measurements were performed by chronoampermetry at the potential of 0.35 V for 100 s in a diluted and undiluted human serum sample. The human serum was derived from male AB plasma (from Sigma). Comparison tests were performed with a commercially available Blood Glucose Monitoring System with the brand name of Ultra2®. The data were collected from five samples for each concentration.

7.3. Results and discussion

Scheme 7.1 illustrates the procedure proposed in this study for the fabrication of the TiO_2 nanowire based biosensor. A facile thermal oxidation (TO) method was developed for the direct growth of TiO_2 nanowires with different dimensions on Ti substrates (Scheme 7.1a & b). Subsequently, a thin layer of carbon was deposited on the surfaces of the TiO_2 nanowires using chemical vapour deposition (Scheme 7.1c). Finally, glucose oxidase was immobilized onto the carbonized TiO_2 nanowires activated using facile electrochemical method (Scheme 7.1d).

7.3.1. Surface morphological studies

To study the size effect, we explored whether a thermal oxidation method might be employed in the creation of TiO_2 nanowires with different dimensions, as it has been used previously in the synthesis of one-dimensional silica and ZnO nanostructures.[29-31] We successfully developed and modified the TO technique to directly grow TiO_2 nanowires with controllable dimensions. Figure 7.1 and 7.2 show typical SEM images of the TiO_2 nanowires having a length of ~ 1 μm (Figure 7.1) and ~ 2 μm (Figure 7.2), grown at 600 and 650˚C, respectively, for 3 h on titanium plates.

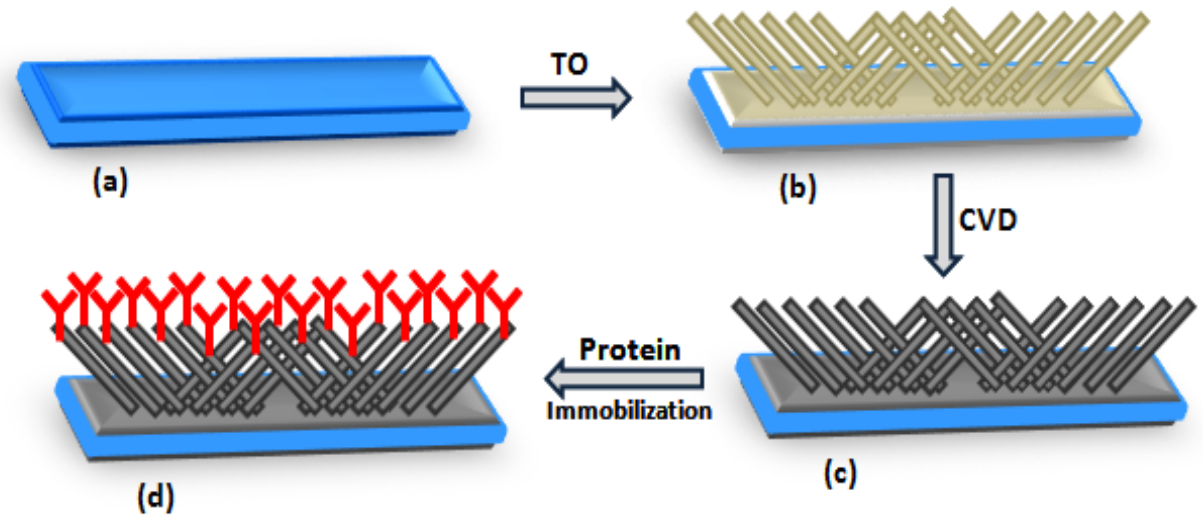

Scheme 7.1. Diagram for the preparation of the TiO_2 nanowire based biosensor. (a) a bare titanium plate; (b) TiO_2 nanowires grown on titanium plate by H_2O assisted thermal oxidation method; (c) deposition of a thin layer of carbon on TiO_2 nanowires by CVD ; (d) immobilization of enzyme.

The electron diffraction pattern in Figure 7.3A facilitated the identification of the crystal structure of the TiO_2 nanowires as being in the tetrahedral rutile phase.

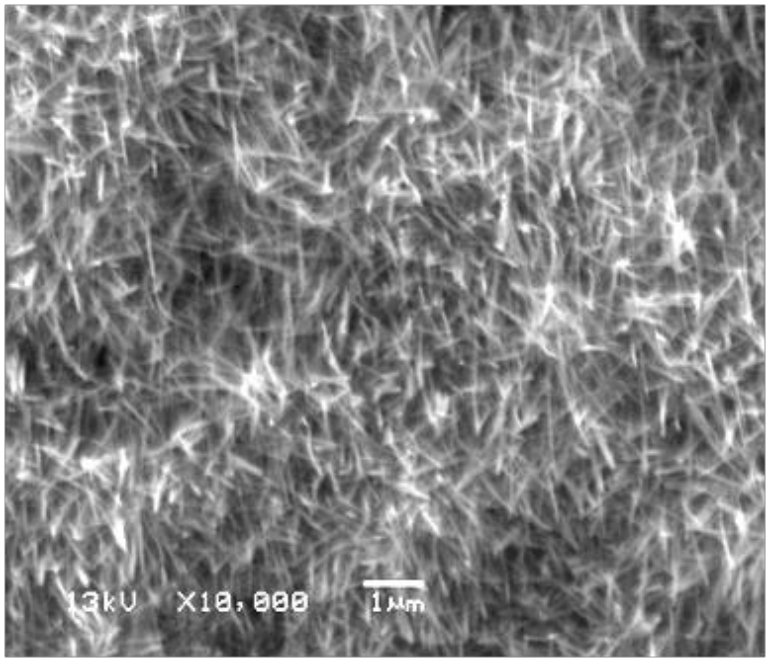

Figure 7.1. SEM images of carbon-modified TiO_2 nanowires with dimensions of 50 nm × 1 μm.

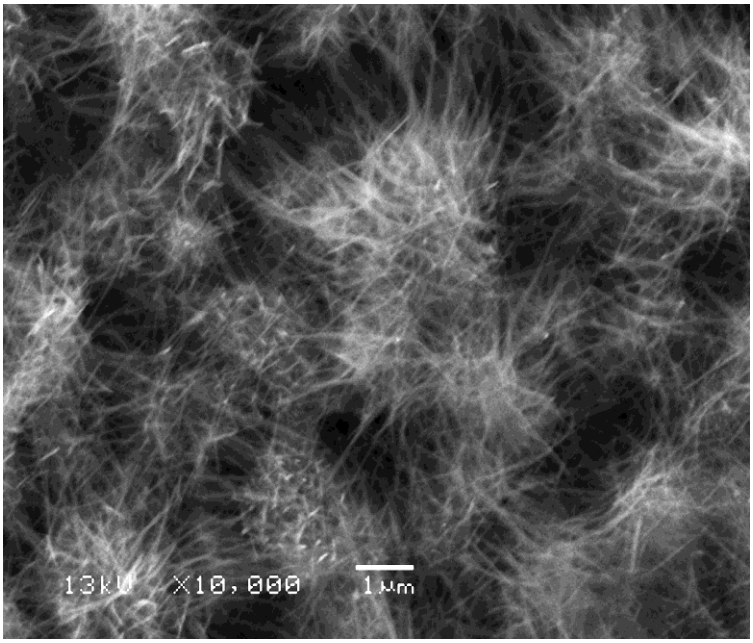

Figure 7.2. SEM images of carbon-modified TiO_2 nanowires with dimensions of 80 nm × 2 μm.

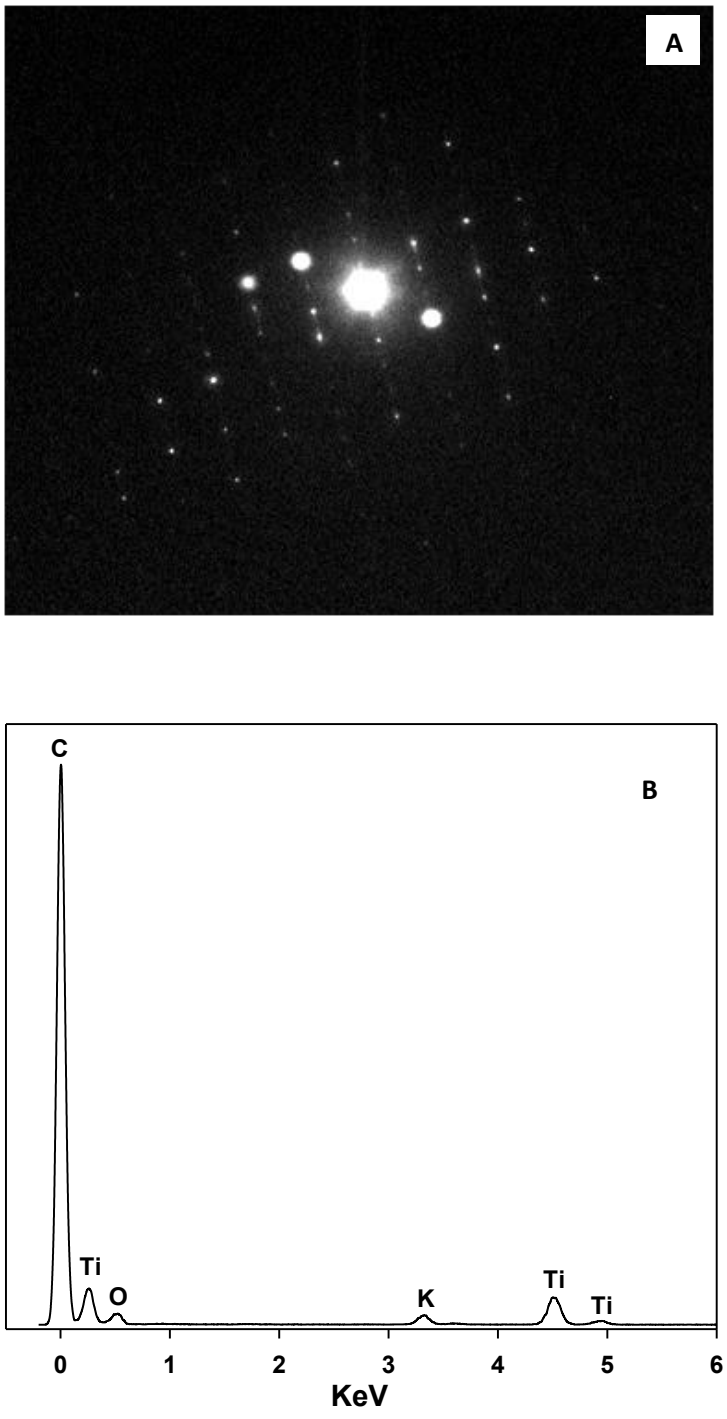

Figure 7.3. SAED pattern of nanowires (A), and the corresponding EDS spectrum (B).

EDS shows a very strong peak for carbon that was deposited on the surfaces of TiO_2 nanowires using CVD (Figure 7.3B). Two additional peaks are related to titanium and oxygen. The small peak associated with potassium emerges from the remnants of the precursors. The TEM images of an individual TiO_2 nanowire are shown in Figures 7.4 and 7.5. Hemicylindrical-shaped TiO_2 nanowires with dimensions of ca. 50 nm × 1 μm (Figure 7.4) and 80 nm × 2 μm (Figure 7.5) were observable. From the cross-sectioned SEM images and the TEM images, it was estimated that the number of the formed nanowires could be up to 3.1×10^{10} and 1.6×10^{10} per cm^2 with the length of 1 and 2 μm, respectively.

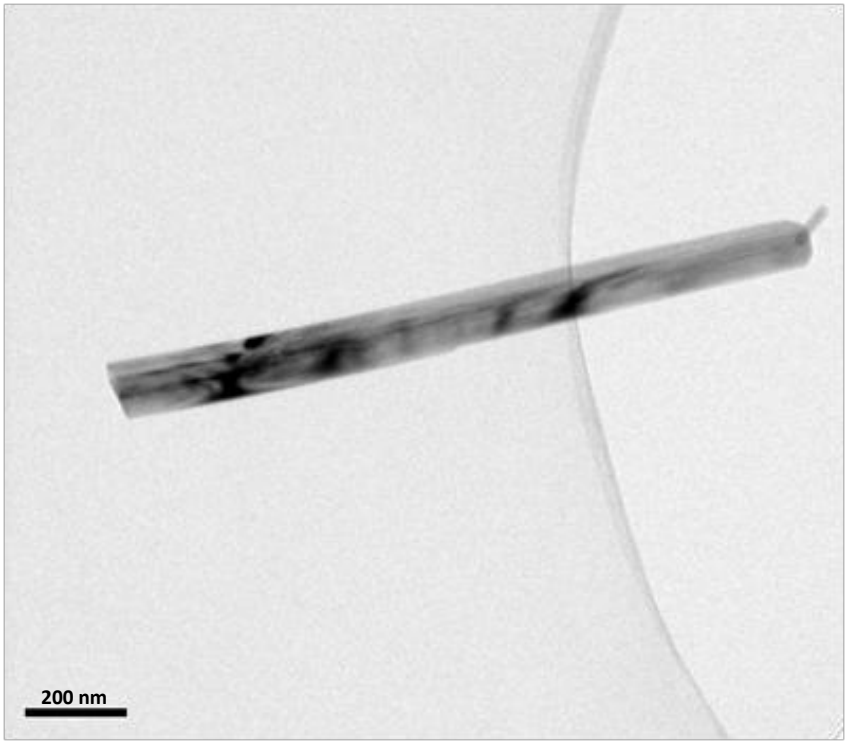

Figure 7.4. TEM images of an individual TiO_2 nanowire with dimensions of 50 nm × 1 μm

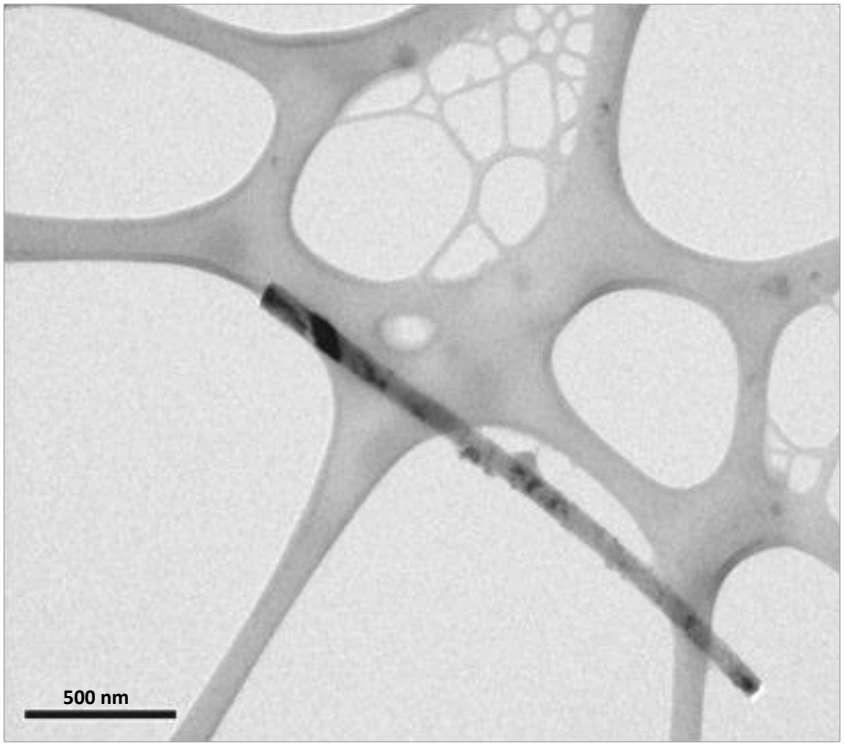

Figure 7.5. TEM images of an individual TiO_2 nanowire with dimensions of 80 nm × 2 μm.

7.3.2. Electrochemical characterization

Figure 7.6A presents the cyclic voltammograms (CVs) of the TiO_2 electrode with nanowire dimensions of ~50 nm × 1 μm (denoted as Electrode**1**) prior to and following carbonization recorded in a $K_3Fe(CN)_6$ solution. A pair of well-defined redox peaks appeared at 0.323 and 0.182 V before carbonization and at 0.312 and 0.186 V after carbonization. Obviously, carbonization improved the electron transfer rate as the peak-to-peak separation decreased ~15 mV. In addition, with carbonized TiO_2 nanowires a huge increase of the peak current from 99.04 to 4305 μA was observed. Under the same conditions, the CVs of the TiO_2 electrode with

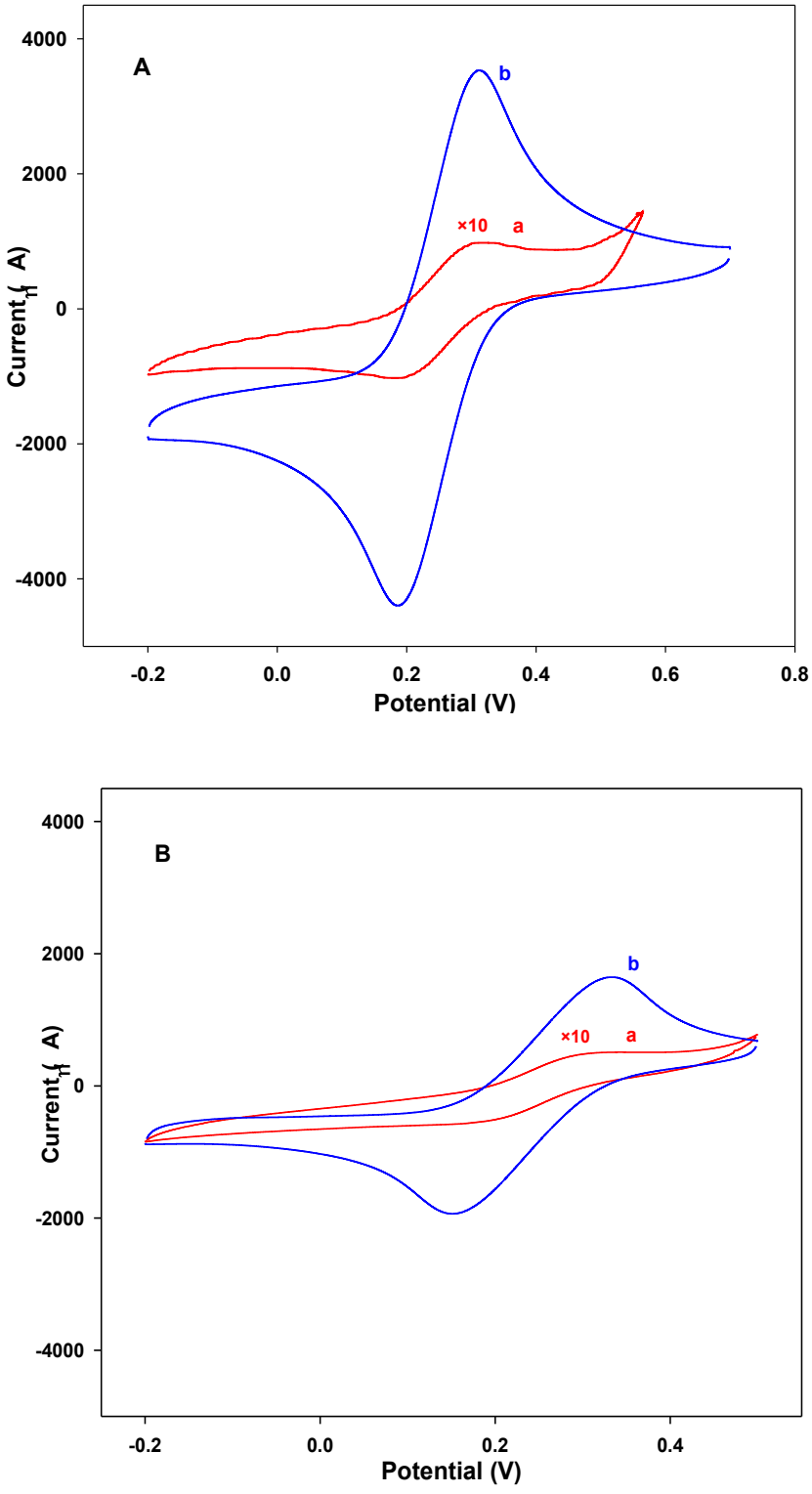

Figure 7.6. Cyclic voltammograms of the TiO_2 electrodes with nanowire dimensions of 50 nm × 1 µm (Electrode**1**) (A) and 80 nm × 2 µm (Electrode**2**) (B) before (a) and after (b) carbonization at the scan rate of 20 $mV.s^{-1}$ in $K_3Fe(CN)_6$ + 0.1 M KCl + PBS solution at pH 7.4.

nanowire dimensions of ~80 nm × 2 μm (denoted as Electrode**2**) exhibited current response peaks of 56.80 and 2063 μA at 0.333 and 0.151 V before and after the carbonization, respectively (Figure 7.6B). This indicates that a much higher surface area and conductivity were achieved with Electrode**1** configuration, in contrast to that of Electrode**2**. The aggregated structure of Electrode**2** results in a diminished active surface area, which imposes physical limits on electron transfer. The above results indicate that by decreasing the dimensions of the TiO_2 nanowires 80 nm × 2 μm to 50 nm × 1 μm, the electron transfer efficiency improves significantly.

Electron transfer between the active site of glucose oxide (GO_x) and the electrode surface is the limiting factor in the operation of electrochemical glucose biosensors. To investigate whether the fabricated TiO_2 nanowires are capable of communicating with the active sites of proteins, we immobilized GO_x as a probe. To assess the ideal nanowire dimensions that will enable the establishment and tailoring of the electrical contact between the redox center of GO_x and the electrode surface, we tested four different electrodes. The first two electrodes were designated Electrode**1** and Electrode**2**. Additional two electrodes were comprised of a TiO_2 film and a bare titanium plate, which was devoid of nanostructuring. The latter two electrodes were utilized as controls. Using the equations described by Sheesan and Whitman, we subsequently calculated the time required for the monolayer of GO_x to be adsorbed onto the nanosensors.[32-33] For the control electrodes, GO_x was immobilized over a range of time intervals in order to obtain optimum results.

To assess electrode coverage and immobilization efficiency, cyclic voltammetry was conducted with the electrodes before and after the immobilization of GO_x in a buffer solution at pH 7.4. As expected, the CV of the carbonized Electrode**1** is featureless in the potential range of

-0.2 to 0.5 V in a phosphate buffer solution (Curve *a* of Figure 7.7A), while subsequent to the immobilization of GO_x, the electrode generates a pair of well-defined redox peaks at 0.203 and 0.154 V with an oxidation current peak of 7.64 μA (Curve *b* of Figure 7.7A). These redox peaks are attributed to the active sites of GO_x, identified as flavin adenine dinucleotide (FAD). Accordingly, the formal potential of GO_x on the TiO_2 nanowires is 0.178 V, which is more positive than the redox potential of the $FAD/FADH_2$ couple, -0.15 V (vs. Ag/AgCl).[34-35] It is surmised that this overpotential might originate from a barrier introduced by the TiO_2 nanowires, which bridges the enzyme to the bulk electrode. In contrast, the CV of Electrode**1** prior to carbonization shows no redox peaks upon the immobilization of GO_x since the conductivity of the uncarbonized TiO_2 nanowires is not sufficient for the electron transfer process (Figure 7.7B).

Under the same conditions, the CVs of Electrode**2** were devoid of any defined redox peaks (Figures 7.8A and 7.8B). However, following GO_x immobilization, the redox peaks attributed to the carbon-oxygen functionalities[28] is broadened, which indicates the blockage of some active parts of Electrode**2** by the enzyme (Figure 7.8A).

The amount of the electroactive GO_x immobilized on Electrode**1**, $\Gamma = Q/nFA$, (where Q is the charge, n is the electron transfer number, F is the faraday constant, and A is the geometric surface area of the working electrode), was calculated to be 7.11×10^{-11} $mol.cm^{-2}$. Thus, the number of active GO_x molecules on the electrode surface is 4.28×10^{13} per cm^2, which corresponds to 86% coverage with a random, densely packed GO_x monolayer. This value is ~ 50 fold larger than the number of GO_x immobilized on a smooth surface, since each molecule of GO_x occupies an area of ~100 nm^2.[36-37] The Γ calculation for Electrode**2** was somewhat dubious since the redox peaks of GO_x were not salient enough.

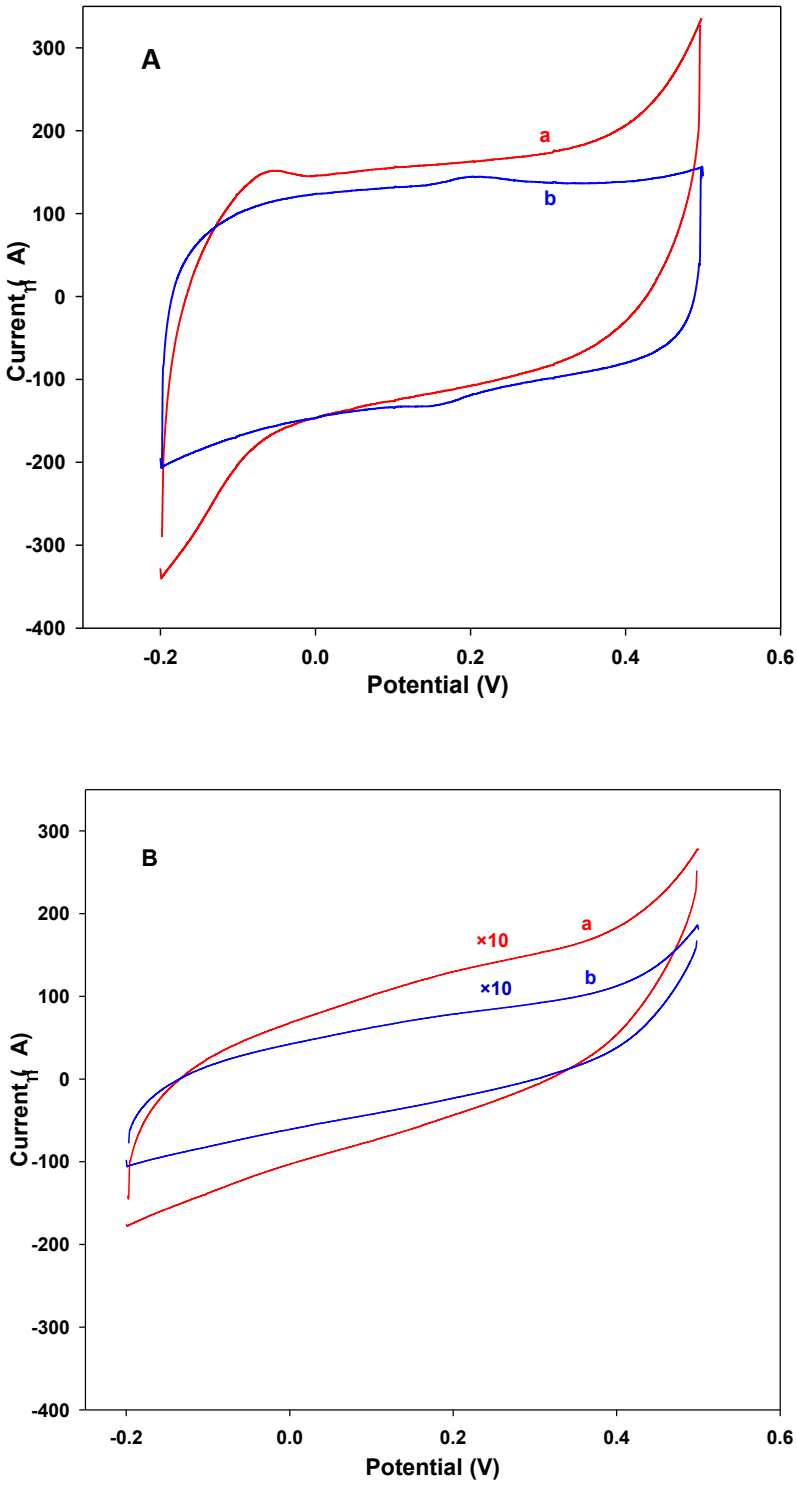

Figure 7.7. Cyclic voltammograms of carbon-modified Electrode**1** (A), and un-carbonized Electrode**1** (B), before (a) and after (b) immobilization of GO_x recorded at the scan rate of 20 $mV.s^{-1}$ in PBS pH 7.4.

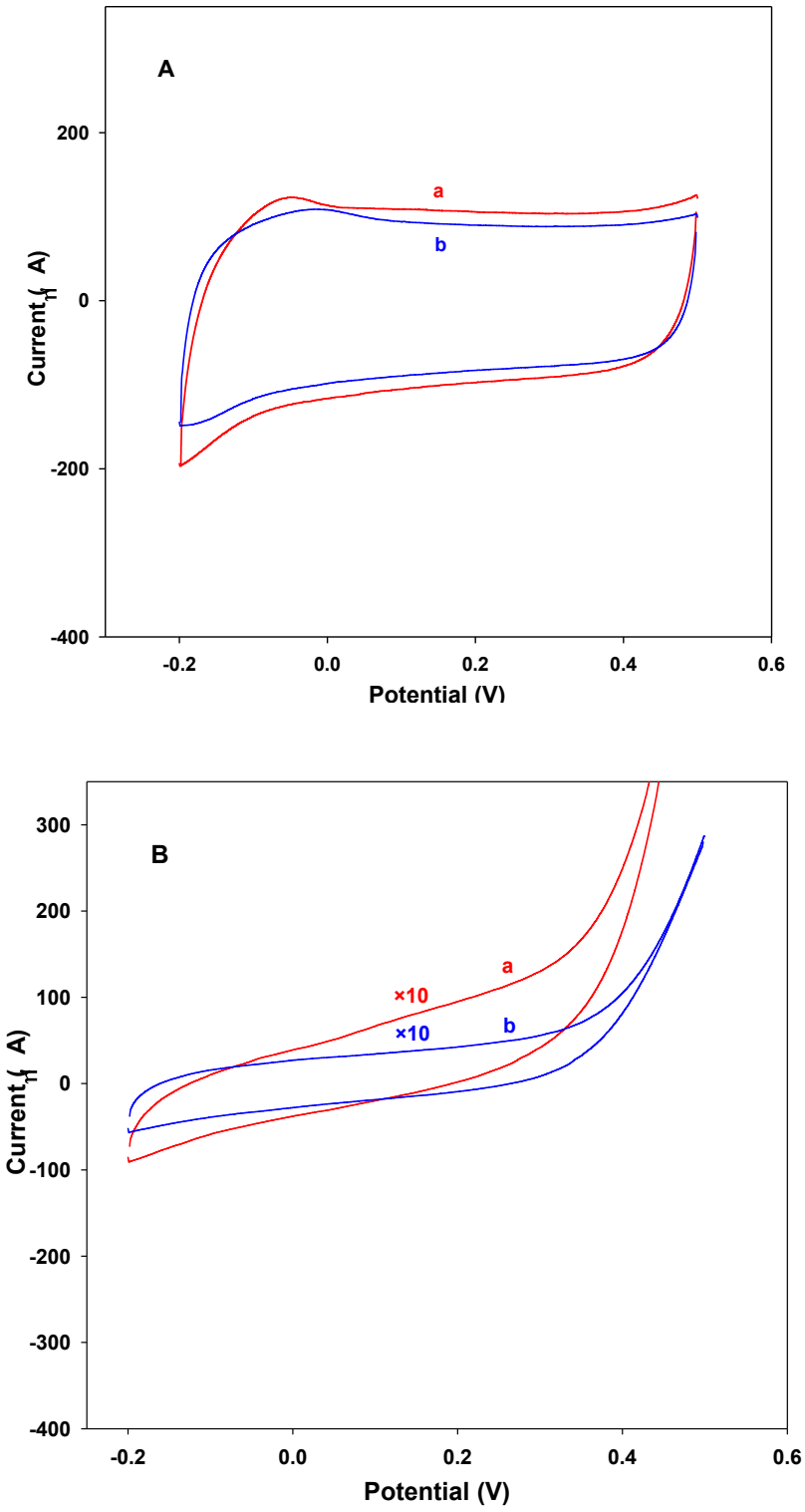

Figure 7.8. Cyclic voltammograms of carbon-modified Electrode**2** (A), and un-carbonized Electrode**2** (B), before (a) and after (b) immobilization of GO_x recorded at the scan rate of 20 $mV.s^{-1}$ in PBS pH 7.4.

In order to evaluate the impact of nanostructuring on the efficiency of GO_x immobilization, the CVs of the Electrode**1** were obtained at different scan rates (Figure 7.9A). The plot of ΔE_p *vs*. log *v* is displayed in Figure 7.9B, where ΔE_p is the potential separation of the anodic and cathodic peak, and *v* is the scan rates. The peak-to-peak separation is linearly dependent on the logarithm of the scan rates when $\Delta E_p > 200/n$, where n is the number of electrons involved in the reaction. This is in good agreement with Laviron theory.[38]

The experimental electron transfer coefficient α was thus calculated to be 0.43. This confirms our hypothesis that the carbonized TiO_2 nanowires may plug into the reaction center of GO_x. From this plot, we further estimated the interfacial electron transfer rate constants (k_s) to be 1.27 s^{-1}. This k_s value is quite similar to the ones reported in the literature for direct electron transfer of GO_x on carbon nanotubes,[39-40] indicating that the carbonized TiO_2 nanowire behaves individually and that the faradaic current increases significantly due to the large active area.

There is a great interest in developing mediator-free electrochemical biosensor for glucose monitoring in diabetes management. Since the direct electron transfer of GO_x immobilized on the carbonized TiO_2 nanowires was observed, we further explored whether the immobilized GO_x could be effective to detect glucose in the absence of a mediator. Figure 7.10 presents the CVs of Electrode**1** recorded in a phosphate buffer solution in the absence (Curve a) and in the presence of glucose (Curve b).

As shown in Figure 7.10, after the injection of glucose, an oxidation current appeared at ~0.1 V and increased with the increase of the electrode potential up to 0.20 V; it retained the maximum value in the potential range from 0.2 to 0.4 V.

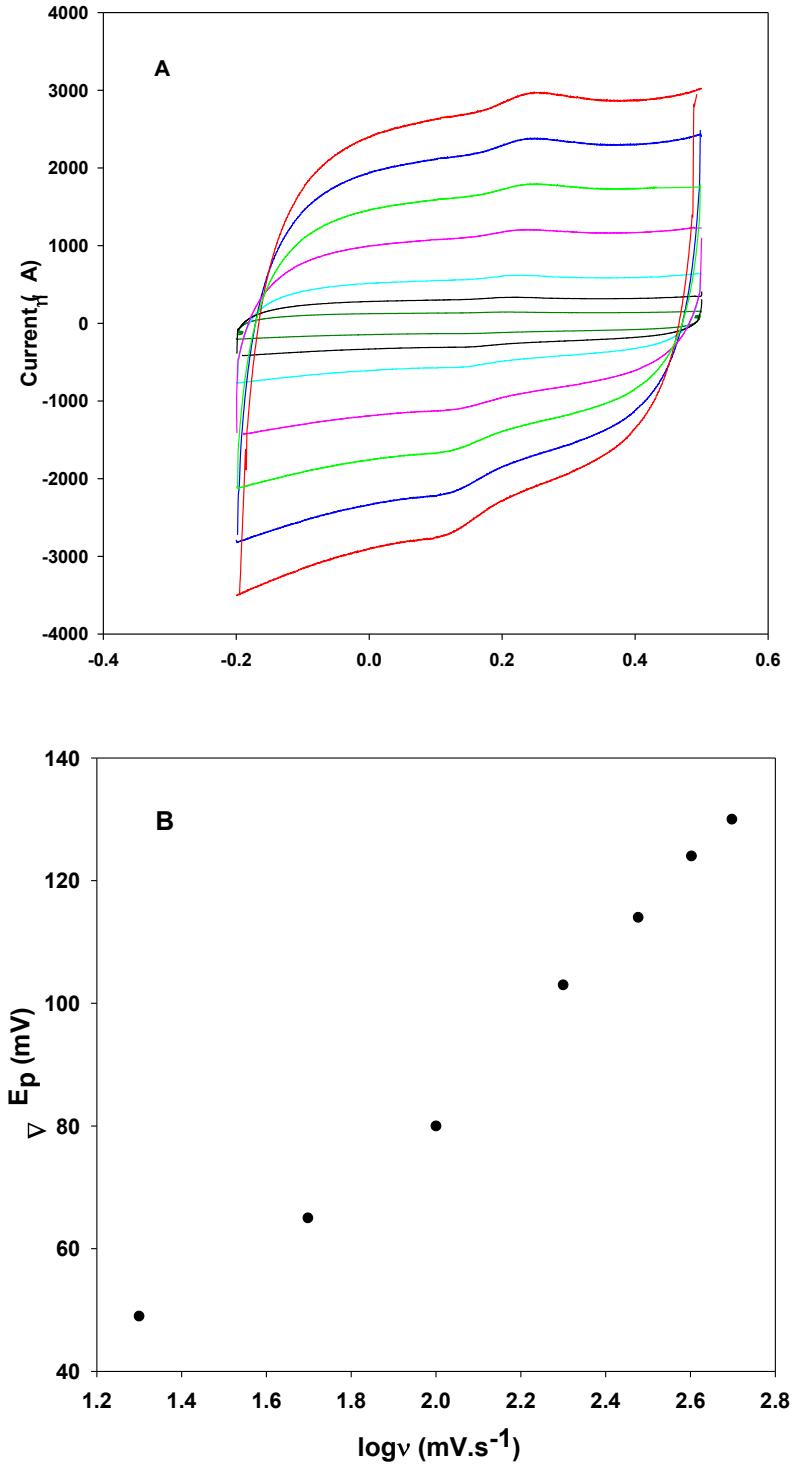

Figure 7.9. (A) Cyclic voltammograms of Electrode**1** after GO_x immobilization at different scan rates (20, 50, 100, 200, 300, 400, 500 $mV.s^{-1}$), and (B) Laviron plots corresponding to the separation between redox peaks of the CVs as a function of scan rates.

In the presence of oxygen, the cyclic voltammogram of Electrode**1** showed greatly increased reduction peak current (curve a, Figure 7.10), while the oxidation peak current decreased, showing an obvious electrocatalytic process toward the reduction of dissolved oxygen according to the following equations:

$$GO_x\ (FAD) + 2e^- + 2H^+ \rightarrow GO_x\ (FADH_2) \qquad (1)$$

$$GO_x\ (FADH_2) + O_2 \rightarrow GO_x\ (FAD) + H_2O_2 \qquad (2)$$

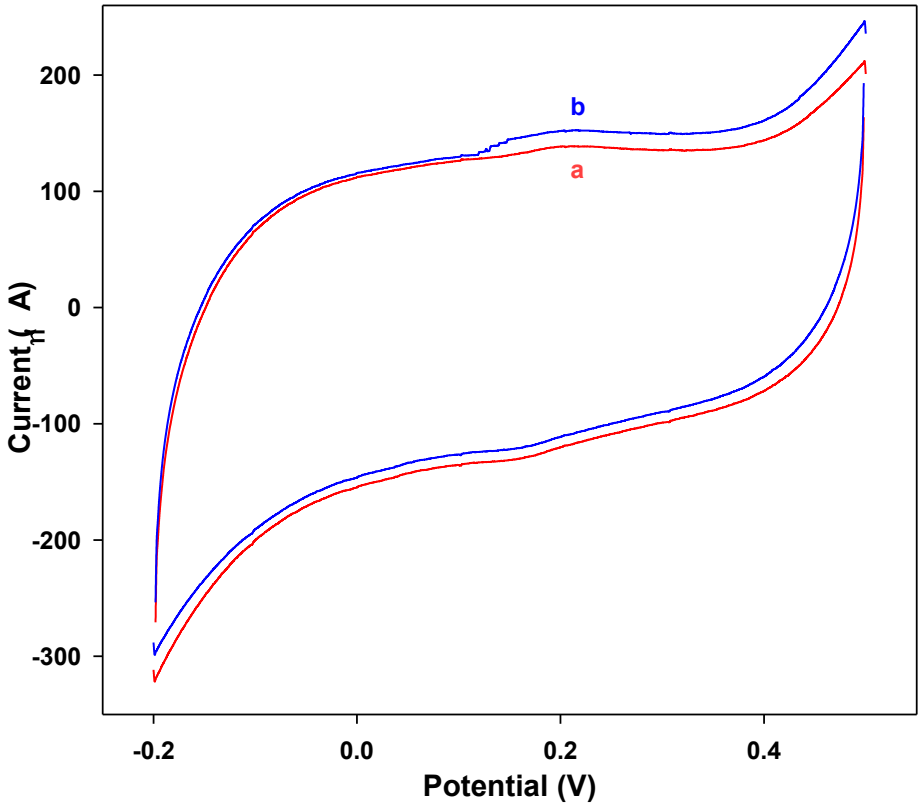

Figure 7.10. Cyclic voltammograms of Electrode**1** after GO_x immobilization in O_2 saturated PBS at pH 7.4 (a) and upon addition of 2 mM glucose (b).

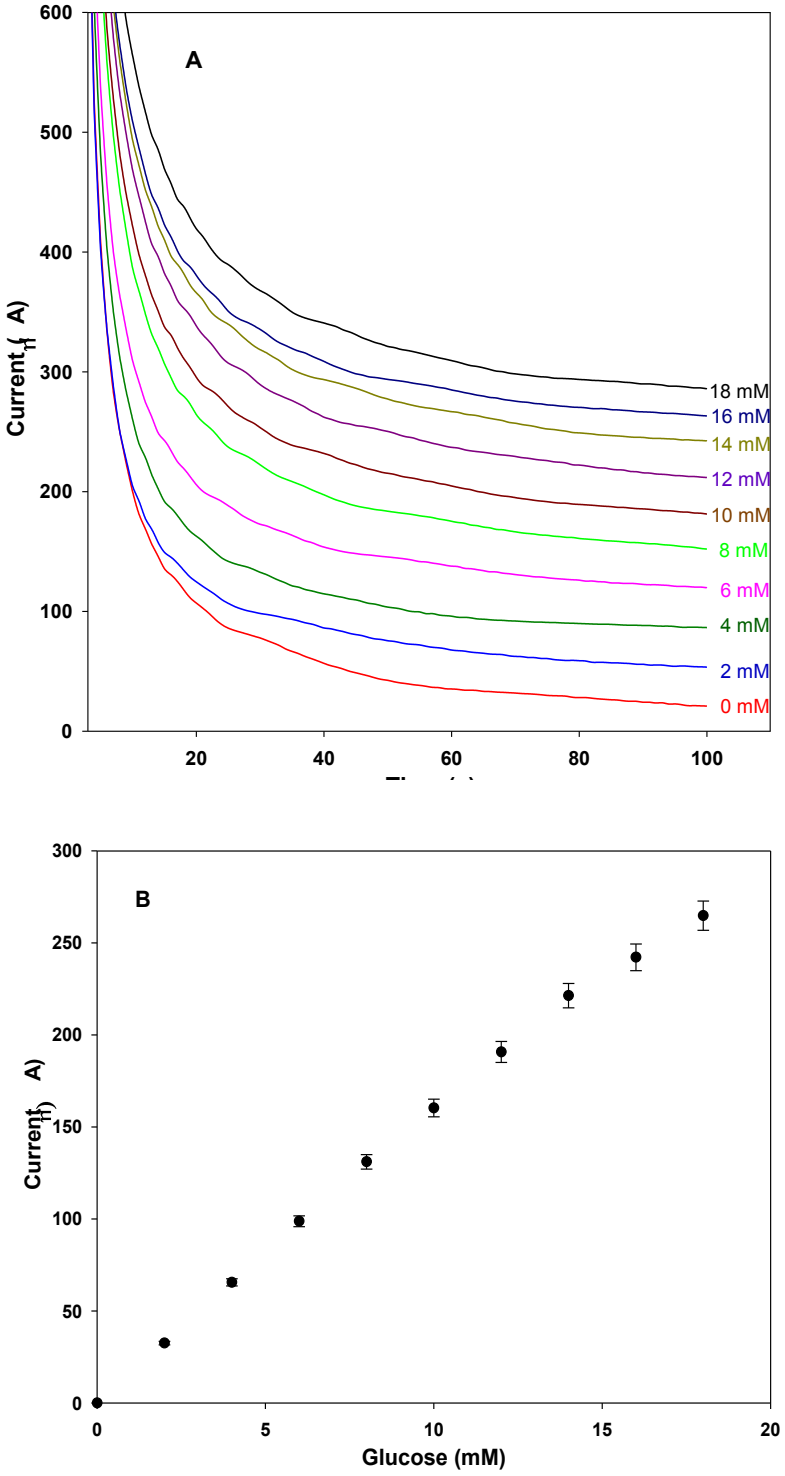

Figure 7.11. (A) Chronoamperometric response of Electrode**1** after GO_x immobilization in O_2 saturated PBS at pH 7.4 upon injection of different concentrations of glucose, and (B) the corresponding calibration curve.

This was a typical EC catalytic process, in which oxygen regenerated GO_x (FAD) and enhanced the reduction peak current of FAD. When glucose was added into this system, the reduction peak current decreased (curve b, Figure 7.10). Thus the glucose restrained the electrocatalytic reaction due to the enzyme-catalyzed reaction between the oxidized form of GO_x, GO_x (FAD), and glucose, Equation (3):

$$\text{Glucose} + GO_x\,(\text{FAD}) \rightarrow \text{Gluconolactone} + GO_x\,(FADH_2) \qquad (3)$$

With increasing glucose concentration, the peak current for the electrocatalytic reduction decreased, while the oxidation peak current increased, producing a glucose biosensor. To determine the linear dynamic range of the carbonized TiO_2 nanowire based biosensor, Electrode**1** was tested when exposed to different concentrations of glucose at E = 0.35 V (Figure 7.11A and B). The linear current response range was wide, up to ~18 mM, which is well beyond the normal physiological glucose level (3 - 8 mM). The sensitivity and detection limit of biosensor were calculated to be 15.0 $\mu A.mM^{-1}.cm^{-2}$ (RSD = 3%, N = 5) and 0.4 mM (S/N = 3), respectively. For comparison, Electrode**2** was also tested under the same conditions; a narrow linear range (1- 6 mM) and a low sensitivity, 4.2 $\mu A.mM^{-1}.cm^{-2}$ (RSD = 5%, N = 5), were obtained for its response to glucose. In contrast, the GO_x immobilized on the TiO_2 thin film and the titanium plate without nanostructuring could not generate a detectable response.

7.3.2. Selectivity of the TiO_2 Nanowire based biosensor

We further studied the selectivity of the carbonized TiO_2 nanowire based biosensor.

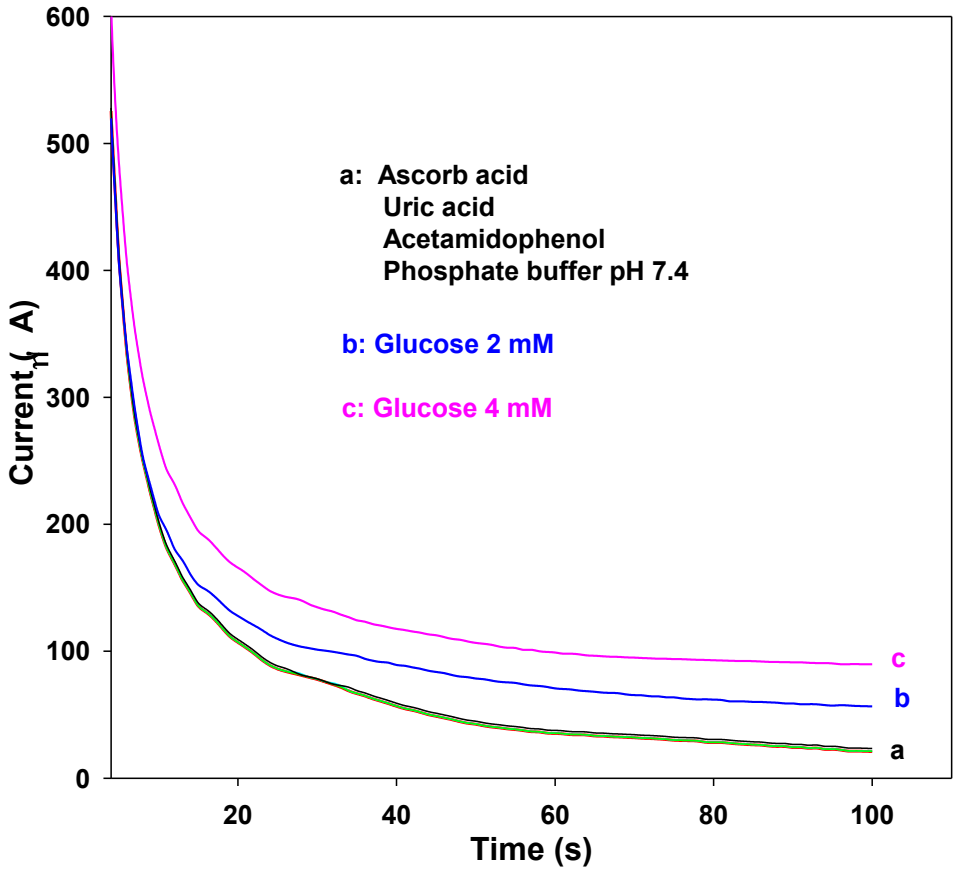

Figure 7.12. Chronoamperometic response of Electrode**1** after GO_x immobilization to interference species (0.1 mM uric acid (UA),0.1 mM 3- acetamidophenol (AP), and 0.1 mM ascorbic acid (AA)) (a) and in the presence of 2 mM (b) and 4 mM (c) glucose in PBS at pH 7.4.

As seen in Figure 7.12, the four *i* – *t* curves of Electrode**1** recorded in 0.1M PBS and upon subsequent injection of ascorbic acid, uric acid and acetamidophenol were overlapped (Curve *a*), showing that the fabricated biosensor is insensitive to the common interfering species. In contrast, the salient response to glucose was observed upon the further injections of 2 mM glucose (Curve *b* and *c* of Figure 7.12) with the same high sensitivity measured in the absence of the interfering species shown in Figure 7.11A.

7.3.3. Real sample analysis

The carbonized TiO_2 nanowire based biosensor was further tested using a real sample, human

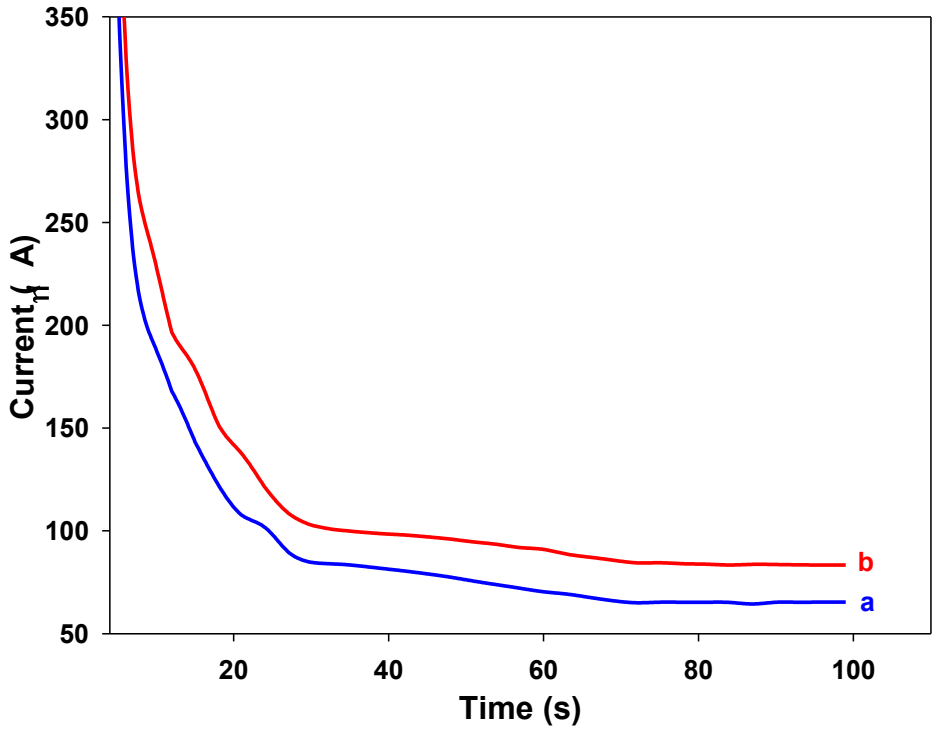

Figure 7.13. Chronoamperometic response of Electrode**1** after GO_x immobilization to diluted (a) and undiluted (b) human serum samples.

serum with a normal glucose level. Figure 7.13 presents the chronoamperograms of a diluted serum sample (in a 0.1 M phosphate buffer solution, pH 7.4) (Curve *a*) and an original undiluted serum sample (Curve *b*). Their corresponding glucose concentration were calculated to be 4 ± 0.01 mM (N = 5) and 5.1 ± 0.01 mM (N = 5), respectively. Those values were in excellent agreement with the data obtained by a commercial blood glucose monitoring assay, showing that the carbonized TiO_2 nanowire based biosensor is amenable in medical diagnostics.

7.4. Conclusion

In summary, the results described herein represent an important advance in understanding the size effect of nanomaterials on electron transfer of immobilized biological species and provide insights in the development of high-performance biosensing systems. We have developed a facile approach for the synthesis of TiO_2 nanowires with controllable dimensions. As demonstrated here, the carbonized TiO_2 nanostructures with different dimensions interact dissimilarly with GO_x. We discovered that GO_x requires a TiO_2 nanowire sensing entity that is smaller than 80 nm × 2 μm in order to sufficiently promote the direct electron transfer throughout the nanosensor and to react with glucose. Our study has revealed that the carbonized TiO_2 nanowires with a diameter of ~50 nm and a length of ~1μm are capable of communicating with the prosthetic group of enzymes with a relatively high interfacial electron transfer rate in the absence of a mediator. The developed carbonized TiO_2 nanowire based glucose biosensor exhibits a wide linear range up to 18 mM, high sensitivity and selectivity. In addition, as previous studies have shown, TiO_2 is inherently biocompatible,[41] its stability can be further enhanced upon protein adsorption, and its protein-conjugated implants do not release particulates into surrounding tissues.[42] Thus, we believe that the carbonized TiO_2 nanowire based biosensors warrant further study for *in vivo* analysis, with the aim of developing implanted biosensing devices.

References

1. Kong, J.; Franklin, N. R.; Zhou, C.; Chapline, M. G.; Peng, S.; Cho, K.; Dai, H., Nanotube Molecular Wires as Chemical Sensors. *Science* **2000,** *287*, 622-625.

2. Chen, X.; Dong, S., Sol-Gel-Derived Titanium OxideCopolymer Composite Based Glucose Biosensor. *Biosens. Bioelectron.* **2003,** *18*, 999-1004.

3. Morrow, T. J.; Li, M.; Kim, J.; Mayer, T. S.; Keating, C. D., Programmed Assembly of DNA-Coated Nanowire Devices. *Science* **2009,** *323*, 352.

4. Adair, . . arette, M. . Alt no lu, E. I.; Kester, M., Nanoparticulate Alternatives for Drug Delivery. *ACS Nano* **2010,** *4*, 4967-4970.

5. Sekiguchi, Y.; Mitsuhashi, N.; Inoue, Y.; Yagisawa, H.; Mimura, T., Analysis of Sugar Phosphates in Plants by Ion Chromatography on a Titanium Dioxide Column with Pulsed Amperometric Detection. *J. Chromatogr. A* **2004,** *1039*, 71-76.

6. Willner, I.; Katz, E., Integration of Layered Redox Proteins and Conductive Supports for Bioelectronic Applications. *Angew. Chem. Int. Ed.* **2000,** *39*, 1180-1218.

7. Wang, J., Electrochemical Glucose Biosensors. *Chem. Rev.* **2007,** *108*, 814-825.

8. Bartlett, P. N.; Booth, S.; Caruana, D. J.; Kilburn, J. D.; Santamaría, C., Modification of Glucose Oxidase by the Covalent Attachment of a Tetrathiafulvalene Derivative. *Anal. Chem.* **1997,** *69*, 734-742.

9. Anne, A.; Demaille, C.; Moiroux, J., Elastic Bounded Diffusion and Electron ropagation: Dynamics of the Wiring of a Self-Assembly of Immunoglobulins Bearing Terminally Attached Ferrocene Poly(ethylene glycol) Chains According to a Spatially Controlled Organization. *J. Am. Chem. Soc.* **2001,** *123*, 4817-4825.

10. Abad, J. M.; Gass, M.; Bleloch, A.; Schiffrin, D. J., Direct Electron Transfer to a Metalloenzyme Redox Center Coordinated to a Monolayer-Protected Cluster. *J. Am. Chem. Soc.* **2009,** *131*, 10229-10236.

11. Ahmadalinezhad, A.; Kafi, A. K. M.; Chen, A., Glucose Biosensing Based on the Highly Efficient Immobilization of Glucose Oxidase on a Prussian Blue Modified Nanostructured Au Surface. *Electrochem. Commun.* **2009,** *11*, 2048-2051.

12. Liu, Y.; Tuleouva, N.; Ramanculov, E.; Revzin, A., Aptamer-Based Electrochemical Biosensor for Interferon Gamma Detection. *Anal. Chem.* **2010,** *82*, 8131-8136.

13. Son, K. J.; Ahn, S. H.; Kim, J. H.; Koh, W.-G., Graft Copolymer-Templated Mesoporous TiO_2 Films Micropatterned with Poly(ethylene glycol) Hydrogel: Novel Platform for Highly Sensitive Protein Microarrays. *ACS Appl. Mater. Interfaces* **2011,** *3*, 573-581.

14. Ahmadalinezhad, A.; Chen, A., High-Performance Electrochemical Biosensor for the Detection of Total Cholesterol. *Biosens. Bioelectron.* **2011,** *26*, 4508-4513.

15. Mun, K.-S.; Alvarez, S. D.; Choi, W.-Y.; Sailor, M. J., A Stable, Label-free Optical Interferometric Biosensor Based on TiO_2 Nanotube Arrays. *ACS Nano* **2010,** *4*, 2070-2076.

16. Rusling, J. F.; Sotzing, G.; Papadimitrakopoulosa, F., Designing Nanomaterial-Enhanced Electrochemical Immunosensors for Cancer Biomarker Proteins. *Bioelectrochemistry* **2009,** *76*, 189-194.

17. Chen, A.; Holt-Hindle, P., Platinum-Based Nanostructured Materials: Synthesis, Properties, and Applications. *Chem. Rev.* **2010,** *110*, 3767-3804.

18. Cui, Y.; Wei, Q.; Park, H.; Lieber, C. M., Nanowire Nanosensors for Highly Sensitive and Selective Detection of Biological and Chemical Species. *Science* **2001,** *293*, 1289-1292.

19. Liu, S.; Chen, A., Coadsorption of Horseradish Peroxidase with Thionine on TiO_2 Nanotubes for Biosensing. *Langmuir* **2005,** *21*, 8409-8413.

20. Peng, X.; Chen, A., Large-Scale Synthesis and Characterization of TiO_2-Based Nanostructures on Ti Substrates. *Adv. Funct. Mater.* **2006,** *16*, 1355-1362.

21. Roy, P.; Berger, S.; Schmuki, P., TiO_2 Nanotubes: Synthesis and Applications. *Angew. Chem. Int. Ed.* **2011,** *50*, 2904-2939.

22. Wu, G.; Nishikawa, T.; Ohtani, B.; Chen, A., Synthesis and Characterization of Carbon-Doped TiO_2 Nanostructures with Enhanced Visible Light Response. *Chem. Mater.* **2007,** *19*, 4530-4537.

23. Wu, M.; Lin, G.; Chen, D.; Wang, G.; He, D.; Feng, S.; Xu, R., Sol-Hydrothermal Synthesis and Hydrothermally Structural Evolution of Nanocrystal Titanium Dioxide. *Chem. Mater.* **2002,** *14*, 1974-1980.

24. Feng, X.; Shankar, K.; Varghese, O. K.; Paulose, M.; Latempa, T. J.; Grimes, C. A., Vertically Aligned Single Crystal TiO2 Nanowire Arrays Grown Directly on Transparent Conducting Oxide Coated Glass: Synthesis Details and Applications. *Nano Lett.* **2008,** *8*, 3781-3786.

25. Wang, Y.; Tang, X.; Yin, L.; Huang, W.; Rosenfeld Hacohen, Y.; Gedanken, A., Sonochemical Synthesis of Mesoporous Titanium Oxide with Wormhole-like Framework Structures. *Adv. Mater.* **2000,** *12*, 1183-1186.

26. Kafi, A. K. M.; Chen, A., A Novel Amperometric Biosensor for the Detection of Nitrophenol. *Talanta* **2009,** *79*, 97-102.

27. Li, Y.; Liu, X.; Yuan, H.; Xiao, D., Glucose Biosensor Based on the Room-Temperature Phosphorescence of TiO_2/SiO_2 Nanocomposite. *Biosens. Bioelectron.* **2009,** *24*, 3706-3710.

28. Ahmadalinezhad, A.; Wu, G.; Chen, A., Mediator-Free Electrochemical Biosensor Based on Buckypaper with Enhanced Stability and Sensitivity for Glucose Detection. *Biosens. Bioelectron.* **2011,** *DOI: 10.1016/j.bios.2011.09.030*.

29. Liao, K.-t.; Shimpi, P.; Gao, P.-X., Thermal Oxidation of Cu Nanofilm on Three-Dimensional ZnO Nanorod Arrays. *J. Mater. Chem.* **2011,** *21*, 9564-9569.

30. Fan, R.; Wu, Y.; Li, D.; Yue, M.; Majumdar, A.; Yang, P., Fabrication of Silica Nanotube Arrays from Vertical Silicon Nanowire Templates. *J. Am. Chem. Soc.* **2003,** *125*, 5254-5255.

31. Kuo, D.-H.; Fang, J.-F.; Chen, R. S.; Chen, C. A.; Huang, Y. S., ZnO Nanomaterials Grown with Fe-Based Catalysts. *J. Phys. Chem. C* **2011,** *115*, 12260-12268.

32. Sheehan, P. E.; Whitman, L. J., Detection Limits for Nanoscale Biosensors. *Nano Lett.* **2005,** *5*, 803-807.

33. Soleymani, L.; Fang, Z.; Lam, B.; Bin, X.; Vasilyeva, E.; Ross, A. J.; Sargent, E. H.; Kelley, S. O., Hierarchical Nanotextured Microelectrodes Overcome the Molecular Transport Barrier to Achieve Rapid, Direct Bacterial Detection. *ACS Nano* **2011,** *5*, 3360-3366.

34. Degani, Y.; Heller, A., Direct Electrical Communication Between Chemically Modified Enzymes and Metal Electrodes. I. Electron Transfer From Glucose Oxidase to Metal Electrodes via Electron Relays, Bound Covalently to the Enzyme. *J. Phys. Chem.* **1987,** *91*, 1285-1289.

35. Xiao, Y.; Patolsky, F.; Katz, E.; Hainfeld, J. F.; Willner, I., "Plugging into Enzymes": Nanowiring of Redox Enzymes by a Gold Nanoparticle. *Science* **2003,** *299*, 1877-1881.

36. Hecht, H. J.; Kalisz, H. M.; Hendle, J.; Schmid, R. D.; Schomburg, D., Crystal Structure of Glucose Oxidase from Aspergillus niger Refined at 2·3 Å Reslution. *J. Mol. Biol.* **1993,** *229*, 153-172.

37. Bourdillon, C.; Demaille, C.; Gueris, J.; Moiroux, J.; Saveant, J. M., A Fully Active Monolayer Enzyme Electrode Derivatized by Antigen-Antibody Attachment. *J. Am. Chem. Soc.* **1993,** *115*, 12264-12269.

38. Laviron, E., General Expression of the Linear Potential A Sweep Voltamogram in the case of Difficultiness Electrochemical Systems. *J. Electroanal. Chem.* **1979,** *101*, 19-28.

39. Cai, C.; Chen, J., Direct Electron Transfer of Glucose Oxidase Promoted by Carbon Nanotubes. *Anal. Biochem.* **2004,** *332*, 75-83.

40. Guiseppi-Elie, A.; Lei, C.; Baughman, R. H., Direct Electron Transfer of Glucose Oxidase on Carbon Nanotubes. *Nanotechnology* **2002** *13*, 559-564.

41. Roy, P.; Berger, S.; Schmuki, P., TiO_2 Nanotubes: Synthesis and Applications. *Angew. Chem. Int. Ed.* **2011,** *50*, 2904-2939.

42. Vamanu, C. I.; HøI, P. J.; Allouni, Z. E.; Elsayed, S.; Gjerdet, N. R., Formation of Potential Titanium Antigens Based on Protein Binding to Titanium Dioxide Nanoparticles. *Int. J. Nanomedicine* **2008,** *3*, 69-74.

Chapter 8

Synthesis and Electrochemical Study of Nanoporous Palladium-Cadmium for Non-Enzymatic Glucose Detection

8.1. Introduction

Over the past few decades strategies for the design of glucose sensing systems have been focused on development of suitable techniques that enable high sensitivity and selectivity at low cost. The importance of glucose monitoring originates from its applications in the food industry, blood diagnostics and fuel cells. Since glucose oxidase is selective to glucose and shows fairly stable activity in a pH range of 2 to 8,[1-2] it has been widely used to construct various amperometric biosensors for glucose detection. Efforts to develop and improve glucose sensors, particularly based on amperometry, have proceeded over five decades since Clark and Lyons first reported the development of an enzyme-based electrode in 1962.[3] Subsequently, in 1967, Updike and Hicks incorporated glucose oxidase (GO_x) within a gel on an oxygen electrode and detected glucose concentrations in a biological fluid.[4] As the reaction centers of enzymes are isolated, the transfer of electrons between glucose oxidase and the electrode surface may be enhanced by the integration of a variety of synthetic mediators into the structures of enzymatic glucose sensors.[2, 5] However, mediators have the tendency of leaching into the test solution and hence, create an unstable/unreliable response. To diminish the necessity of utilizing synthetic mediators, glucose sensors were investigated for transferring electrons directly from the enzyme to the electrode by electrically wiring its active redox site to the electrode surface. Thus, regardless of the concentration of co-substrates such as oxygen or redox mediators, direct

electron transfer could transform the enzymatic oxidation process of glucose into an amperometric signal. The most important advantage of this design is the selective response of the electrode to glucose in the presence of additional electroactive interfering species. However, GO_x quickly loses its activity at pH levels of below 2 and above 8, as well as in solutions that contain ionic detergents.[6] Furthermore, the thermal and chemical instability of GO_x limits enzymatic glucose sensors from being amenable for the continuous monitoring of fermentation processes or within the human body where sterilization is required. Aside from temperature, pH, and toxic chemicals, the responses of enzymatic glucose sensors may be influenced by humidity. Fluctuations in humidity may be significantly harmful to the activity of electrodes when they are in use as well as during storage,[7-8] with the result of providing unreliable data. To overcome these drawbacks, the electrocatalytic oxidation of glucose without the use of enzymes has been increasingly investigated.[9-29] Continued efforts toward the development of this idea have culminated in the realization of the electrocatalytic oxidation of glucose and its mechanism on bare metal surfaces. Early mechanistic studies revealed that glucose oxidation on metal surfaces suffers from very slow kinetics, which is unable to generate significant faradaic current. Most pure metals, including platinum, exhibit an unsatisfactory sensitivity to glucose. For example, the sensitivity of flat platinum with a roughness factor of 2.6 in a phosphate buffer barely exceeds 0.14 μAcm^{-2} for 6 mM glucose. Besides low sensitivity, platinum electrodes are subject to poisoning via the adsorption of intermediates that arise from glucose oxidation,[21] which results in poor selectivity. This phenomenon further reduces the activity of platinum-based glucose sensors. In addition, the absence of enzymes leads to non-specific electrode responses to other electroactive species such as ascorbic acid.

Regarding its mechanism of operation, the electrochemical oxidation of glucose molecules involves the complex processes of adsorption, electron transfer, and subsequent chemical rearrangement, which are combined with the reactions on the surfaces of the electrocatalysts.[2] On the other hand, amperometric studies of glucose oxidation using conventional electrodes showed that the electrochemical performance of enzyme-free electrodes is heavily influenced by the pH of the test solution, and that their maximum response current can be achieved when the evaluation is performed under high pH conditions (0.1 M NaOH solution).[10-11, 13-16] In contrast, exposing electrodes to a highly basic medium inevitably causes surface degradation and imposes limits on the longevity of the electrocatalysts.[30] To overcome the aforementioned drawbacks toward the design of a high performance glucose oxidation system, the electrocatalytic activity of enzyme-free electrodes are of great interest insofar as investigations into cathodic operation potentials (to minimize the interfering effects of electroactive species), and neutral pH conditions (to avoid electrocatalyst surface damage).

In recent years, three dimensional nanomaterials have been investigated for their electroanalytical performance in a broad range of applications, from batteries to sensors. For example, precious metal nanoparticles[15, 24, 31] have exhibited efficient electrocatalytic activity in response to glucose oxidation. These results illustrated that the faradic current responses of nanomaterial-based electrodes are influenced by both the structure and resident active sites of nanomaterials. However, further broad-based applications are somewhat limited as these materials are costly, and they suffer from surface poisoning. Alternately, transition metals and their alloys have been extensively explored.[12, 14, 16, 25-27, 30] Among the transition metals, Pd-based alloys offer a class of practical materials for gas sensing[32] and other catalytic applications.[33-34] The application of these materials would be expanded by their compatible combination with an

appropriate electroactive transition metal such as cadmium to develop binary nanostructured building blocks. The dimensions, geometries, and composition of these nanomaterials may be manipulated to further improve the performance of glucose electrooxidation.

In this work, for the first time, we report on the fabrication and characterization of a non-enzymatic electrode for the direct oxidation of glucose in a mediator-free based upon palladium-cadmium (PdCd) nanostructured materials. The Pd-Cd binary nanostructure was synthesized via a labile, convenient, template-free, single-step hydrothermal method. The surface morphology, composition and crystal structure of the resultant nanoparticles were investigated in detail. The fabricated glucose sensor was configured to measure glucose with high sensitivity and selectivity under a wide range of potentials and pH.

8.2. Experimental

8.2.1. Materials

$PdCl_2$ (Alfa Aesar, 99.9%), $Cd(NO_3)_2$ (Alfa Aesar, 99.9%), ammonium formate (Aldrich, 99.995%), *d*-glucose (Sigma), ascorbic acid (AA) (Sigma-Aldrich), uric acid (UA) (Sigma), and 3-acetamidophenol (AP) (Aldrich) were used as received. All chemicals were of analytical grade. The phosphate buffer solution (PBS, 0.1 M, pH 7.4) was comprised of Na_2HPO_4 and NaH_2PO_4. Solutions of glucose, AA, UA and AP were prepared using PBS immediately before each experiment. Glucose stock solutions were allowed to mutarotate overnight prior to use. Nanopure water (18.2 MΩ cm) was utilized in the preparation of all solutions.

8.2.2. Fabrication of PdCd/GC Electrode

A hydrothermal method was employed in the synthesis of variably composed nanoporous PdCd. Briefly, a solution of $PdCl_2$ 0.05 M and $Cd(NO_3)_2$ 0.05 M precursors with stoichiometric ratios, and 1 ml ammonium formate (10 M) serving as the reducing agent was diluted to 10 ml with water and transferred to a Teflon-lined autoclave. The autoclave was subsequently sealed, and heated at 180^{o}C for 2 h. After cooling to room temperature, the PdCd nanomaterials were rinsed, ultrasonicated and centrifuged three times. Glassy carbon electrodes (GC, 3 mm in diameter, CH Instruments) were polished with alumina powder prior to each experiment, rinsed thoroughly with doubly distilled water, and ultrasonicated in 1:1 HNO_3, ethanol and water for 15 min, after which they were allowed to dry at room temperature. A solution consisting of 3 µl of 6 mg/ml PdCd nanomaterials in Nafion® (0.5% in methanol) was then added to the GC electrodes. The electrodes were allowed to dry at room temperature.

8.2.3. Instruments and Electrochemical Experiments

All electrochemical experiments were performed using an electrochemical workstation (CHI660B, CH instrument Inc.), interfaced with an in-house-built, three-electrode glass cell (50 mL). A platinum coil was used as the counter-electrode and was flame-annealed before each experiment. Ag/AgCl (saturated KCl) was used as the reference electrode. GC electrodes coated with Pd-Cd nanoparticles was employed as the working electrodes. Amperometric measurements of glucose were carried out in a 0.1 M phosphate buffer solution (pH 7.4) at selected potentials. Currents at each glucose concentration were recorded subsequent to the onset of transient steady states, which were attained under the constant stirring of the solution. All solutions were de-

aerated with ultrapure argon (99.999%) prior to measurements, and argon was passed above the solution during the experiments. All measurements were conducted at room temperature.

8.3. Results and discussion

8.3.1. Morphological characterization of nanoporous PdCd

Figures 8.1 and 8.2A present a typical SEM image and EDS spectrum of the nanoporous PdCd, respectively which were synthesized by a hydrothermal method. The SEM image reveals that the three-dimensional random porous structures, with diameters of tens to hundreds of nanometers, were formed by the close proximity of the PdCd nanoparticles, with a size range of from 50–500 nm. Solitary Pd and Cd peaks appear in the EDS spectrum, and no discernible carbon or oxygen signals are seen in this spectrum. This verified that the synthesized nanoporous PdCd was free of organic surface-resident impurities.

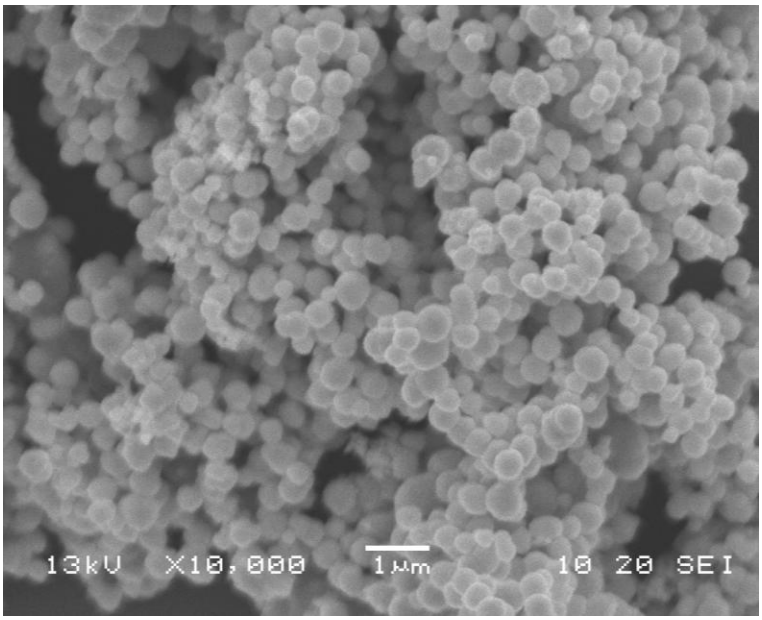

Figure 8.1. Typical SEM image of the nanoporous PdCd.

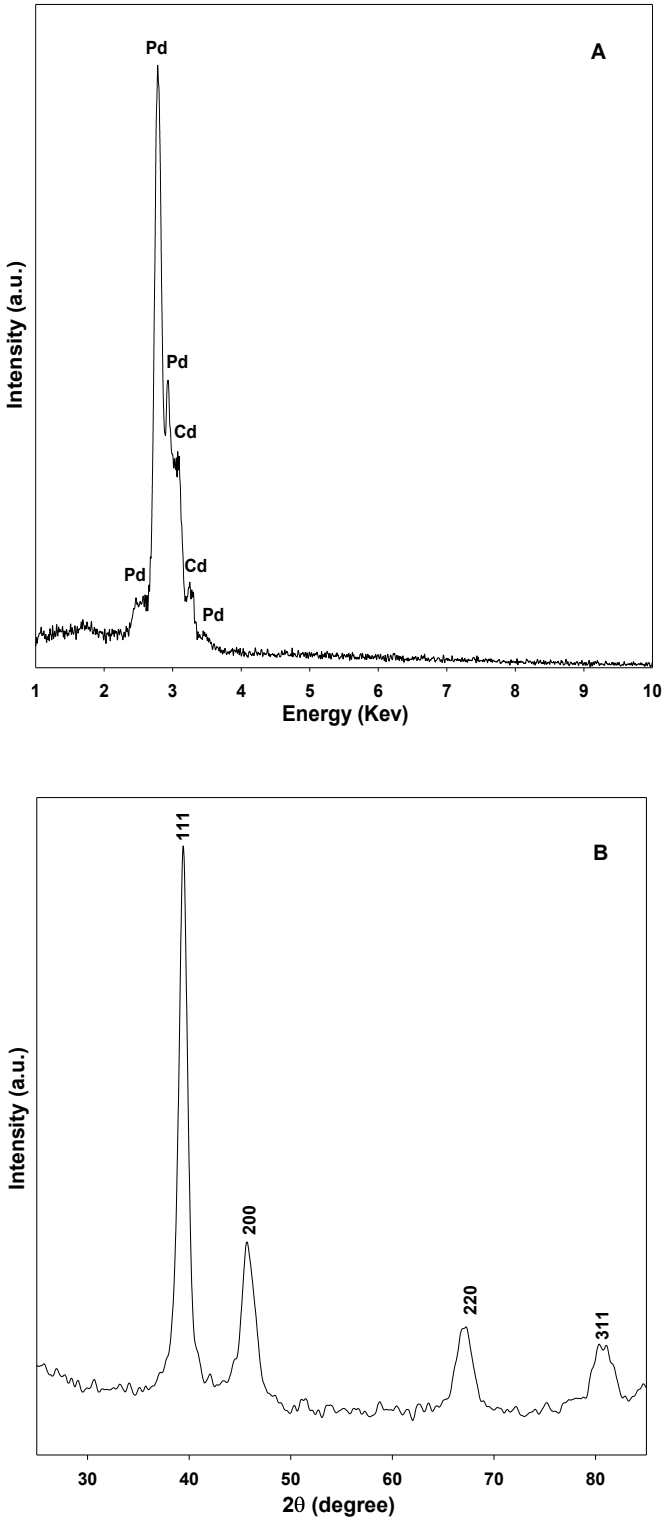

Figure 8.2. (A) the EDS spectrum and (B) XRD patterns of the prepared nanoporous PdCd film.

The crystalline nature of the Pd nanomaterials in nanoporous PdCd was confirmed by XRD studies, as shown in Figure 8.2B. The pattern of the PdCd nanostructures depicts all of the major peaks of palladium at 39.33(111), 45.71(200), 66.97(220) and 80.65(311) which are shifted slightly to smaller 2θ values, rather than pure palladium, 42.02 (111), 46.56 (200), 68.04 (220), and 82.05°(311). This is indicative of increased *d*-spacing and a dilation of the lattice constant, due to the incorporation of the Cd atoms into the Pd fcc lattice.[34] The XRD pattern of Pd nanomaterials is in good agreement with that of the reference pattern for the fcc (face centered-cubic) palladium (JCPDS 46-1043). No hexagonal Cd peaks appear, indicating that alloyed Pd-Cd intermetallic nanostructures were formed.

8.3.2. Evaluation of the electrochemical performance of the PdCd/GC electrode

To assess whether the percentage of cadmium has an impact on the electrochemical behaviour of the electrodes, cyclic voltammetry was conducted for the electrodes containing nanoporous PdCd with the ratio of (Pd:Cd) 100:0, 90:10, 80:20, 70:30 in a phosphate buffer solution (0.1 M, pH 7) at the scan rate of 50 $mV.s^{-1}$ and at the potential range of -1000 to 400 mV . As shown in Figure 8.3, by increasing the percentage of cadmium up to 20%, both the oxidation and reduction peak currents increase. Conversely, a current decrease is indicated when 30% cadmium was introduced into the nanoporous structure, signifying that cadmium lowers the activity of the fabricated binary nanostructure when the ratio of PdCd exceeds 80:20. We further studied the electrocatalytic response of the electrodes in the presence of 1 mM glucose in the PBS buffer solution (0.1 M, pH 7).

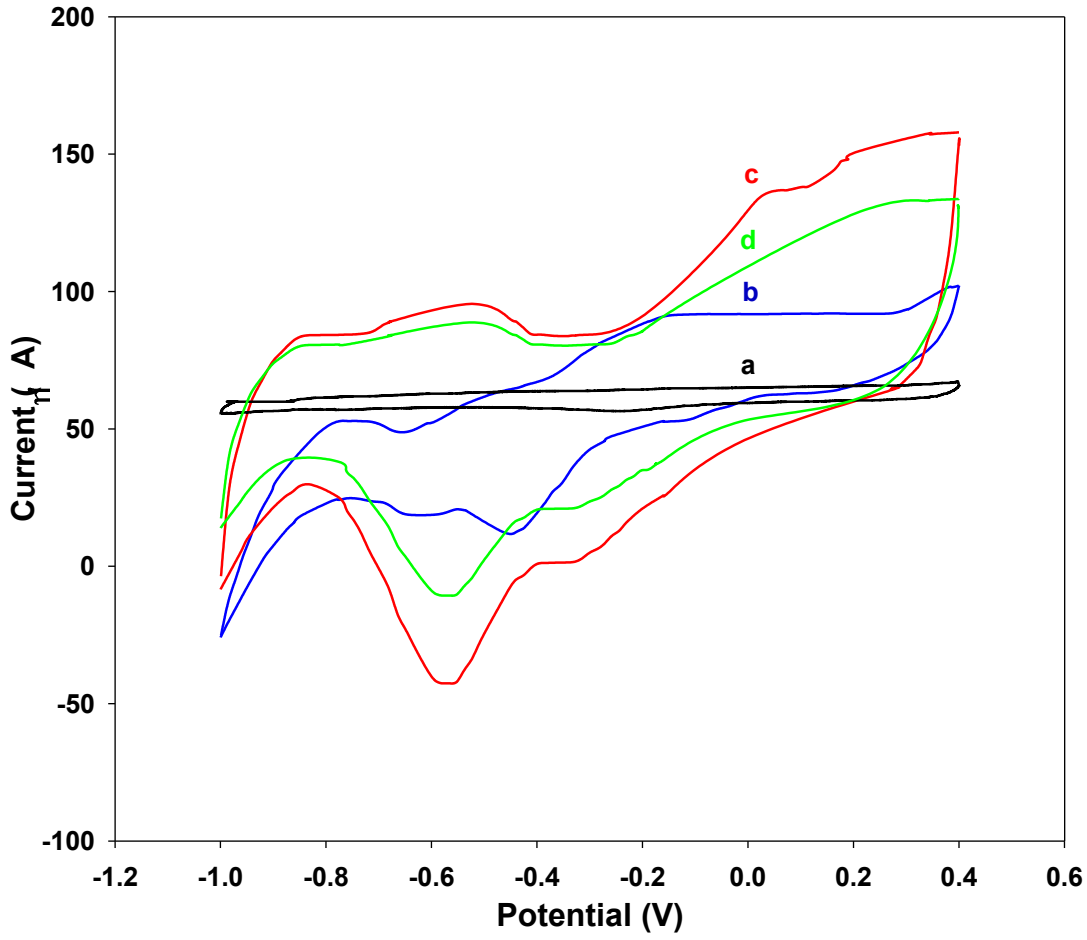

Figure 8.3. Cyclic voltammograms of Pd-Cd/GC electrodes with (a) 0%, (b) 10% (c) 20% (d) and 30% loadings of Cd, in PBS (0.1M, pH 7) at a scan rate of 50 $mV.s^{-1}$.

Figure 8.4 presents the CVs of the glassy carbon electrode containing Pd:Cd 80:20, prior to, and following the addition of 1 mM glucose. In the absence of glucose, the voltammogram of the electrode shows the characteristic features of palladium-cadmium, including the hydrogen adsorption/desorption waves at a negative potential region (-1000 to -400 V); a flat double layer region at intermediate potential (-400 to -150 V); and the cadmium oxide and palladium oxide

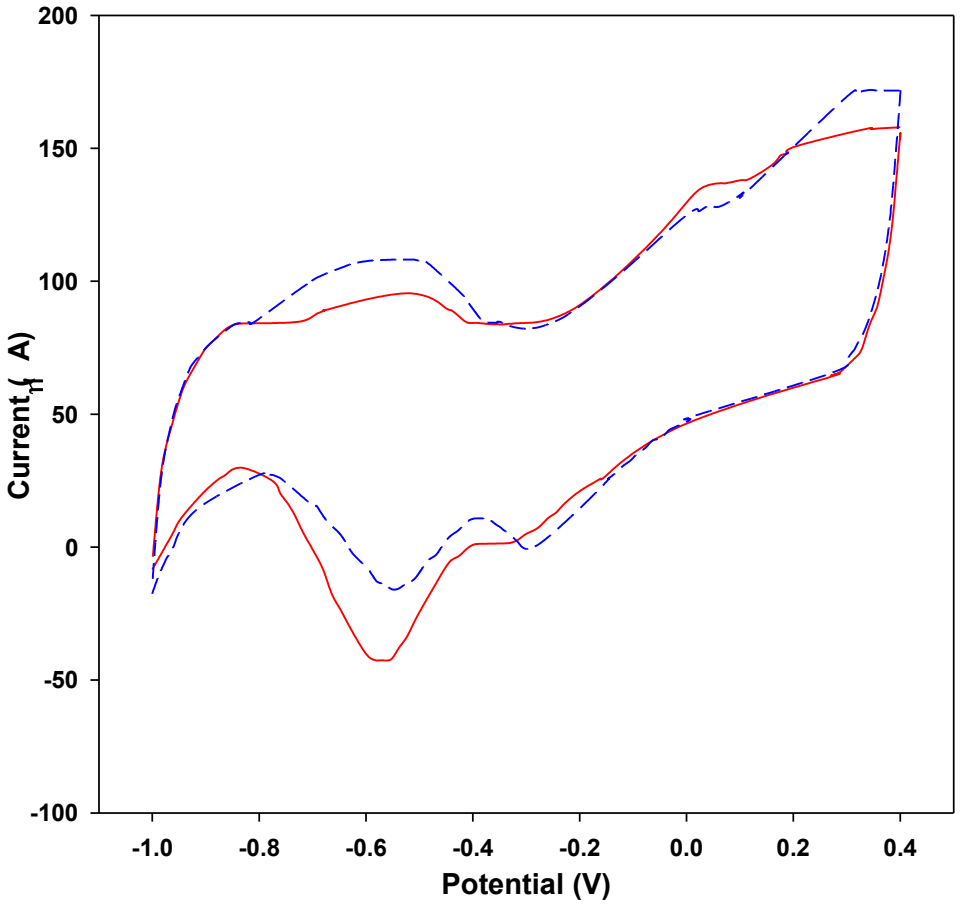

Figure 8.4. Cyclic voltammograms of the Pd-Cd/GC electrode in PBS (0.1M, pH 7.4) in the absence (solid line) and presence (dashed line) of 1 mM glucose at a scan rate of 50 $mV.s^{-1}$ in PBS solution (pH 7).

formation region at the positive potentials (0 to 400 V). Cathodic peaks at ca. -300 and -600 V corresponding to the reduction of palladium oxide and cadmium oxide are observed in the negative potential scan.[35] Upon the addition of glucose (1 mM), the voltammetric characteristics of the PdCd/GC electrode with 20% cadmium change drastically and show a very complicated electrochemical behavior. However, the CVs of the other three electrodes containing 0, 10 and 30% cadmium did not show any salient response to glucose. Therefore, the PdCd20% electrode was selected for further evaluation. As shown in Figure 8.4, the GC electrode containing PdCd20% shows a strong current response towards the electro-oxidation of glucose and its

intermediates at a variety of potentials. At low potential, the first peak emerges at -500 mV and broadens with increasing glucose concentrations, which might be attributed to the electrosorption of glucose; forming glucose intermediates such as enediols. At potentials of above -450 mV the further oxidation of glucose and its intermediates may occur, forming products such as gluconolactone or gluconic acid.[21]

8.3.3. Effect of potential and pH on the PdCd/GC electrode

The electrocatalytic performance of nanomaterials may generally be evaluated by measuring current at fixed operating potentials in the presence of a specific analyte. Hence, for the electrochemical sensing of glucose, it is critical to define an optimum detection potential, at which a maximum current response for glucose oxidation is achievable. The electrooxidation of glucose on a PdCd20%/GC electrode was investigated at operating potential range of -600 to 400 mV utilizing amperometry. Figure 8.5A illustrates the dependence of the glucose current response of the electrode on the operating potential. The current response in the presence of 3 mM glucose decreased when the cathodic potential was lowered from -600 to -400 mV. However, we witnessed an improvement in the standard deviation of the electrode response at-400 mV (RSD = 4.3%). By further decreasing the cathodic potential to -300 mV, the response current declined significantly.

The change in current nearly diminished to the potential range of -200 to 200 mV. At 300 mV, a jump in the response current was observed while the standard deviation increased (RSD = 10%). Therefore, an operating potential of -400 mV was selected as an optimal value, since a large and reliable response of the electrode to glucose was obtained at this potential.

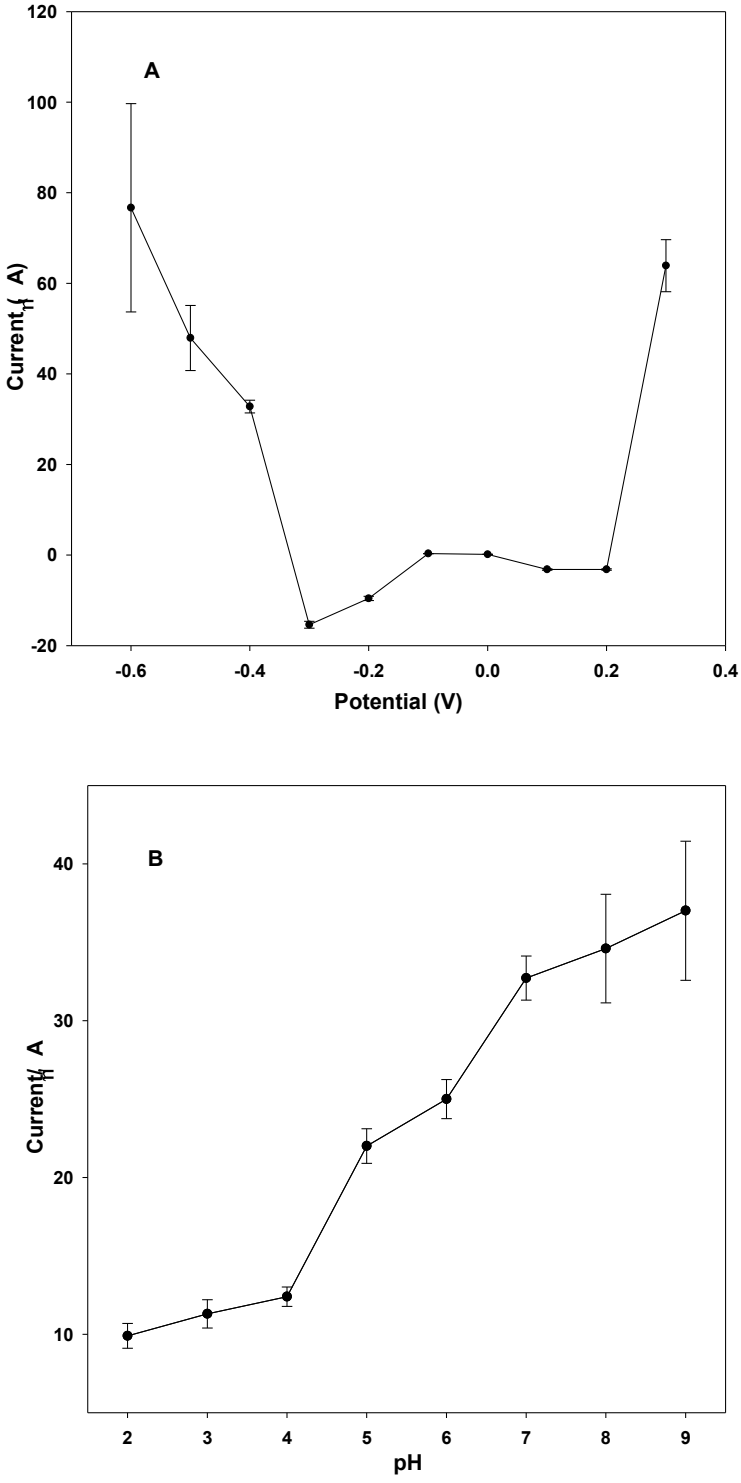

Figure 8.5. (A) Dependence of catalytic current of the Pd-Cd/GC electrode at different applied potentials measured in PBS (0.1M, pH 7) containing 3 mM glucose. (B) Effect of pH on the catalytic current of the Pd-Cd/GC electrode in PBS containing 3 mM glucose.

To study the effect of pH on the electrocatalytic activity of the electrode, amperometry was conducted in pH range of from 2 - 9 in the presence of 3 mM glucose. As shown in Figure 8.5B, the electrode response current increases in conjunction with elevated pH levels. However, the standard deviation for five different electrodes reached 12% at pH 9.0. In addition, unlike most other non-enzymatic sensors,[10-11, 13-16] the present sensor system demonstrates remarkable performance without surface contamination at neutral pH (PBS buffer 0.1 M), which makes it an excellent candidate for practical applications.

8.3.4. Amperometric performance of PdCd20%/GC electrode in the oxidation of glucose

To study the performance of the electrode in the continuous monitoring of glucose, the electrochemical responses of the electrode were examined upon the injection of different concentrations of glucose. The response current was continuously recorded at -400 mV in a phosphate buffer solution (pH 7) while the solution was being constantly stirred. As is shown in Figure 8.6A, the current for the electrooxidation of glucose at the PdCd20%/GC electrode increases in step with increasing glucose concentrations up to 10 mM. The sensitivity calculated from the calibration curve (Figure 8.6B) is 146.21 $\mu AmM^{-1}cm^{-2}$ ($y=10.33x+1.70$, $R = 0.9975$) with a detection limit of 0.05 mM (S/N = 3). The high sensitivity of the fabricated sensor may be ascribed to the extensive surface area of nanoporous PdCd in conjunction with the high electrochemical activity of the binary nanostructured system, which can in turn guarantee the accessibility of glucose to the active surface domains of the electrode. Electrode-to-electrode reproducibility was examined and validated through the fabrication of five distinct electrodes, which were constructed under identical conditions and compositions. Accordingly, the relative standard deviation, following the evaluation of the five electrodes, was estimated to be 5%.

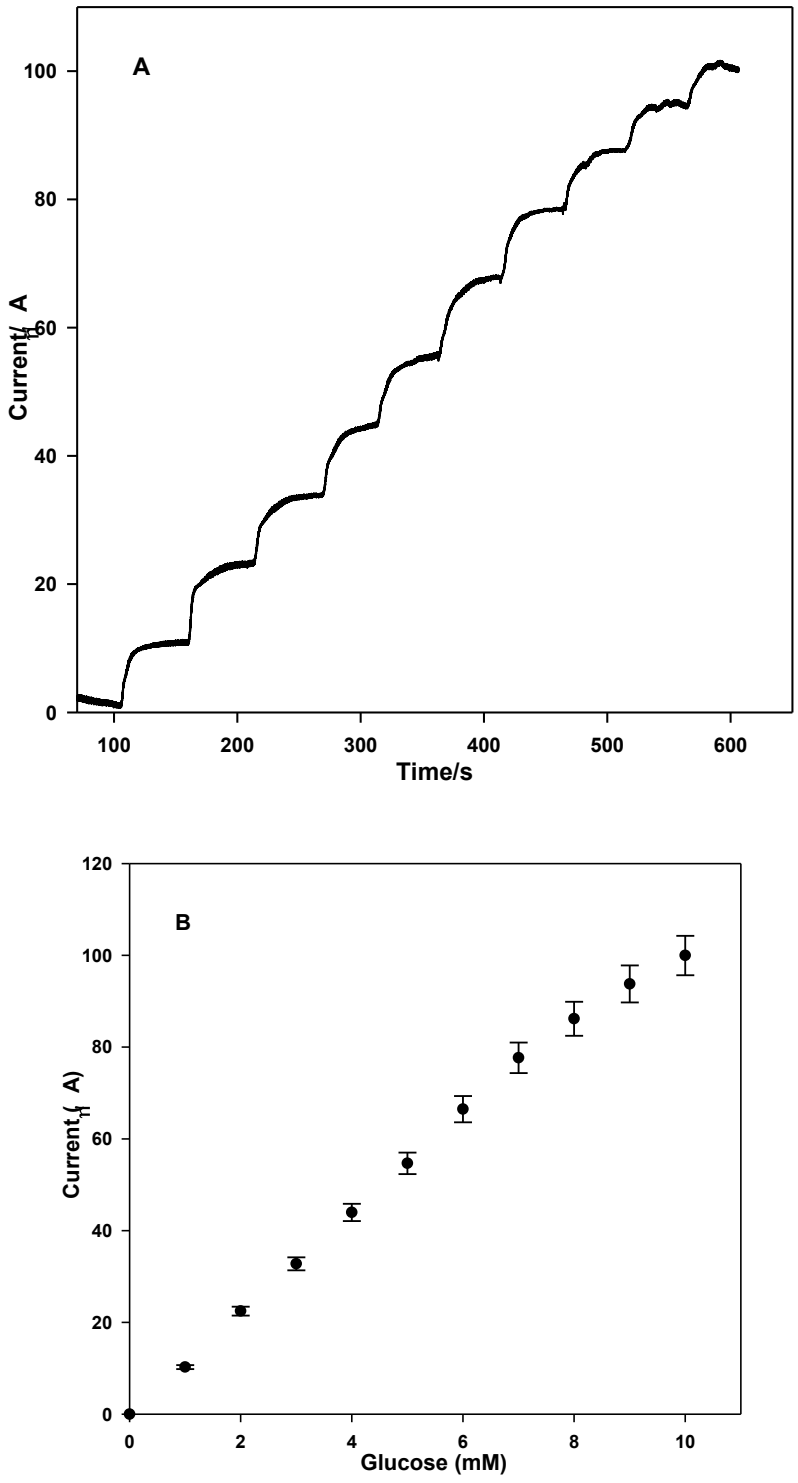

Figure 8.6. (A) Amperometric response to successive additions of 1mM glucose into PBS (0.1M, pH 7) at -0.4V; (B) and the corresponding calibration curve for the response of the Pd-Cd/GC electrode.

In addition, the time required for the electrode to reach 95% of the steady-state current response to glucose was about 8 s (Figure 8.6A).

Table 8.1 Comparison of different glucose sensors based on nanostructured materials.

Electrode	Sensitivity ($\mu AmM^{-1}cm^{-2)}$	Linear dynamic range (mM)	Operating potential (V)
Pt-PbNA/Pt[12]	11.25	1-11	-0.20
NPG[29]	41	0-15	0.2
3DGF/ITO[10]	46.6	0.005- 10	-0.30
AuNP[15]	160	1-8	0.25
NiCFP[16]	420	2e-3 - 2.5	0.6
$Ni(OH)_2$ NP/FTO[36]	446	0.01–0.75	0.4
Pt/MCs[28]	8.52	0-7.5	0.1
This work	146.21	0-10	-0.4

Pt-PbNA: Pd-Pb nanowire array, 3DGF: three-dimensional inverse-opal gold film, ITO: Indium-tin oxide; AuNP: Gold nanoparticles; NiCFP: Ni nanoparticle-loaded carbon nanofiber paste; Pt/MCs: Pt nanoparticles/mesoporous carbons; NPG: Nanoporous gold; $Ni(OH)_2$ NP/FTO: $Ni(OH)_2$ nanoparticle modified fluorine doped tin oxide.

The sensor exhibited good stability and a negligible voltammetric current decrease was observed during continuous operation (RSD = 4.3%). To test the long-term stability of the electrode, it underwent testing for glucose monitoring once a week. The results revealed that the sensor

maintained nearly 90% of its initial current response to glucose after one month. Table 8.1 compares the performance of the proposed sensor and other reported glucose sensors.

8.3.5. Selectivity of glucose sensor in the presence of interferants

To investigate the selectivity of the PdCd/GC electrode, we tested its response to the

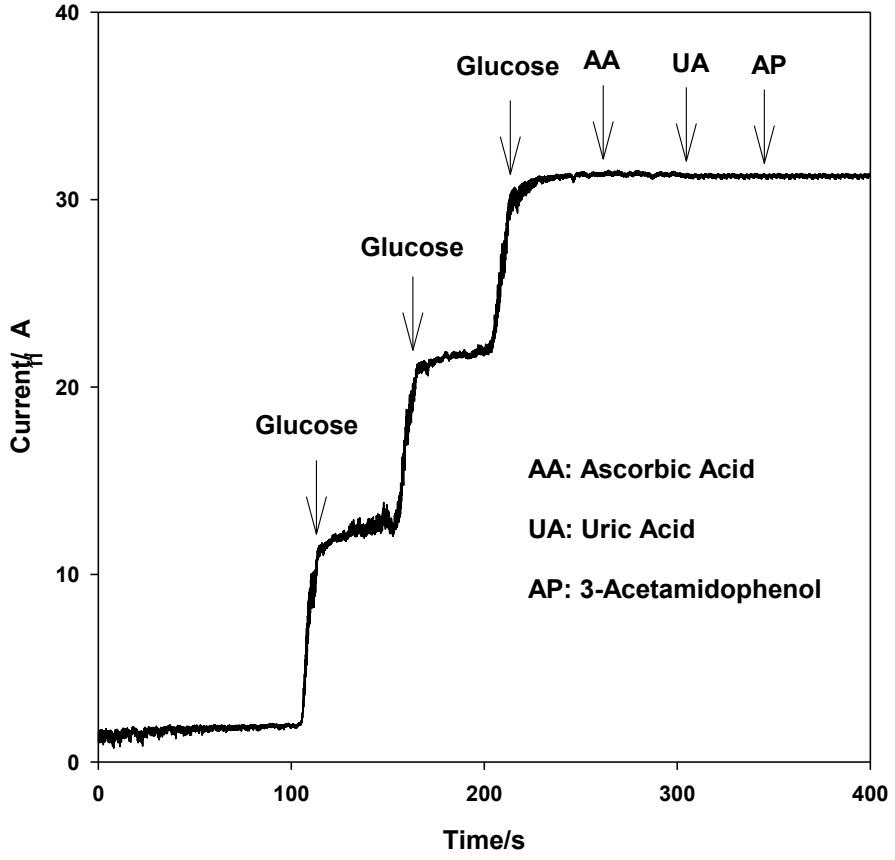

Figure 8.7. Effect of interferants, 0.1 mM ascorbic acid (AA), 0.1 mM acetaminophen and 0.02 mM uric acid (UA), on the response of the Pd-Cd/GC electrode in the presence of glucose in PBS solution (pH 7) at -0.4 V.

common interferant species including 0.1 mM ascorbic acid (AA), 0.02 mM uric acid (UA) and 0.1 mM acetamidophenol (AP). Figure 6 shows the amperometric response of the PdCd20%/GC

electrode to the interferants in the presence of 3 mM glucose. Clearly, there is no change in the current upon the addition of the interferants. Thus, the sensor allows for the highly selective quantification of glucose at a negative potential and a neutral pH.

8.4. Conclusions

In summary, an enzyme-free glucose sensor was successfully fabricated, which was based on PdCd binary nanostructured system. A hydrothermal method was used in the synthesis of nanoporous PdCd with variable compositions. The stable incorporation of PdCd nanostructures onto glassy carbon electrodes was facilitated by the use of Nafion®. The electrode exhibited a salient current response to electro-oxidation of glucose with high sensitivity and selectivity at an optimized potential. The resulting nanosensor is capable of sustainably detecting glucose via amperometry at the negative potential of -400 mV (Ag/AgCl), where interference from the oxidation of common interfering species such as AA, AP, and UA is effectively avoided. The electrode has a number of other desirable attributes including a low detection limit, short response time, satisfactory linear concentration range, excellent stability, and high reproducibility. In addition, the high sensitivity of the electrode to glucose at neutral pH (pH = 7) confirms its potential in multiple analytical applications.

References

1. White, B. J.; Harmon, H. J., Novel Optical Solid-State Glucose Sensor Using Immobilized Glucose Oxidase. *Biochem. Biophys. Res. Commun.* **2002,** *296*, 1069-1071

2. Park, S.; Boo, H.; Chung, T. D., Electrochemical Non-Enzymatic Glucose Sensors. *Anal. Chim. Acta* **2006,** *556*, 46–57.

3. Clark, L. C.; Lyons, C., Electrode Systems For Continuous Monitoring in Cardiovascular Surgery. *Ann. N.Y. Acad. Sci.* **1962,** *102*, 29-45.

4. Updike, S. J.; Hicks, G. P., The Enzyme Electrode. *Nature* **1967,** *214*, 986-988.

5. Ahmadalinezhad, A.; Kafi, A. K. M.; Chen, A., Glucose Biosensing Based on the Highly Efficient Immobilization of Glucose Oxidase on a Prussian Blue Modified Nanostructured Au Surface. *Electrohem. Commun.* **2009,** *11*, 2048-2051.

6. Wilson, R.; Turner, A. P. F., Glucose Oxidase: An Ideal Enzyme. *Biosens. Bioelectron.* **1992,** *7*, 165-185.

7. Mano, N.; Mao, F.; Heller, A., Characteristics of a Miniature Compartment-less Glucose−O_2 Biofuel Cell and Its Operation in a Living Plant. *J. Am. Chem. Soc.* **2003,** *125*, 6588–6594.

8. Moussy, F.; Harrison, D. J.; OLBrien, D. W.; Rajotte, R. V., Performance of Subcutaneously Implanted Needle-Type Glucose Sensors Employing A Novel Trilayer Coating. *Anal. Chem.* **1993,** *65*, 2072-2077.

9. Larew, L. A.; Johnson, D. C., Concentration Dependence of the Mechanism of Glucose Oxidation at Gold Electrodes in Alkaline Media. *J. Electroanal. Chem.* **1989,** *262*, 167.

10. Bai, Y.; Yang, W.; Sun, Y.; Sun, C., Enzyme-Free Glucose Sensor Based on A Three-Dimensional Gold Film Electrode. *Sens. Actuat. B: Chem.* **2008,** *134*, 471-476.

11. Li, L.-H.; Zhang, W.-D., Preparation of Carbon Nanotubes Supported Platinum Nanoparticles by An Organic Colloidal Process for Nonenzymatic Glucose Sensing. *Microchim. Acta* **2007,** *163*, 305-311.

12. Bai, Y.; Sun, Y.; Sun, C., Pt-Pb Nanowire Array Electrode for Enzyme-Free Glucose Detection. *Biosens. Bioelectron.* **2008,** *24*, 579-585.

13. Chen, J.; Zhang, W.-D.; Ye, J.-S., Nonenzymatic Electrochemical Glucose Sensor Based on MnO_2/MWNTs Nanocomposite. *Electrochem. Commun.* **2008,** *10*, 1268-1271.

14. Kang, X.; Mai, Z.; Zou, X.; Cai, P.; Mo, J., A Sensitive Nonenzymatic Glucose Sensor in Alkaline Media with A Copper Nanocluster/Multiwall Carbon Nanotube-Modified Glassy Carbon Electrode. *Anal. Biochem.* **2007,** *363*, 143-150.

15. Kurniawan, F.; Tsakova, V.; Mirsky, V. M., Gold Nanoparticles in Nonenzymatic Electrochemical Detection of Sugars. *Electroanalysis* **2006,** *18*, 1937-1942.

16. Liu, Y.; Teng, H.; Hou, H.; You, T., Nonenzymatic Glucose Sensor Based on Renewable Electrospun Ni Nanoparticle-Loaded Carbon Nanofiber Paste Electrode. *Biosens. Bioelectron.* **2009,** *24*, 3329-3334.

17. Vassilyev, Y. B.; Khazova, O. A.; Nikolaeva, N. N., Kinetics and Mechanism of Glucose Electrooxidation on Different Electrode-Catalysts .1. Adsorption and Oxidation on Platinum *J. Electroanal. Chem.* **1985,** *196*, 105-125.

18. Ye, J. S.; Wen, Y.; Zhang, W. D.; Gan, L. M.; Xu, G. Q.; Sheu, F. S., Nonenzymatic Glucose Detection Using Multi-Walled Carbon Nanotube Electrodes. *Electrochem. Commun.* **2004,** *6*, 66-70.

19. Adzic, R. R.; Hsiao, M. W.; Yeager, E. B., Electrochemical Oxidation of Glucose on Single Crystal Gold Surfaces. *J. Electroanal. Chem. Interfac. Electrochem.* **1989,** *260*, 475-485.

20. de Mele, M. F. L.; Videla, H. A.; Arv´ıa, A. J., The Electrooxidation of Glucose on Platinum Electrodes in Buffered Media. *Bioelectrochem. Bioenerg.* **1983,** *10*, 239.

21. Ernst, X.; Heitbaum, J.; Hamann, C. H., The Electrooxidation of Glucose in Phosphate Buffer Solutions: Part I. Reactivity and Kinetics Below 350 mV/RHE. *J. Electroanal. Chem.* **1979,** *173*, 173-183

22. Hsiao, M. W.; Adzic, R. R.; Yeager, E. B., The Effects of Adsorbed Anions on the Oxidation of D-Glucose on Gold Single Crystal Electrodes. *Electrochim. Acta* **1992,** *37*, 357.

23. Hsiao, M. W.; Adzic, R. R.; Yeager, E. B., Electrochemical Oxidation of Glucose on Single Crystal and Polycrystalline Gold Surfaces in Phosphate Buffer *J. Electrochem. Soc.* **1996,** *143*, 759-767

24. Lee, Y. J.; Park, D. J.; Park, J. Y., Fully Packaged Nonenzymatic Glucose Microsensors With Nanoporous Platinum Electrodes for Anti-Fouling. *Sens, J., IEEE* **2008,** *8*, 1922-1927.

25. Chou, C.-H.; Chen, J.-C.; Tai, C.-C.; Sun, I.-W.; Zen, J.-M., A Nonenzymatic Glucose Sensor Using Nanoporous Platinum Electrodes Prepared by Electrochemical Alloying/Dealloying in a Water-Insensitive Zinc Chloride-1-Ethyl-3-Methylimidazolium Chloride Ionic Liquid. *Electroanalysis* **2008,** *20*, 771-775.

26. Holt-Hindle, P.; Nigro, S.; Asmussen, M.; Chen, A., Amperometric Glucose Sensor Based on Platinum–Iridium Nanomaterials. *Electrochem. Commun.* **2008,** *10*, 1438-1441.

27. Wang, J.; Thomas, D. F.; Chen, A., Nonenzymatic Electrochemical Glucose Sensor Based on Nanoporous PtPb Networks. *Anal. Chem.* **2008,** *80*, 997–1004.

28. Su, C.; Zhang, C.; Lu, G.; Ma, C., Nonenzymatic Electrochemical Glucose Sensor Based on Pt Nanoparticles/Mesoporous Carbon Matrix. *Electroanalysis* **2010,** *22*, 1901-1905.

29. Seo, B.; Kim, J., Electrooxidation of Glucose at Nanoporous Gold Surfaces: Structure Dependent Electrocatalysis and Its Application to Amperometric Detection. *Electroanalysis* **2010,** *22*, 939-945.

30. Cui, H.-F.; Ye, J.-S.; Liu, X.; Zhang, W.-D.; Sheu, F.-S., Pt-Pb Alloy Nanoparticle/Carbon Nanotube Nanocomposite: A Strong Electrocatalyst for Glucose Oxidation. *Nanotechnology* **2006,** *17*, 2334-2339.

31. Park, S.; Boo, H.; Lee, S. Y.; Kim, H.-M.; Kim, K.-B.; Kim, H. C.; Chung, T. D., Apparent Electrocatalysis on 3D Nanoporous Platinum Film Electroplated from Hexagonal Lyotropic Liquid Crystalline Phase of Triton X-100. *Electrochim. Acta* **2008,** *53*, 6143-6148.

32. Favier, F.; Walter, E. C.; Zach, M. P.; Benter, T.; Penner, R. M., Hydrogen Sensors and Switches from Electrodeposited Palladium Mesowire Arrays *Science* **2001,** *293*, 2227-2231.

33. Huang, Y.; Zhou, X.; Liao, J.; Liu, C.; Lu, T.; Xing, W., Synthesis of Pd/C Catalysts with Designed Lattice Constants for the Electro-Oxidation of Formic Acid. *Electrochem. Commun.* **2008,** *10*, 1155-1157.

34. Adams, B. D.; Wu, G.; Nigro, S.; Chen, A., Facile Synthesis of Pd-Cd Nanostructures with High Capacity for Hydrogen Storage. *J. Am. Chem. Soc.* **2009,** *131*, 6930-6931.

35. Nepomnyashchii, A. B.; Alpuche-Aviles, M. A.; Pan, S.; Zhan, D.; Fan, F.-R. F.; Bard, A. J., Cyclic Voltammetry Studies of Cd^{2+} and Zn^{2+} Complexation with Hydroxyl-Terminated Polyamidoamine Generation 2 Dendrimer at A Mercury Microelectrode. *J. Electroanal. Chem.* **2008,** *621*, 286-296.

36. Martins, P. R.; Aparecida Rocha, M.; Angnes, L.; Eisi Toma, H.; Araki, K., Highly Sensitive Amperometric Glucose Sensors Based on Nanostructured α-$Ni(OH)_2$ Electrodes. *Electroanalysis* **2011**, DOI: 10.1002/elan.201100271.

Chapter 9

Conclusion, Future Prospects and Challenges

As the prevalence of diabetes is increasing worldwide and as curing of the two types of diabetes remains elusive, humanity is likely to further benefit from advances in monitoring of glycemia. In this regard, the enormous activity in the field of glucose biosensors is a reflection of the major clinical importance of the topic. Such huge demands for effective management of diabetes have made the disease a model in developing novel approaches for other types of biosensors for diagnosis of cholesterol, cancer, infections and other diseases.

Electrochemical glucose monitoring has contributed massively to improving the lives of diabetic people. Accordingly, for nearly 50 years we have witnessed tremendous progress in the development of electrochemical glucose biosensors. Elegant research on new sensing concepts, coupled with numerous technological innovations, has thus opened the door to widespread applications of electrochemical glucose biosensors. Such devices account for nearly 85% of the world market of biosensors. Major fundamental and technological advances have been made for enhancing the capabilities and improving the reliability of glucose measuring devices. Such intensive activity has been attributed to the tremendous economic prospects and fascinating research opportunities associated with glucose monitoring. The success of glucose blood meters has stimulated considerable interest in in-vitro and in-vivo devices for monitoring other physiologically important compounds. Similarly, new materials (membranes, mediators, electrocatalysts, etc.) and concepts, developed originally for enhancing glucose biosensors, now benefit a wide range of sensing applications.

Even though progress in this field is rapid, the ultimate goal of achieving long-term, accurate and continuous glucose monitoring in patients has not yet been fulfilled, and there are still many challenges and obstacles related to the achievement of a highly stable and reliable continuous glycemic monitoring. Such monitoring of moment-to-moment changes in blood glucose concentrations is expected to lead to a substantial improvement in the management of diabetes. The motivation of providing such tight diabetes control thus remains the primary focus of many researchers.

Nanoscale sensors have the potential to drastically improve continuous glucose monitoring capabilities and improve patient quality of life. Macrosensors can be compromised during implantation through the degradation of the sensor and fibrous capsule formation. Nanosensors might avoid these drawbacks, allowing more long-term monitoring and reaching the goal of a closed-loop artificial pancreas. Several questions remain about the ability for these approaches to impact clinical care, including biocompatibility and sensor lifetime.

Therefore, the questions that need to be answered are:

1. Can we design biosensors with biocompatible components?
2. Can nanomaterials size and shape have an impact on the bio-recognition components in a biosensor?
3. Can nanomaterials be designed to help improve sensor lifetime?
4. Do nanomaterials improve current sensors at a level that offsets the increased cost of manufacture?
5. Can nanoscale sensors minimize tissue encapsulation and protein fouling?

6. Can nanosensors be administered in locations to minimize glucose transport time lag?

In the present dissertation, we devoted our full commitment and efforts to answer the first three questions. However, the last three questions need to be addressed through further research for patients to benefit from this technology.

First, we demonstrated a novel glucose biosensor based on the highly efficient immobilization of GO_x on a Prussian blue-modified nanoporous Au surface. The nanoporous Au was directly grown through a facile hydrothermal method and modified by electrodeposited Prussian blue (PB). Our study showed that owing to its large surface area and strong adsorption ability for enzyme binding, high chemical stability, low inherent toxicity and high conductivity the nanoporous Au substrate provides an excellent matrix for the immobilization of GO_x. The small K_m value of the biosensor indicates that the immobilized GO_x possesses high enzymatic activity and that the fabricated biosensor exhibits a high affinity for glucose. Our electrochemical tests showed that the fabricated biosensor exhibits fast amperometric response, a low detection limit, extremely high sensitivity, good reproducibility and high selectivity for the detection of glucose.

To adopt the excellent properties of nanoporous gold in a mediator-free biosensor, we modified its structure and fabricated a cholesterol biosensor by co-immobilizing enzymes (cholesterol oxidase, cholesterol esterase and horseradish peroxidise) on its surface. The immobilized cholesterol oxidase effectively catalyzes the oxidation of cholesterol while the cholesterol esterase catalyzes the hydrolysis of esterase-esterified cholesterol, thus allowing the determination of the total cholesterol. Meanwhile, the immobilized horseradish peroxidase (HRP) facilitates the detection of the H_2O_2 generated by the catalytic conversion of cholesterol to

cholest-4-en-3-one. The developed cholesterol biosensor showed high selectivity as tested toward common interfering species such as ascorbic acid, uric acid, lactic acid and glucose. A very low Michaelis-Menten constant indicates a very high activity of the immobilized enzymes. Under the physiological condition (pH 7.4), the designed biosensor exhibited reliable cyclic voltammetric responses, high sensitivity, and a wide linear range up to 300 $mg.dl^{-1}$. The developed biosensor was also successfully used to measure the total cholesterol in real food samples. The high-performance along with the ease of fabrication and low costs makes the new biosensor promising for the detection of total cholesterol in both clinical diagnostics and the food industry.

Furthermore, to improve the long-term stability of the biosensor we used buckypaper (aggregated carbon nanotubes) networks to design a mediator-free glucose biosensor based on the co-immobilization of GO_x and HRP on the activated buckypaper. Direct electrochemistry of GO_x on the buckypaper was observed. The glucose biosensor showed a high sensitivity, low detection limit, fairly wide linear dynamic range, over 80 days life-time for continuous monitoring of glucose. The selectivity response of the biosensor in the presence of common interferent species was studied under the physiological condition and the result showed that the biosensor is worth to be further tested in real sample analysis. These properties of the buckypaper-based biosensor, coupled with the biocompatibility of its components are important factors which could be attractive for real-time in vivo glucose monitoring and lead to a substantial improvement in the management of diabetes. The facile and robust buckypaper-based platform proposed in this study opens many opportunities for the development of high-performance electrochemical biosensors for medical diagnostics and environmental monitoring.

According to our previous work carbon-based nanostructured biosensors exhibit considerable longevity. Thus, we developed a modified method to synthesize carbon-modified TiO_2 nanowires with controllable size. As demonstrated in chapter 7, carbonized TiO_2 nanostructures, with different dimensions, interact differently with GO_x. We discovered that GO_x requires a TiO_2 nanowire smaller than 80 nm × 2 μm in order to sufficiently promote electron transfer throughout the sensor and reaction with glucose in a continuous behavior. This confirms that the modified TiO_2 nanowire is capable of communicating with the prosthetic group of enzyme. The carbonized TiO_2 nanowire based biosensor was further tested using a real sample, human serum with a normal glucose level. The values measured by the fabricated biosensor were in excellent agreement with the data obtained by a commercial blood glucose monitoring assay, showing that the carbonized TiO_2 nanowire based biosensor is amenable in medical diagnostics.

In addition, as previous studies showed TiO_2 is inherently biocompatible and obtains more stability upon protein adsorption and its protein-conjugated implants do not release particles to the surrounding tissues. Therefore, we suggest that carbonized TiO_2 nanoparticles can further be studied for *in vivo* analysis with the aim of developing implanted biosensors.

To study the behaviour of nanomaterials in an enzyme-free medium, we synthesized Palladium-Cadmium (Pd-Cd) nanostructure. Then, we deposited the nanomaterials on a glassy carbon electrode. The fabricated electrode has strong and sensitive current responses to glucose. The sensor is capable of sensing glucose amperometrically at a very negative potential, -400 mV (Ag/AgCl), where the interference from the oxidation of common interfering species such as AA, AP, and UA is effectively avoided. In addition, the high sensitivity of the electrode in neutral pH (7.4) corroborates its longevity. The electrode has many other desirable properties including low detection limit, high sensitivity, short response time, and satisfactory linear

concentration range. However, its response in very low potential and its biocompatibility, life time and mechanical stability are three main issues that need to be investigated in the future.

Table 9.1 summarizes the properties of the glucose sensors which were designed and fabricated in this research project.

Table 9.1 Some of the important properties of the glucose sensors reported in this dissertation.

Sensor	Detection Limit (mM)	Sensitivity ($\mu A.mM^{-1}.cm^{-2}$)	Mechaelis Menten Constant (mM)	Lifetime (days)	Linear Dynamic Range (mM)
Ti/NPAu/PB/GO_x	0.0025	177	2.1	60	0-2.04
Ti/Au/BP/GO_x-HRP	0.01	20	4.6	> 80	0-9
Ti/TiO_2/C/GO_x	0.4	15	9.5	> 70	0-18
PdCd/GC	0.05	146	N/A	30	0-10

Ti: Titanium; NPAu: Nanoporous gold; PB: Prussian blue; GOx: Glucose oxidase; BP: Buckypaper; HRP: Horseradish peroxidise; C: Carbon; PdCd: Palladium/Cadmium; GC: Glassy carbon electrode; N/A: Not Applicable

In all works presented in this dissertation, we tested the selectivity of the biosensor toward common interference species in blood and finally in our last fabricated biosensor, we reported on tests in human serum samples and described the comparable sensitivity of the biosensor to conventional testing techniques, which is promising for future applications of these sensors.

The research and development of nanosensors for the management of diabetes will remain an important research area in the future. Following the single-use strips, which now accurately monitor glucose concentrations in 300 nL samples of blood, their already small subcutaneous sensors will be further miniaturized, and their 5-7 day operating lives will be extended. Through

increasingly accurate and continuous measurement of the first and second generation of glucose biosensors, the diabetic user will be adequately forewarned if and when corrective action is needed to maintain a healthier narrower, closer to normal, glycemic range. The pain of blood glucose monitoring could be eliminated and the constant worry of diabetic people is now being eliminated through “smart tattoo”. The closed-loop pancreas would eliminate the need for the patient to perform these steps because it would perform similar to a natural pancreas. Continuous monitoring, like that achieved by the systems discussed here, is a necessary part of this long-term goal. To help fulfill this goal, future work should also emphasize testing these sensors in comparison with commercially available sensors to better demonstrate the advantages or disadvantages of the nanosensors. These direct comparisons would help justify the additional cost and effort to overcoming the manufacturing challenges associated with nanosensors compared with standard sensors. The cost and effort of the large-scale manufacture of new sensor approaches must provide either extreme improvements in accuracy with minimal additional new cost or an improvement in patient quality of life. This is a large problem to overcome for the approaches that incorporate nanomaterials into electrochemical detection approaches or detect glucose through direct oxidation, because the patient must still undergo the same sampling methods (finger-stick), yielding no improvement in quality of life. To have an impact on diabetes, these sensors must demonstrate extremely high improvements in response because cost is unlikely to decrease below current manufacturing approaches.

Success in this direction demands a detailed understanding of the underlying biochemistry, physiology, surface chemistry, electrochemistry, and material chemistry. As this field enters its sixth decade of intense research, we expect significant efforts that couple the fundamental sciences with technological advances. This stretching of the ingenuity of researchers will result

in advances including the use of nanomaterials for improved electrical contact between the redox center of GO_x and electrode supports, enhanced "genetically engineered" GO_x, new "painless" in-vitro testing, artificial (biomimetic) receptors for glucose, advanced biocompatible membrane materials, the coupling of minimally invasive monitoring with compact insulin delivery system, new innovative approaches for noninvasive monitoring, and miniaturized long-term implants.

Finally, from all our works in the area of enzyme-analyte-nanomaterials interactions, we believe that surface morphology may also play an important role in other interfacial biomolecular probe-target interaction, such as nucleic acid hybridization and antigen-antibody interactions. Therefore, the observations reported in this dissertation may guide the development of both sensors and materials with great capabilities to improve the lives of patients living with diabetes, cancer and other diseases through progress in electrochemistry and biotechnology.